1-1-1970

An experimental investigation into the response of a turbulence-type amplifier, and laminar/turbulent jet study.

Thomas Ignatius Marian Vaz
University of Windsor

INFORMATION TO USERS

This manuscript has been reproduced from the microfilm master. UMI films the text directly from the original or copy submitted. Thus, some thesis and dissertation copies are in typewriter face, while others may be from any type of computer printer.

The quality of this reproduction is dependent upon the quality of the copy submitted. Broken or indistinct print, colored or poor quality illustrations and photographs, print bleedthrough, substandard margins, and improper alignment can adversely affect reproduction.

In the unlikely event that the author did not send UMI a complete manuscript and there are missing pages, these will be noted. Also, if unauthorized copyright material had to be removed, a note will indicate the deletion.

Oversize materials (e.g., maps, drawings, charts) are reproduced by sectioning the original, beginning at the upper left-hand corner and continuing from left to right in equal sections with small overlaps.

AN EXPERIMENTAL INVESTIGATION

INTO THE RESPONSE OF A

TURBULENCE-TYPE AMPLIFIER,

AND LAMINAR/TURBULENT

JET STUDY.

A Thesis

Submitted to the Faculty of Graduate Studies Through
the Department of Mechanical Engineering in Partial
Fulfillment of the Requirements for the Degree
of Master of Applied Science at the
University of Windsor

by

Thomas Ignatius Marian Vaz

B.E. (Mechanical), College of Engineering,

Guindy, Madras, India, 1968

Windsor, Ontario, Canada

1970

UMI Number: EC52842

UMI®

ABN2020

Approved by:

W. S. Collins

H. J. Tucker

S. P. Peter

321798

ABSTRACT

The experimental results of an investigation into the response times to switch off and switch on an open type of turbulence amplifier are presented.

In this study, the Reynolds number of the supply jet was varied from 2300 to 3800, the delay times were determined for different distances down the jet. The control jet velocity was varied from 50 to 80 ft./sec.

The transition time from the turbulent to laminar state was very appreciable when compared to the laminar-turbulent transition time.

After an initial experimental study of the 0.054" jet, a 0.25" i.d. tube was installed to study the turbulence intensity and mean-velocities prevailing in the jet. Measurements were made using hot-wire probes.

The laminar length of the jet between Reynolds numbers of 1000 and 11,000 were determined. The experimental points fell close to the straight line

$$L/d = -0.00185Re + 22.33$$

iii

ACKNOWLEDGEMENTS

I would like to express my sincere gratefulness to my advisor Professor Henry J. Tucker for his encouragement, guidance, and assistance during the course of this investigation.

Gratitude is also due to my parents who had made nothing wanting for me.

The help that Dr. K. Sridhar gave me in this project is gratefully acknowledged.

My thanks are also due to Mr. O. Brudy of the Central Research Shop and to Mr. L.F. Cory of the Electronic Shop. I further wish to thank Mr. Roy F. Allen for taking pains to type this work.

CONTENTS

vi

LIST OF FIGURES

vii

ix

x

LIST OF SYMBOLS

Symbol

a	exponent of velocity in the hot-wire response equation
C	constant used in the hot-wire response equation
d	inner diameter of tube
e'	fluctuating voltage of the hot-wire
$\sqrt{\overline{e'^2}}$	r.m.s. value of the fluctuating voltage
$\overline{E}$	bridge d.c. voltage
$\overline{E}_o$	bridge d.c. voltage at zero flow velocity
I	probe current
l_s	length of supply tube
L	distance of the transition point from the exit of the supply tube
m	constant
M	slope of the hot-wire calibration curve
Q	heat flux
R	probe resistance
Re_s	Reynolds Number of the supply jet based on the average velocity at the exit of the tube
r	radial distance in the jet
S	sensitivity of the hot-wire used
u'	fluctating component of velocity
$\sqrt{\overline{u'^2}}$	r.m.s. value of the fluctating velocity in the x direction
$\overline{U}$	mean-velocity at any point in the jet

xi

Symbol

$\overline{U}_o$ mean-velocity at the exit of the supply
          tube

$\left(\overline{U}_c\right)_o$ center-line mean-velocity at the exit

          of the supply tube

$\left(\overline{U}_c\right)_{turbulent}$ mean center-line velocity in the

          turbulent supply jet

Vc control jet average velocity at exit

          of control tube

x axial distance along the jet

xii

1. INTRODUCTION

In March 1960, the Harry Diamond Laboratory introduced a new class of fluid control device known as the turbulence amplifier developed by Auger (2). It is a low pressure switching device having no-moving parts. This amplifier is basically a two-state device which operates as a NOR element capable of performing all conventional logical operations.

The turbulence amplifier shown in Fig. 1 consists of a supply tube emitting a laminar jet directed into a collector tube separated by a gap. The control jet tube is located near the exit of the supply jet. The function of the control jet is to induce turbulence in the laminar jet.

Figure 1 and Fig. 2 explain the principle of operation in a turbulence amplifier. When the laminar flow is directed into the collector, the pressure and flow recovered is appreciable. The amplifier is now said to be 'ON'. A very small control flow will cause the laminar flow to break up into turbulence further upstream than it would naturally, resulting in the intense mixing of the jet and surrounding fluid and hence loss of captured output flow. This is the 'OFF'

1

state of the amplifier.

Figure 3 shows the oscillogram of the signals from two probes, one placed near the exit of the control jet tube and the other in the place where the entrance to the collector would have been.

The 'ON' and 'OFF' state as illustrated in Fig. 1 and Fig. 2 are shown on this oscillogram. Other terms used in this investigation are as follows:-

DELAY TIME-LAMINAR:- is the time taken from the control 'start on' point to the point at which the supply jet starts becoming turbulent.

FALL TIME:- is the time between the start of the fall of the velocity and the appearance of fully turbulent velocity fluctuations (OFF state of the amplifier). In other words it is the conversion time from laminar to turbulent flow.

DELAY TIME-TURBULENT:- is the time between the control 'start off' point to the point at which the turbulent state starts to return to the laminar state.

RISE TIME or conversion time from turbulent to laminar flow is the time interval between the end of the turbulent fluctuations and the attainment of its original 'ON' level.

The fluidic turbulence amplifier has found wide application due to its reliability in different environments, low supply pressures, complete input signal

2

isolation from other inputs and its high power gain.

The narrow range in the Reynolds number, the supply tube length and the critical alignment between the supply tube and the collector restricts the operation of the turbulence amplifier. Other disadvantages of this type of amplifier are the sensitivity of the laminar jet to acoustic disturbances, and the erratic transition from the turbulent to the laminar state. The unequal switch-on and switch-off times introduce difficulties in the reliable operation of circuits containing these amplifiers. A major drawback in this type of amplifier is the appreciable time to switch-on (turbulent-laminar transition time) when compared to the switch-off time or the laminar-turbulent transition time. The object of this study was to make an experimental investigation into these times.

3

2. LITERATURE SURVEY

2.1 Jet Flow

McNaughton and Sinclair (14) using flow visualization observed four main types of vertical jets, namely:-

1) the dissipated-laminar jet (Reynolds number of the jet less than 300) wherein a parallel-sided, non-eddying jet rose a short distance into the vessel and then mushroomed,

2) the fully laminar jet (Reynolds number between 300 and 1000) wherein the laminar length of the jet became equal to the length of the vessel,

3) the semi-turbulent jet (Reynolds number between 1000 and 3000) wherein turbulent eddies appeared at the top of the laminar jet,

4) the fully turbulent jet (Reynolds number greater than 3000) wherein there are two regions - a forward moving, turbulent, conical jet and a slower moving backflow region which surrounds the jet and moves towards the inlet. The types of breakdown observed in this work were similar to those mentioned by Reynolds (16).

Schlichting (19) derived theoretically the circular laminar jet velocity profile. He assumed that the jet issued from a point aperture, giving as

4

it does an infinite velocity. Squire (21) also obtained a solution for the axially symmetrical jet, and showed that in the central part of the jet the flow was very similar to that deduced by Schlichting.

Andrade and Tsien (1) carried out an experimental work on the distribution of velocity in a liquid-into liquid jet from a cylindrical tube with tapering approach. There was excellent agreement between their experimental work and Schlichting's theoretical predictions, except in the immediate neighbourhood of the orifice. Andrade and Tsien had to account for the fact that the jet issued from an orifice of finite size. They did this experimentally determining the effective origin of the point source and including this in Schlichting's equation.

2.2 The Transition Phenomena and Laminar Length of the Jet.

The boundary layer surrounding the immersed jets used in the turbulence amplifier can either attenuate or amplify any instabilities existing in it, depending on the Reynolds number of the jet. Rosenhead (17) shows the amplification and attenuation regions separated by the neutral stability curve. The amplification mechanism exists in the boundary layer. The boundary layer grows at the expense of the regions immediately

5

around it. Since the laminar boundary layer grows
quickly, the jet transition is rapid. Once turbulent,
the jet dissipates its energy in the immersing medium.
Transition to turbulence in the jet is closely controlled
by the character of the boundary layer. In turn, bound-
ary layer transitions depend on initial disturbance
size. Most studies of transition to turbulence in lam-
inar jets have been concerned with the vortex evolution
in the free shear layer.

Becker and Massaro (5) using smoke photography
investigated the phenomena of instability, such
as the rolling up of the cylindrical vortex layer into
ring vortices, the coalescence of ring vortex pairs
and the eventual disintegration into turbulent eddies
as a function of the Reynolds number. This work agrees
with the theory given by Wille (22) that the transition
of a laminar jet is governed by the growth and decay
of the annular vortices.

Jets at sufficiently high Reynolds numbers where
the angle of viscous spreading is small are unstable to
infinitesimal disturbances, but little data could be
obtained by Batchelor and Gill (4) about the critical
Reynolds number or the mode of disturbance that grows
most rapidly at a given Reynolds number.

Sato (18) observed in the region where the lam-
inar flow becomes unstable, two kinds of sinusoidal

6

velocity fluctuations; one was symmetrical and the other anti-symmetrical with respect to the centerline of the jet. The relative intensity of the two modes of fluctuation was strongly dependant on the mean-velocity distribution. The transition of the jet according to Sato was initiated by sinusoidal velocity fluctuations, which were weak at first and then amplified as the distance downstream increased.

Inlet disturbances, appearing as vortices which arrive at the outlet of the supply tube, even though greatly damped, could also be the cause for early transition to turbulence. Wille (22) identified vortex motions as the origin of the transition phenomena. Usually these vortices must be generated in the free shear layer, however, if they are present in the flow when the jet emerges from the supply tube, they are immediately available as a possible transition triggering mechanism.

The laminar length of a free jet is strongly dependant upon the Reynolds number of the flow at the jet exit. For Reynolds numbers between 1000 to 2400, Marsters (12) obtained a correlation of the form:-

$$\frac{L}{d} = A \, Re^{-B}$$

where   L = laminar length

d = inside diameter of tube

A = 10^9

Average value of B = 2.3

7

In another investigation, McKenzie and Wall (13) observed at very low Reynolds number range (Re = 10 to 400), a somewhat different dependance of laminar length L on Reynolds number, namely:-

$$\frac{L}{d} = \frac{10^3}{Re}$$

McNaughton and Sinclair (14) investigated the laminar length L for the jet enclosed inside a vessel. Between Reynolds number of 500 and 2000, they arrived at the following relationship:-

$$\frac{L}{d} = 9.97 \times 10^7 \, Re^{-2.46} \, (D/d)^{-0.48} \, (h/d)^{0.74}$$

where D = diameter of the receiver vessel and

h = length of receiver vessel.

2.3   The Response of the Turbulence Amplifier

According to Siwoff (20) the time for the signal transmission inside the turbulence amplifier (response time) depends on the average speed of the supply jet and the distance x between the supply tube and the collector. Therefore to obtain a fast response amplifier, x should be kept as small as possible. Siwoff also concludes that if amplifier stability is sacrificed, faster response can be obtained by increasing the supply jet Reynolds number; both requirements will lead to a choice of small supply tube diameters. Siwoff claims to have improved the response time of the turbulence amplifier

8

by placing a knife-edge at 2/3 the distance between the supply tube and the collector. The location of the edge, exerted an influence on the degree of turbulisation. The conversion time of the supply jet from laminar to turbulent and the time from turbulent to laminar was found to be considerably reduced when compared to the case having no edge between the supply and collector tubes. Furthermore, the absolute value of the zero output signal decreases. The edge provides an additional source of disturbance, taking part of the function of the control jet.

Gradetsky and Dmitriev (7) introduced a diffuser at different distances between the supply tube and the collector. The presence of the diffuser eliminated the residual pressure. Also it was found that on increasing the control pressure, there was an increase in the slope of the P output vs P control characteristic with the presence of the diffuser in the flow.

Auger (3) mentions the possibility that higher switching speeds could be realized by overdriving, which entails the use of very strong signals, but that the cyclical switching period will be limited by the relatively lengthy interval required to reestablish laminar flow.

9

Hayes (8) investigated the signal transport delay phenomena based on the velocity profile variations in the free laminar jet. He found the turbulence amplifier "switch-off" depended upon the signal transport effects, while the "switch-on" depended on jet cavity secondary flow as well as signal transport effects.

3. OUTLINE OF EXPERIMENTAL PROGRAM

Very little work has been carried out on a jet flow having a parabolic profile at the exit of the tube. Hayes (8) assumed that there was a region from the exit of the tube where the center-line mean-velocity remained constant (potential core region). He found this length theoretically. It was generally thought that the delay time-laminar was entirely dependent on the center-line mean-velocity of the supply jet. Hence, Hayes calculated this time based on the center-line mean-velocity.

This experimental investigation was carried out partly to see if a region of constant center-line mean-velocity in the jet could be detected, and also to verify if the delay time-laminar depended entirely on the center-line mean velocity of the supply jet. To accomplish this, a large tube was chosen. Turbulence quantities, mean-velocities and laminar length of the jet were also determined.

The small tube which was originally built for the turbulence amplifier was removed and the large tube was fitted because it was felt that the size of the hot-wire probe was appreciable when compared to the diameter of the small tube.

11

3.1 Small Jet

With the 0.054" i.d. supply tube, l_s/d ratio 116, used in the turbulence amplifier, the following were measured:-

1) the mean-velocity profiles at different axial stations in the jet for Reynolds numbers of 2342 and 3050,

2) the center-line mean-velocity of the turbulent jet for Reynolds numbers of 2342, 3050, and 3820 with the control jet continuous at 70 ft./sec.,

3) the effect of the collector on the transition point of the jet for the range of Reynolds numbers between 2342 and 3820.

3.2 Large Jet

Using a 0.25" i.d. tube with the same l_s/d ratio the following were measured:-

1) the mean-velocity profiles at different axial stations in the jet, for Reynolds numbers of 2342 and 3050,

2) the axial-symmetery in the jet,

3) the effect of increasing the Reynolds number from 2342 to 5000 on the mean center-line velocity,

4) the turbulence intensity along the center-line of the jet for Reynolds numbers between 2342 to 5000,

12

5) the turbulence intensity radially across
the jet at different x/d stations for a Reynolds number
of 3050,

6) the laminar length of the jet for Reynolds
numbers between 1000 and 11,000.

3.3 Determination of the Response Time

This investigation was carried out on an open
configuration of the turbulence amplifier. The collect-
or was removed after an initial investigation showed
that its presence did not noticably effect the delay
time. The location of the hot-wire probes were al-
ready mentioned in the introduction. With the def-
inition of the times involved listed in the introd-
uction, the following were measured:-

1) the delay time-laminar and the fall time
for distances from 0.3" to 0.6" down the supply jet.
This investigation was carried out for Reynolds
numbers of 2342, 2780, 3050, 3540, and 3820. The
control jet velocities were 56.75 ft/sec., 70 ft./sec.
and 83 ft./sec.,

2) the delay time-turbulent and the rise time
for distances from 0.3" to 0.6" down the supply jet;
these times were determined for the same range of
Reynolds numbers of the supply jet and the control
jet velocities as mentioned above,

13

3) all of the above times were again determined after turning the control jet through 30° from its original normal position.

14

4. APPARATUS AND INSTRUMENTATION

A schematic arrangement of the apparatus is shown in Fig. 4. Before the flow enters the settling chamber or the control jet tube, it passes through line filters, pressure regulators, gauges, and needle valves as shown in the diagram. Information on the components is presented in a tabular form in Appendix A.

4.1 Apparatus for Response Time Determination

In order to provide a steady air supply to the jet, a large settling chamber was provided with screens and flow straighteners as shown in Fig. 5. A bell-mouth entrance led to the inlet of a stainless steel hypodermic tube having an internal diameter of 0.054" and a length of 6.25". This can also be seen in Fig. 10. This appreciable entrance length was arrived at using Langhaar's formula based on a Reynolds number of 2000, in order to attain a fully developed parabolic profile at the exit of the tube.

Two static pressure taps 0.040" diameter at 90° apart were provided on the settling chamber exit end.

The collector unit having the same diameter opening as the supply tube as shown in the close-up view of the apparatus (Fig. 7), could be mounted on

15

the horizontal traversing mechanism and also very easily removed. The collector was removed after an initial investigation showed that its presence did not noticeably affect the delay times.

The horizontal graduated platform could be levelled accurately using the levelling screws on the four corners (Fig. 11). This was checked using a caliper height gauge. Four adjusting screws, two on the front and two on the back faces of the same horizontal platform enabled the probe movement to be aligned with the axis of the jet.

The control jet was the same type of hypodermic tubing used as in the main supply tube, namely 0.054" i.d. but 1" long having a small bell-mouth at its entrance. Behind the bell-mouth, a camera shutter was placed (Fig. 7 and Fig. 14), and the speed set at 1/100 second.

The fast opening and closing of the shutter blades interrupted the jet giving a control input pulse which was very steep in its rise and fall. These points were well defined, enabling times to be accurately read off on the oscilloscope. The repeatability in the control jet pulse, each time the shutter is released, as observed on an oscilloscope was remarkably good, proving the usefullness of this device.

16

The type 55A25 miniature straight hot-wire probe is attached to the type 55A28 right-angle miniature probe support which rests on a slot located at a suitable height such that the wire is in close proximity to the outlet of the control jet tube (Fig. 7). To align the wire, so that it spans across the center of the tube and also to bring it back as close as possible to the control jet outlet without breaking the wire, two micrometer screws were provided (40 threads per inch), one to move the probe up and down, and the other micrometer screw to move the wire back and forth (Fig. 7). The final check to see if the wire spanned exactly across the diameter of the control jet tube was made using a powerful magnifying glass. The length of the wire happened to be the same as the inside diameter of the control jet tube. Similar micrometer screws (Fig. 9) were provided for the main horizontal traverse so that the Type 55A25 miniature hot-wire probe could be moved along the center-line of the supply jet. In most of the experimental data the wire was moved 0.05" downstream at a time, except when studying the flow fluctuations in the transition zone.

4.2   Set-Up Using Large Tube

Since the wire length was appreciable when compared to the diameter of the main supply tube, a larger

17

diameter supply tube was chosen to study the mean velocity distribution and the turbulence quantities in the jet. The diameter of the tube chosen was 0.25" with a length of 29", giving an 1/d ratio of 116, which was the same as the 1/d ratio in the 0.054" diameter tube, based on a Reynolds Number of 2000 to give a fully developed parabolic profile at the exit of the tube. The flow entered this long tube through a bell-mouth entrance (Fig. 10) after passing through the settling chamber. The settling chamber was the same as that which was used in the case of the 0.054" diameter tube. The whole settling chamber unit could be moved back so that the exit of the tube coincided with the zero mark on the graduations that were made on the main horizontal traverse.

4.3   Probing Assembly

To probe into the large diameter jet (Fig. 12), the type 55A25 miniature straight hot-wire probe was held by the type 55A21 miniature probe support. This probe support was held tightly in a holder having a slot to accomodate it. The holder itself could be moved making sure that the wire travels exactly across the diameter of the tube. The wire can be moved up and down using a vernier with a micrometer gauge, capable of measuring 0.001".

This vernier caliper is mounted to an arm which

18

moves in a slot cut in a metal plate. The slot cut is
such that the whole micrometer assembly carrying the
probe could be turned through 90° (Fig. 13). By doing
this, the axial-symmetery in the jet could be investigated.

4.4   Instrumentation

The hot-wire probes placed in the control jet
and in the supply jet are connected to two independant
DISA 55A01 constant temperature anemometers ME C-97 and
ME C-116. The bridge d.c. outputs (d.c. voltmeter
accuracy = $\pm1\%$) from these two anemometers were taken
into channel 1 and channel 2 of type 564 storage oscillo-
scope. The type 3B3 Tektronix plug-in time-base unit
used on the oscilloscope was capable of generating nor-
mal as well as delayed sweeps. The time base was accurate
within 3% when using both normal and delayed sweeps. The
horizontal time scale was set at 0.5 m.secs./cm. Each
cm. was divided into five parts by drawing vertical lines
right through on the graticule of the oscilloscope. The
two signals obtained were stored, and were accurately
read off on the scribed graticule of the oscilloscope.

Though the DISA constant temperature anemometer
has its own bridge r.m.s. voltage meter (accuracy = 2%)
the pointer of the indicating meter sometimes fluctuates.
Therefore a Brüel and Kjaer random noise voltmeter type
2417 (accuracy = 1% at full scale deflection) with a long

19

time constant was used to measure the correct r.m.s. level. The meter time constant in the instrument was adjusted to the lowest value where no fluctuation of the pointer was visible.

A Hewlett-Packard Model 3440A digital voltmeter with a 4-digit presentation (accuracy = $\pm 0.05\%$ of reading) of the bridge d.c. voltage was used rather than taking the d.c. voltage meter reading provided with the anemometer.

To provide a pulse to externally trigger the oscilloscope, a GE253 bulb shining on a Clairex CL902 photocell was used. In operation the light beam is interrupted by a small vane attached to the shutter cocking lever providing the pulse to scope trigger input.

Figure 16 shows all the connections to the different instruments used.

5. EXPERIMENTAL PROCEDURE

5.1   Determination of Response Time

The different time delays involved in this tur-
bulence amplifier configuration as defined in the in-
troduction were first investigated.

Using the needle valves, the velocity of the
main supply jet and the control jet could be accurately
adjusted. The average velocity at the exit of the main
supply tube is determined from the position of the
spherical float on the flowmeter, this already having
been calibrated (Appendix E).

The control jet tube was placed 0.1" from the
exit plane of the supply tube. Using the micrometer
screws provided, the straight hot-wire probe was
located in front of the control jet, care being taken
not to interfere with the laminar flow from the supply
tube. The velocity of the control jet was determined
from the d.c. voltage reading of the anemometer when
the shutter was open. This d.c. voltage corresponded
to a particular average velocity at the exit of the
control jet tube obtained from the calibration curve
(Appendix D).

21

This investigation was carried out for Reynolds number of supply being 2342, 2780, 3050, 3540, and 3820 with control jet velocities of 56.75 ft./sec., 70 ft./sec., and 83 ft./sec.

A second normal hot-wire was used for the output side. By means of the three micrometer screws as shown in Fig. 9, the wire was made to span across the diameter of the main supply tube. This whole assembly could be made to move along the center-line of the jet, the main horizontal traverse is shown in Fig. 11. All the data was obtained when the wire was moved downstream 0.3" to 0.6" from the exit plane of the supply tube. This distance was well within the laminar region for the whole range of Reynolds numbers of supply.

Having connected the hot-wire probes to two separate hot-wire anemometers, the bridge d.c. output from these were fed into channel 1 and channel 2 of the oscilloscope. After adjusting for the correct control jet velocity, the shutter was cocked. In this position the small vane covers the beam of light which was directed into the photocell. The oscilloscope was set on external trigger mode of operation getting the pulse on breaking the beam of light when the shutter was released. The time-base unit provided on this oscilloscope was capable of generating delayed sweeps.

22

This enabled the transition from laminar to turbulent
and the transition from turbulent back to laminar state
to be studied independantly with a setting of 0.5 m.sec./
div. on the time base. The signals obtained were stored
in the oscilloscope, and the delay times as defined
were read off.

The control jet was turned by an angle of 30°
(Fig. 15) from its normal position and the procedure
repeated as described above to obtain the response
time to switch off and switch on this turbulence amplifier.

5.2   Experiments with the Large Jet

The larger diameter tube, 0.25" i.d. of length
29" with a bell-mouth entrance and having the same l/d
ratio as in the case of the hypodermic tubing, was
screwed onto the settling chamber. The same spherical
float flowmeter was used. The settling tank was moved
back so that the zero on the horizontal graduations
coincided with the exit plane of the tube. The whole
of the control jet assembly and output probe assembly
were removed when studying this jet.

The type 55A25 straight hot-wire probe being
used was calibrated (Appendix C). The probe holder
was placed in a slot provided for it. This was mounted
on a micrometer vernier caliper capable of moving the
wire 0.001" up or down. The zero on this gauge is set

23

corresponding to when the wire is at the center. As seen from Fig. 29, the laminar length is defined as the distance up to which the r.m.s. voltage is less than 20 m.v. With this definition the hot-wire was moved along the center-line of the jet and the transition point located for each Reynolds number of the supply jet.

To determine the mean-velocity in the jet (for Reynolds number of 2342 and 3050), the d.c. voltage reading of the anemometer was observed on a Hewlett-Packard digital voltmeter. The mean-velocity profiles for different axial stations were plotted by operating the micrometer screw, moving the wire 0.01" at a time (Fig. 12) and noting the d.c. voltage reading. Calculation of mean-velocity is shown in Appendix B. To check for axial symmetery in the jet, the arm carrying the caliper unit to which the probe was fastened was turned through 90° (Fig. 13) along the circular slot. The probing in this direction for the different axial stations downstream was done in a manner as described above.

In the determination of the turbulence intensity at different points in the jet, a reading of the d.c. voltage and r.m.s. voltage had to be taken. Calculation of turbulence intensity is shown in Appendix B. A Bruel and Kjaer meter was used to measure the correct

24

r.m.s. level, the time constant in this instrument was set to damp out the fluctuations in the pointer.

6. RESULTS AND DISCUSSION

6.1 Large Diameter Jet

Figure 17 shows the non-dimensional mean-velocity profile measured 0.025" away from the exit plane of the supply tube; $\overline{U}_o$ is the mean center-line velocity at the exit of the tube and d is the inner diameter of the tube. Noting the bridge d.c. voltage at different r (radial distances from the center-line), the mean-velocity $\overline{U}$ calculated from Equation (3) Appendix B is plotted in this Figure. Comparing this experimental curve with the equation of a parabola $y^2 = -4ax$, it is found that the experimental points are in close agreement, showing that with this l_s/d ratio chosen (based on Langhaar's formula (11)), a fully developed parabolic profile was obtained at the exit of the tube. This exit velocity profile is desirable in a turbulence amplifier.

Figures 18 to 21 show the mean-velocity profiles in the jet at different x/d locations downstream for a Reynolds number of 2342 and 3050. As seen from the velocity distributions, the center-line mean-velocity decreases with distance from the exit of the jet. In the laminar region there is a very small decrease in

26

the mean center-line velocity. Also in this region there is no noticeable spread of the laminar jet. The profile at x/d = 24 is in the turbulent region as seen from the sharp decrease in the center-line mean-velocity.

After obtaining these velocity profiles in the jet by traversing the hot-wire as shown in Fig. 12, the probe was now turned through 90° as shown in Fig. 13 and velocity profiles obtained. This was done at a Reynolds number of 3050 for different x/d stations in the jet to check for axial symmetry. The results are shown in Fig. 20 and Fig. 21. The jet appeared to be quite symmetrical in the laminar region. In the turbulent region, due to the scatter of the points, it was not possible to determine if the jet was symmetrical or not.

The decrease in the center-line mean-velocity for Reynolds numbers between 2342 and 5000 is shown in Fig. 22. The location of the laminar-turbulent transition point, especially for the high Reynolds numbers, is easily observed. The transition point moves closer to the exit plane of the supply tube with increase in Reynolds number; this is evident from the curves. The non-dimensional center-line mean-velocity finally approaches each other far downstream for the

27

different Reynolds numbers. Also, for all the Reynolds numbers, the curves collapsed into a single curve for x/d less than 12.

The variation in the relative turbulence intensity along the axis of the jet for different Reynolds numbers of the supply in the range of operation of the turbulence amplifier is shown in Fig. 23 (Plot non-dimensionalized where d is the inner diameter of the supply tube). The bridge d.c. voltage and r.m.s. bridge voltage fluctuation for every axial station in the jet is noted. Referring to Appendix B Equation (4), the r.m.s. of the fluctuating component of the velocity u'^2 could be computed and hence the relative turbulence intensity $\dfrac{u'^2}{\bar{u}_o}$. For all the Reynolds numbers, the relative turbulence intensity increased sharply in the turbulent region, reaching a maximum value before dying out. By increasing the Reynolds number of the supply jet, the relative turbulence intensity peaks increased in magnitude and moved upstream. As suggested by Boyd (6), the appearance of these peaks were probably due to the coalescence of ring vortices which resulted in a sudden concentration of the velocity fluctuation. The relative turbulence intensity gradually dies out to about the same level for all the Reynolds numbers at appreciable distances downstream.

Figure 24 shows the radial turbulence intensity

28

profiles at different x/d stations in the jet of
Reynolds number 3050. At the beginning of transition
and at the same radial distance from the center-line,
two local maximums appear on either side of the center-
line. A little further downstream at x/d = 18 these
two local maxima collapse into a single local maximum
on either side of the center-line, with the center-
line turbulence intensity still a local minimum. In
the turbulent region this local minimum gradually
disappears and is replaced by a local maximum at the
center-line. The appearance of the maximum intensity
at the jet center-line and the corresponding disappear-
ance of all the peaks may be attributed to the coal-
escence of individual vortices characteristics of
the final stages of vortex decay. With the coales-
cence of these vortices, their accompanying velocity
fluctuations are finally able to penetrate the center-
line of the jet. True turbulence begins to develop
after x/d = 22 as seen from the turbulence intensity
distributions.

The laminar length of the jet between Reynolds
numbers of 1000 to 11,000 is shown in Fig. 25. The
experimental points fall close to the straight line
$L/d = -0.00185Re + 22.33$.

In Fig. 26 the curve obtained by Marsters (12)

29

is shown. Marsters obtained a correlation of the form $\frac{L}{d} = 10^9 Re^{-2.3}$ for the Reynolds number range between 1000 to 2400. He used different tubing materials and different l_s/d ratios. By comparing his curve with the straight line relationship obtained in this experiment, it is observed that close agreement is reached only at the higher Reynolds numbers. This is probably because Marsters in his experiment filled the settling chamber with glass wool. In the experimental investigation screens were used.

6.2   Small Jet

Using the same settling chamber, the 0.25" i.d. tube was now replaced by the 0.054" i.d. tube ($l_s/d = 116$ was the same in both cases). The mean-velocity profiles in the jet at different x/d locations downstream for Reynolds numbers of 2342 and 3050 are shown in Fig. 18 to Fig. 21. The result of using the hot-wire when using this tubing was that the center-line mean-velocity in the jet was affected. For a Reynolds number of 2342 the effect was noticeable especially at x/d = 12, and for a Reynolds number of 3050 at x/d = 8. This was most likely due to the appreciable size of the hot-wire in comparison with the tube diameter.

The control jet with a velocity of 70 ft./sec. was kept continuously on. The decrease of the turbulent

30

jet velocity along the center-line of the jet for Reynolds numbers of 2342, 3050, and 3820 were shown in Fig. 27. Schlichting (19) noted that for a circular turbulent jet, the center-line velocity decreases with the reciprocal of the distance x. This is the case in Fig. 28 for a Reynolds number of 3050 and 3820. For the very low Reynolds number of 2342, no conclusion could be reached due to the scatter of the points.

To arrive at a suitable definition for the distance of the transition point from the exit of the tube, different Reynolds numbers of the supply jet were investigated as shown in Fig. 29. The milli-volt r.m.s. reading is an index of the turbulence level. Moving the probe down the jet results in a gradual increase in the m.v. reading up to 20 m.v. for the whole range of Reynolds numbers of the supply jet considered When the jet is turbulent, the m.v. reading increases very rapidly. In the work, at 20 m.v. the laminar to turbulent transition was defined to take place. After reaching a maximum value, the flow fluctuation (m.v. reading) gradually dies out.

As seen from Fig. 30, the distance of the transition point with increase in the Reynolds number of the supply jet with and without the collector are plotted. This curve is reproduced in Fig. 26. It is seen

31

to compare favourably with the laminar length of the jet obtained using the larger tubing.

By observing Fig. 30, it is noted that the collector in the flow did not appreciably affect the laminar length. Hence, the collector was removed in the study of the delay times. The hot-wire was located exactly where the inlet of the collector would have been.

6.3   Determination of the Response Time

Figure 31 shows typical oscillograms for the on-off transition of the turbulence amplifier. The top signal was obtained by placing the hot-wire near the exit of the control jet tube and the bottom signal obtained by placing the hot-wire in the location, where the entrance to the collector would have been. Both these wires were aligned using micrometer screws. The control jet was placed normal to the supply jet as shown in Fig. 32. The distance downstream was measured from the edge of the control jet. This investigation was carried out for three control jet velocities and five different Reynolds number of the supply. The different delay times involved in a turbulence amplifier have already been defined in the introduction.

Figure 32 shows the variation in the delay time-laminar with distance downstream for each of the Reynolds

32

number of the supply. The control jet velocity was
maintained at 56.75 ft./sec. The delay time-laminar
as expected increases with distance from 0.4 m.sec.
to 1 m.sec. for the whole range of Reynolds numbers.
Also this delay time is less for higher Reynolds
number, for any distance downstream of the supply jet.

Figure 33 shows how the fall time varies with
distance downstream for a control jet velocity of 56.75
ft./sec. For Reynolds number of 3540 there is a
decrease in the fall time; for all other Reynolds numbers
there is an increase with distance downstream.

In Figures 34 and 36 the control jet velocity was
increased to 70 ft./sec. and 83 ft./sec. respectively.
This did not cause any appreciable change in the delay
time-laminar, from the values obtained for a control jet
velocity of 56.75 ft./sec.

For a control jet velocity of 70 ft./sec. and
83 ft./sec. the fall time was erratic at the higher
range of Reynolds number. This is shown in Fig. 35
and Fig. 37.

From Fig. 31 (a), (b), and (c) there seems to be
no vigorous turbulent fluctuations during the period
when the amplifier is turned off. The laminar nature
of the flow is still prevailent. In Fig. 31 (d) where

33

the Reynolds number is increased to 3050, turbulent fluctuations are very prominent. At Reynolds numbers higher than 3050 similar patterns were observed. All these photographic figures 31 (a) to (d) also show clearly the delay time-laminar. It is also observed that the fall time is approximately in the order of twice the delay time-laminar.

The delay time-turbulent and the rise time have already been defined in the introduction. From the trend in the delay time-turbulent as in Figs. 38, 39, and 40 it appears that this time is slightly longer than the delay time-laminar. With the highest value of the control jet velocity of 83 ft./sec. (Fig. 40), we notice a uniform pattern of the increase in delay time-turbulent with distance downstream for different Reynolds numbers of the supply jet. For this value of the control jet velocity we clearly see that the delay time-turbulent decreases with an increase in the Reynolds number of the supply for any particular distance downstream, except for the highest Reynolds numbers of supply of 3540 and 3820, the difference in delay time-turbulent for any particular distance was negligibly small.

The very appreciable rise time is observed in Figs. 38 to 40 when compared with the delay time-

34

turbulent. The rise time increases very sharply with distance in general. The effect that the control jet velocity had on this time could not be predicted due to the erratic nature of this transition as shown in these figures.

From this it is clear that for a turbulent stream to become laminar again requires that the turbulence decay sufficiently for the laminar jet to penetrate it. This penetration takes the form of an erratic and gradually increasing velocity, depending on how vigorous the turbulence is which must be penetrated and also on how stable the laminar stream is in attempting the penetration.

In the switch back to the 'ON' state, the turbulent fluctuations are prominent during the latter period of the transition (Figs. 41 (a) and (b)). This is the case for low Reynolds number of the supply jet where vigorous turbulence is absent. Fig. 41 (c) and (d) shows the switch 'ON' of the amplifier for the higher Reynolds number of the supply.

The control jet was now turned through 30° from its original position as shown in Fig. 42. There was no noticeable change in the delay time-laminar with the increase in the control jet velocity. The delay time-laminar increases with distance from 0.5 m.sec. to 1 m.sec. for the whole range of Reynold numbers of

35

the supply jet as shown in Figs. 42, 44 and 46. These results are similar to when the control jet strikes the main jet at right angles.

For a low control jet velocity of 56.75 ft./sec. (Fig. 43), the fall time increases with distance to a maximum value and then decreases. This is not the case for the highest Reynolds Number of 3820.

By increasing the control jet velocity, it would be difficult to ideally locate the collector to minimise the fall time for any particular Reynolds number of the supply jet. This is evident from Figs. 45 and 47.

Turning the control jet through 30°, the supply jet appeared laminar at low Reynolds number (Fig. 48 (a)). Increasing the Reynolds number of the supply jet beyond 3050, results in intense turbulent fluctuations during the 'OFF' state of the amplifier. The same phenomena were observed with the control jet in the normal position.

Turning the control jet through 30° from its original position, did not greatly affect the delay time-turbulent. The decrease in the delay time-turbulent with increasing Reynolds numbers of the supply jet is evident from Fig. 49, Fig. 50, and Fig. 51. This time is longer than in the case of delay time-laminar especially at lower Reynolds number of the supply jet and also at greater distances downstream.

36

For the control jet at 30°, the rise time increasing with distance follows a more regular pattern than when the control jet was in its normal position.

The supply jet appearing laminar with the introduction of the control jet could be explained as due to the laminar vortices being distorted, without collapsing. They regain their symmetry when the turbulence amplifier switches back to the stable laminar state.

By interchanging the connections of the leads between the two hot-wire anemometers used, a check on the response times of these instruments was made. The times were quite repeatable as seen in Fig. 53, showing that the performance of the two instruments were identical.

Hayes (8) used the center-line mean-velocity of the supply jet to calculate the delay time-laminar. He investigated this time using a theory based on a potential core region (constant mean center-line velocity) in the supply jet. From Fig. 22 it is observed that the mean center-line velocity does not remain constant even for short distances downstream. Hence, there is disagreement between the present findings and those assumed by Hayes.

Using the curve for Reynolds number of 3050 obtained from Fig. 22 and taking an average of the

37

decrease in the center-line velocity between the two locations, the time in m.secs. could be computed. Several points could be obtained in this way (Fig. 54 lowest curve). The experimental curve of the delay time-laminar for Reynolds number of 3050 and control jet velocity 70 ft./sec. is plotted on the same graph with the delay time-laminar calculated from the mean-velocity along the center-line of the laminar jet. From this it is obvious that the delay time-laminar in a turbulence amplifier does not depend entirely on the mean-velocity of the supply jet. By extending the experimental curve, the delay time not associated with the mean jet velocity could be estimated.

The next approach was to investigate the turbulent jet. The control jet velocity was kept continuous at 70 ft./sec. Considering the curve of the center-line mean-velocity of the turbulent jet for Reynolds number of 3050 as shown in Fig. 27, the delay time could be computed by integrating between suitable limits of x. The upper-most curve in Fig. 54 shows this delay time. From the nature of this curve it is obvious that the experimental curve obtained is closer to the case when the delay time-laminar was calculated from the mean-velocity along the center-line of the laminar supply jet. The longer time obtained by experiment could be explained due to the presence of the turbulent front having its influence on the laminar portion of the flow.

38

7. CONCLUSIONS

7.1   Jet Study

1. For Reynolds number of 3050, the 0.25" diameter jet appeared quite symmetrical in the laminar region. This could not be said about the jet in the turbulent region because of the scatter of the points.

2. For the range of Reynolds numbers 2342 to 5000 which was studied here, the center-line mean-velocity decreased slightly in the downstream direction. This agrees with the experimental work of Boyd (6), but is contrary to the assumption made by Hayes (8) of the existance of a potential core region.

3. With increasing Reynolds numbers, the maximum axial turbulence intensity near the transition region increased, the peaks of the curves for the higher Reynolds numbers were closer to the exit of the tube.

4. The radial turbulence intensity distribution in the transition region of the jet was characterized by the presence of local minima at the center-line.

5. The initiation of turbulence appeared to take place near the edge of the jet, in the region of high mean-velocity gradients.

6. In the early part of the turbulent region,

39

this local minimum in the turbulence intensity gradually
disappeared and was replaced by a local maximum at the
center-line. This was probably due to the coalescence
of the ring vortices, characteristic of vortex decay,
as suggested by Boyd (6).

7. The uniform radial turbulence intensity in
the central region of the jet for high x/d, was charact-
eristic of a fully developed turbulent jet flow.

8. The laminar length of the jet between Reynolds
number of 1000 and 11,000 was determined. The experimental
points fell close to the straight line.

$$L/d = -0.00185Re+22.33$$

7.2   Response Time of the Turbulence Amplifier

The experimental findings in a turbulence-type
amplifier of this particular configuration are as
follows:-

1. The delay time-laminar increased with distance
from 0.4 m.secs. to 1 m.secs. for the whole range of
Reynolds number of the supply jet.

2. Increasing the control jet velocity or turn-
ing the control jet through 30° from its original normal
position showed no appreciable change in the delay time-
laminar.

3. Delay time-laminar was shorter for higher
supply Reynolds numbers for any given distance downstream
of the supply jet.

40

4. Operating the turbulence amplifier at high Reynolds numbers and high control jet velocities resulted in an erratic nature of the fall time.

5. The turbulence was very prominent on switch-off with the higher Reynolds numbers of the supply jet irrespective of any control jet velocity. At lower Reynolds numbers, turbulence could not be achieved, the laminar nature of the jet still prevailed. The same conditions were noticed even with the control jet in its 30° position.

6. The delay time-turbulent was slightly longer than the delay time-laminar, especially at lower Reynolds numbers of the supply jet and at greater distances downstream.

7. The delay time-turbulent increased with distance downstream for different Reynolds numbers of the supply jet. Turning the control jet by 30° did not greatly effect this time.

8. The shorter delay time-turbulent with an increase in the Reynolds number of the supply for any particular distance downstream was very evident especially at the highest control jet velocity of 83 ft./sec. A similar affect on the time was found by turning the control jet through 30°.

9. Among all the times, the rise time was most appreciable. This is because for a turbulent stream

41

to become laminar again requires that the turbulence decay enough for the laminar jet to penetrate it.

10. The rise time in general increased very sharply with distance. This time followed a more regular pattern when the control jet was turned through 30°.

11. For low Reynolds numbers of the supply jet, turbulent fluctuations were prominent during the latter period of reverse transition back to the laminar state. For higher Reynolds numbers of the supply, the intense turbulence in the OFF state of the amplifier was followed by an erratic nature of the transition. These same conditions were also noticed when the control jet was in its other position.

12. Hayes (8) investigated the delay time-laminar using the center-line mean-velocity and a potential core region in the supply jet. No such region could be recognized in this experimental investigation, which resulted in disagreement on the delay time-laminar as computed by Hayes.

13. The delay time-laminar did not depend entirely on the velocity of the supply jet. This was seen when comparing the experimental data with the curve obtained by computing this time based on the mean center-line velocity in the laminar jet. The longer time obtained by experiment could be explained due to the fact

42

that the turbulent front had an influence on the laminar portion of the flow when the control jet was introduced.

14. The delay time-laminar calculated from the curve of the center-line mean-velocities in the turbulent jet showed absolutely no agreement with the measured values obtained.

BIBLIOGRAPHY

(1) Andrade, C., and Tsien, L.: "The velocity dist-
    ribution in a liquid-into-liquid jet", Proceed-
    ings of the Physical Society, London, No. 49,
    (1937).

(2) Auger, R.N.: "Pneumatic turbulence amplifier",
    Instruments and control systems, No. 3, (1965),
    pp. 129-133.

(3) Auger, R.N.: "The turbulence amplifier in control
    systems", Proceedings of the fluid amplification
    symposium, Harry Diamond Laboratories, Vol. II,
    (May, 1964), p. 261.

(4) Batchelor, G.K., and Gill, A.E.: "Analysis of
    the stability of axisymmetric jets", Journal of
    Fluid Mechanics, Vol. 14, (1962), pp. 529-551.

(5) Becker, H.A., and Massaro, T.A.: "Vortex evolut-
    ion in a round jet", Journal of Fluid Mechanics,
    Vol. 31, (1968), pp. 435-447.

(6) Boyd, M.A.: "An experimental investigation of the
    effects of transverse secondary flow on the lam-
    inar-turbulent transition of a free axisymmetric
    jet", Thesis submitted for the degree of Master
    of Science, Department of Mechanical Engineering,
    Auburn University, Alabama, (1965).

(7) Gradetsky, V., and Dmitriev, V.: "Some design
    problems of the fluidic digital elements and
    devices", Third Cranfield Fluidics Conference,
    (May, 1968).

(8) Hayes, W.: "Static and dynamic performance char-
    acteristics of fluidic turbulence amplifiers",
    Laboratory technical report LTR-CS-9, (1969),
    Division of Mechanical Engineering, Control
    Systems Laboratory, National Research Council of
    Canada.

(9) Hinze, J.O.: "Turbulence - An introduction to its
    mechanism and theory", McGraw-Hill, New York, (1959).

44

(10) Kirschner, J.: "Fluid amplifiers", McGraw-Hill, New York, (1966).

(11) Langhaar, H.L.: "Steady flow in the transition length of a straight tube", Journal of Applied Mechanics, (June, 1942), pp. A-55 to A-58.

(12) Marsters, G.F.: "Some observations on the transition to turbulence in small, unconfined free jets", Report No. 1-69, (October, 1969), Department of Mechanical Engineering, Queen's University at Kingston.

(13) McKenzie, C.P., and Wall, D.B.: "Transition from laminar to turbulence in submerged and bounded jets", Fluid Amplifier Associates, Ann Arbor, Fluidics Quarterly 4, (1968), pp. 38-47.

(14) McNaughton, K.J., and Sinclair, C.G.: "Submerged jets in short cylindrical flow vessels", Journal of Fluid Mechanics, Vol. 25, (1966), pp. 367-375.

(15) Pai, Shih - I.: "Fluid dynamics of jets", D. Van Nostrand Company, Inc., (1954).

(16) Reynolds, A.J.: "Observation of a liquid-into-liquid jet", Journal of Fluid Mechanics, Vol. 14, (1962), pp. 552-556.

(17) Rosenhead, L.: "Laminar Boundary Layers", Oxford and Clarendon Press, (1963).

(18) Sato, H.: "The stability and transition of a two-dimensional jet", Journal of Applied Mechanics, Vol. 7, Part 1, (1960), p. 53.

(19) Schlichting, H.: "Boundary-Layer theory", McGraw-Hill Book Company, Inc., Sixth Edition, (1968).

(20) Siwoff, F.: "Improvement of the static and dynamic behaviour of the turbulence amplifier by inbuilding of an edge over the distance between the emitter and the collector", Third Cranfield Fluidics Conference, British Hydromechanical Research Association, Paper H2, (1968).

(21) Squire, H.B.: "The round laminar jet", Quarterly Journal of Mechanics and Applied Mathematics, Vol. 4, (1951), pp. 321-329.

45

(22) Wille, R.: "Growth of velocity fluctuations lead-
ing to turbulence in free shear flow", Technical
Report AD418294, (1963).

46

APPENDIX A

Manufacturers	Components	Model	Specifications
Dollinger Corporation Rochester, New York	Pipe-line filter	CPHB-14938-4D-50	———
H.O. Trerice Co. Detroit, Michigan	Pressure regulator	982 X C	Maximum inlet pressure = 250 p.s.i.
H.O. Trerice Co.	Pressure gauge		Range 0 to 100 p.s.i.
Pitney Bowes, Inc. Stamford, Conn.	Fluidic filter	522-58	Particles removed:- 1 micron or larger
Moore Products Co. Spring House, Pa.	Moore Pressure Regulator 1	40 - 2	Maximum supply pressure = 25 p.s.i.
	Moore Pressure Regulator 2	40 - 7	Maximum supply pressure = 50 p.s.i.
	Moore Pressure Gauge 1	7342 - 1	Range 0 to 50" water
	Moore Pressure Gauge 2	7266 - 1	Range 0 to 200" water
Hoke Incorporated Cresshill, N.J.	Needle valves	1335 G2B 1^0 stem	provided with micrometer vernier handle to meter the flow with ultra fine control
Roger Gilmont Instruments, Inc. Greatneck, N.Y.	Spherical float flowmeter	F 1300	Range 0 to 25 cu.ft./hr.

47

APPENDIX B

The Hot-Wire Anemometer

This instrument is widely used in the investigation of turbulent flow. If an electrically heated wire is placed in an air stream, it will be cooled, hence causing a resistance change. The amount of this change can be interpreted as a measure of the fluid velocity. Fundamentally what is measured is the power that is required to keep the temperature constant. Due to its accuracy and high response, the constant temperature anemometer was used. The detecting element of the hot-wire anemometer consists of a platinum plated tungsten wire 0.005 m.m. diameter and 1 m.m. long welded on to two supports. The wire forms one arm of a Wheatstone bridge circuit. The mean flow velocity $\bar{U}$ is indicated by the bridge d.c. voltage and velocity fluctuations are measured by the r.m.s. value of the corresponding bridge voltage fluctuations.

To express the d.c. voltage in terms of the mean velocity, the probe must be calibrated against a reliable measuring instrument such as a Pitot tube (Appendix C).

When a fluid passes over a heated cylinder, the rate of heat transfer is given by:

$$Q = m\sqrt{\bar{U}} + C \qquad \qquad (1)$$

48

If the cylinder is electrically heated, the power input to the cylinder equals the heat transferred.

$$I^2R = Q \qquad\qquad\text{(2)}$$

where   I is the probe current

and   R is the probe resistance

$$I^2R = m\sqrt{\overline{U}} + C$$

$$\frac{\overline{E}^2}{R} = m\sqrt{\overline{U}} + C$$

when $U = 0$, $C = \dfrac{E_0^2}{R}$

$$\therefore\quad \frac{\overline{E}^2}{R} = m\sqrt{\overline{U}} + \frac{\overline{E}_0^2}{R}$$

This relationship is known as King's law.

$$\therefore\quad \sqrt{\overline{U}} = \frac{\overline{E}^2 - \overline{E}_0^2}{mR}$$

$$= \frac{\overline{E}^2 - \overline{E}_0^2}{M} \qquad\qquad\text{(3)}$$

where $\overline{U}$ = mean flow velocity

$M = mR$ = slope of the E^2 vs $\sqrt{\overline{U}}$ calibration curve
(Appendix B)

$\overline{E}$ = bridge d.c. voltage

$\overline{E}_0$ = bridge d.c. voltage at zero flow velocity

In order to find an expression for the local turbulence intensity we shall start with the basic equation:

49

$$\overline{E}^2 = M\overline{U}^a + C$$

$$\therefore \quad (\overline{E} + e')^2 = M(\overline{U} + u')^a + C$$

$$\overline{E}^2 + e'^2 + 2e'\overline{E} = M\overline{U}^a \left(1 + \frac{u'}{\overline{U}}\right)^a + C$$

$$\overline{E}^2 + e'^2 + 2e'\overline{E} = M\overline{U}^a \left[1 + \frac{au'}{\overline{U}} + \frac{a(a-1)}{2!}\left(\frac{u'}{\overline{U}}\right)^2 + \ldots\right] + C$$

Dividing throughout by $\overline{E}^2$

$$1 + \frac{e'^2}{\overline{E}^2} + 2\frac{e'}{\overline{E}} = \frac{M\overline{U}^a}{\overline{E}^2}\left[1 + \frac{au'}{\overline{U}} + \frac{a(a-1)}{2!}\left(\frac{u'}{\overline{U}}\right)^2 + \ldots\right] + \frac{C}{\overline{E}^2}$$

Since $\frac{e'}{\overline{E}} \ll 1$ and $\frac{u'}{\overline{U}} \ll 1,$

$$\therefore \quad 1 + 2\frac{e'}{\overline{E}} = \frac{M\overline{U}^a}{\overline{E}^2}\left[1 + \frac{au'}{\overline{U}} + \ldots\ldots\right] + \frac{C}{\overline{E}^2}$$

$$= \frac{1}{\overline{E}^2}\left[M\overline{U}^a + au'M\overline{U}^{a-1} + C\right]$$

$$= \frac{1}{\overline{E}^2}\left[\overline{E}^2 + au'M\overline{U}^{a-1}\right]$$

$$\therefore \quad e' = \frac{aM\overline{U}^{a-1}}{2\overline{E}} \cdot u'$$

To find the value of $\overline{U}^{a-1}$ starting with the basic equation

$$\overline{E}^2 = M\overline{U}^a + C$$

$$\therefore \quad \frac{\overline{E}^2 - C}{M} = \overline{U}^a$$

50

$$\left(\frac{\overline{E}^2 - C}{M}\right)^{\frac{a-1}{a}} = \left(\overline{U}^a\right)^{\frac{a-1}{a}}$$

$$\overline{U}^{a-1} = \left(\frac{\overline{E}^2 - C}{M}\right)^{\frac{a-1}{a}}$$

$$e' = \frac{aM}{2\overline{E}} \left(\frac{\overline{E}^2 - C}{M}\right)^{\frac{a-1}{a}} \times u'$$

$$= S \times u'$$

where S = sensitivity = $\dfrac{aM}{2\overline{E}} \left(\dfrac{\overline{E}^2 - C}{M}\right)^{\frac{a-1}{a}}$

$$\sqrt{\overline{e'^2}} = S\sqrt{\overline{u'^2}} \qquad\qquad\qquad\qquad (4)$$

In the above: a = exponent of velocity in the hot-wire

response equation.

M = slope of the calibration curve.

C = y-intercept of the calibration curve.

$\overline{E}$ = bridge d.c. voltage.

$\sqrt{\overline{e'^2}}$ = r.m.s. value of fluctuating voltage.

$\sqrt{\overline{u'^2}}$ = r.m.s. value of fluctuating velocity

in the x direction.

Equations (3) and (4) were used in the plots of the
turbulence intensity and mean velocity profiles in the
jet.

51

APPENDIX C

Calibration of the Hot-Wire

The DISA constant temperature hot-wire anemometer 55A01 was taken to the wind tunnel where the calibration was carried out. The wind tunnel was chosen because of the low level of turbulence prevailing. The hot-wire probe was exposed to the flow in the wind tunnel. A pitot static probe stationed close to the hot-wire was connected to a Wilhelm Lambrecht slanting tube micromanometer No. 655 measuring the dynamic pressure, hence giving the mean velocity of flow. Flow velocity was varied using the fan regulator. The anemometer d.c. voltage and the micromanometer reading was noted for each flow velocity. The calibration curve for the hot-wire used is shown in Fig. 55. Calibration facilities were not available for high velocities.

52

APPENDIX D

Calibration of the Control Jet

To determine the volume rate of flow at the outlet of the control jet, the tubes were joined together in the space which was occupied by the shutter blades. The rotameter (ROTA L10 400-6185 accuracy = $\pm 2\%$ calibrated using the precision wet test meter) placed on the inlet side measured the quantity of flow. The hot-wire was placed at the outlet of the 0.054" i.d. tube. Micrometer screws were used to align the wire. The d.c. voltage was read from the constant temperature anemometer to which this probe was connected. A calibration curve was plotted between d.c. reading (volts) and flow rate (cu.ft./hr.) (Fig. 56). The exact location of the hot-wire was noted before carrying out the calibration of the control jet. Care was taken to make sure that the wire was in this same location every time the experiment was carried out.

53

Calibration of the Roger Gilmont F1300 Spherical Float Flowmeter and Rotameter ROTA L10 400-6185.

In the calibration of the above two rotameters, a precision wet test meter was used. It was installed between the needle valve regulating the flow and the rotameter being calibrated. The atmospheric temperature and pressure were noted. The accuracy of the precision wet test meter calibrated by the company is within ½%.

The calibration curve of these two rotameters is shown in Fig. 57 and Fig. 58.
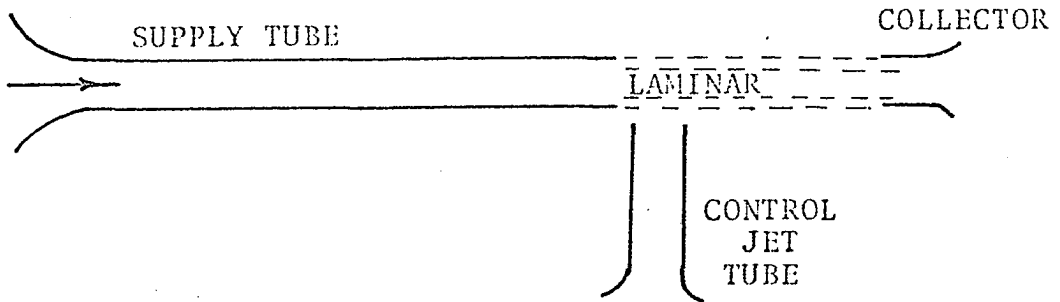
Fig. 1: The turbulence amplifier with no control input.

(The laminar flow is directed into the collector.

The amplifier is 'ON')
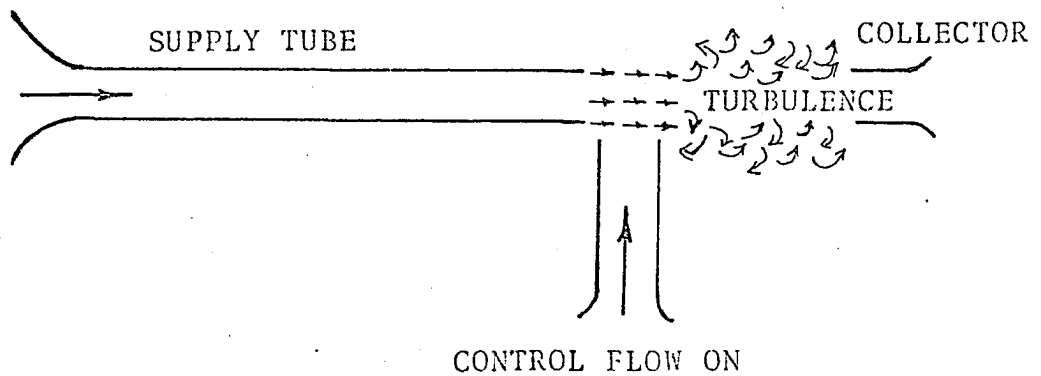
Fig. 2: The turbulence amplifier with control input.

(Introduction of the control jet results in

intense turbulence in the amplifier. The

amplifier is 'OFF')
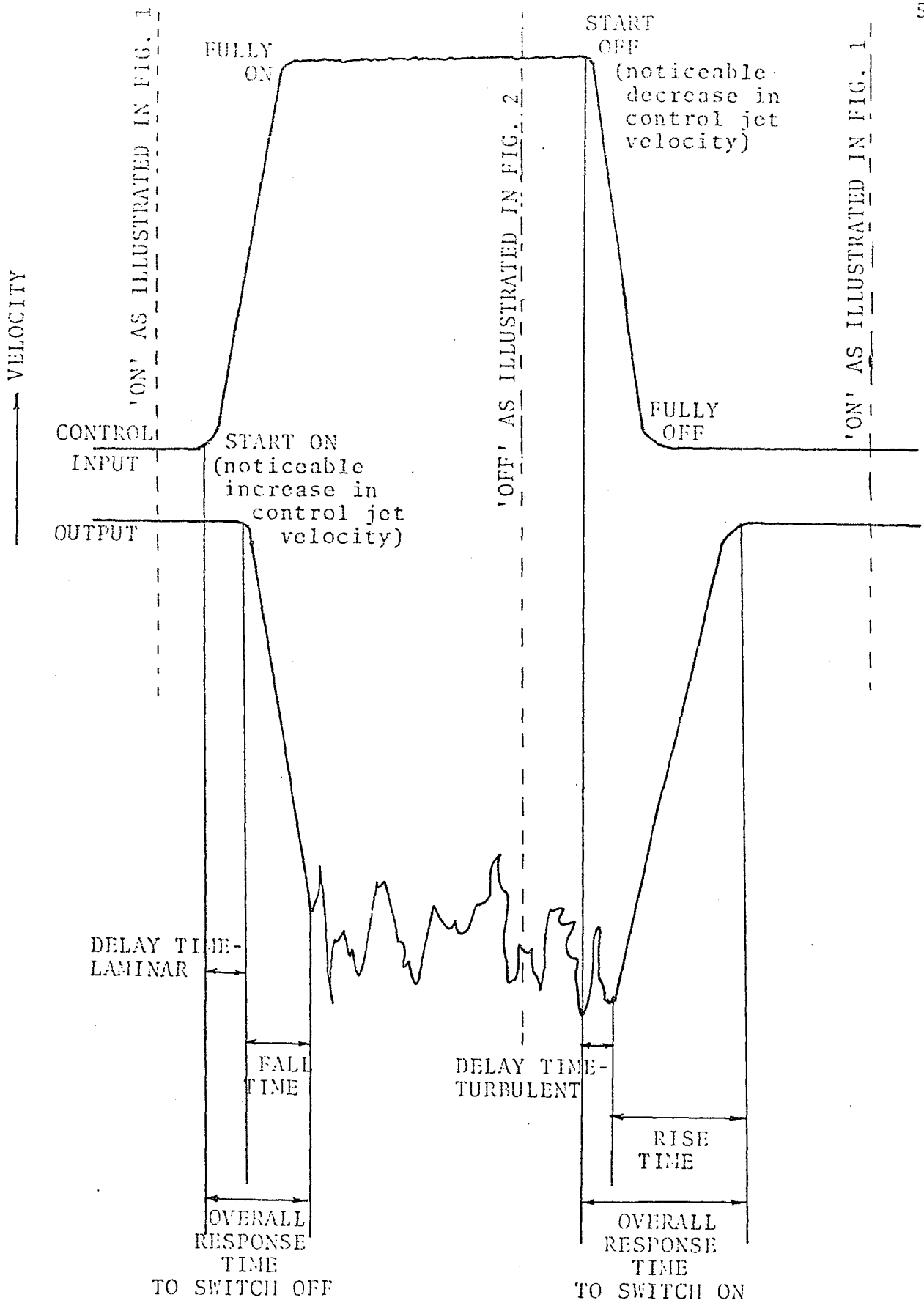
Fig. 3: A typical oscillogram of the signals from the
two probes.

57
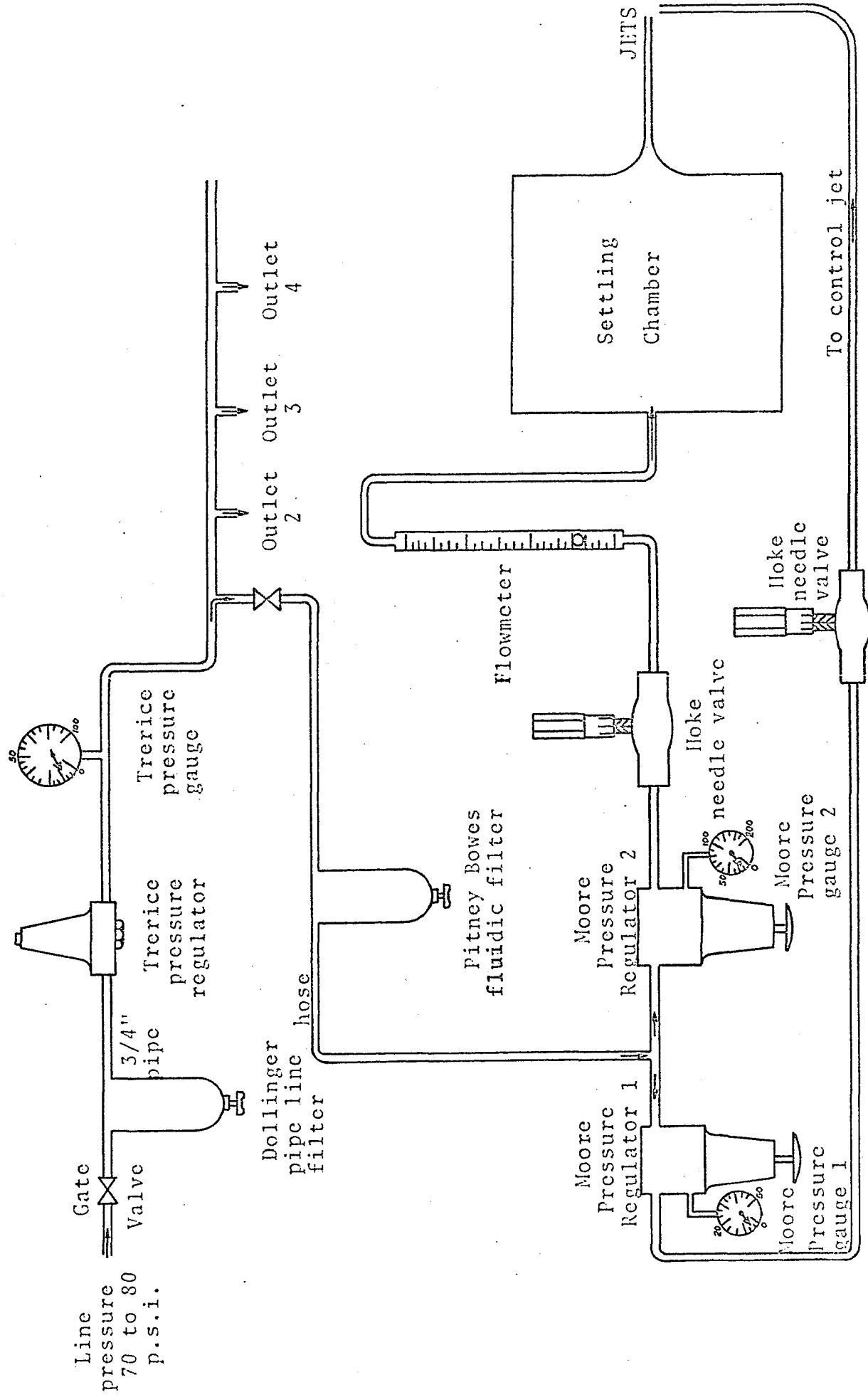
Fig. 4 : Details of air supply, (filtering, measurement and control)

58
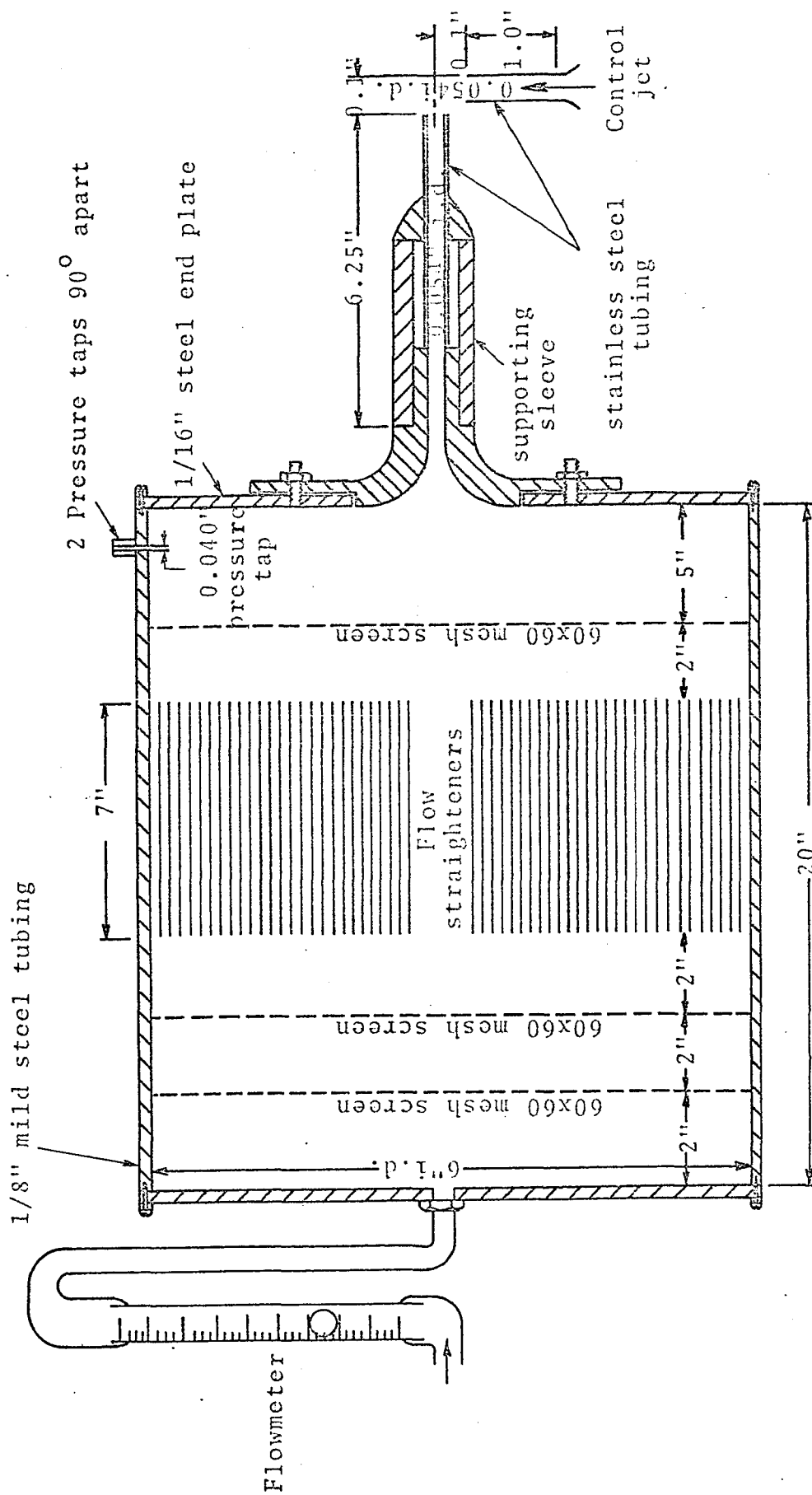
Fig. 5 : Details of the settling chamber and jets
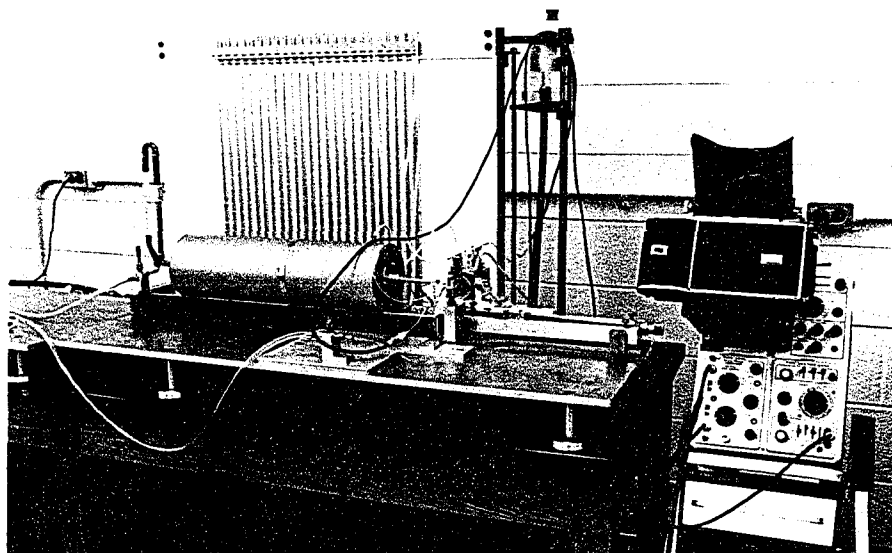
Fig. 6: Overall view of the apparatus.
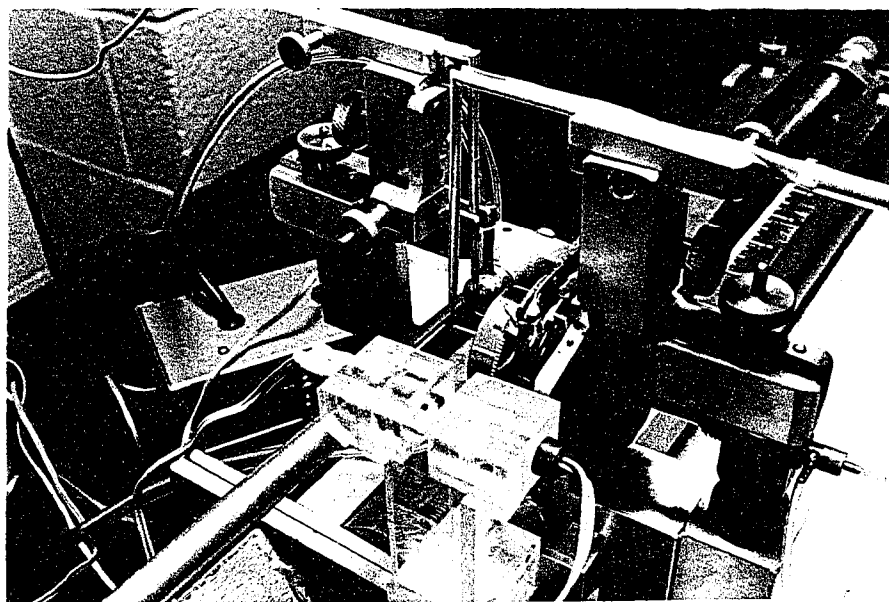
Fig. 7: Close up view of the apparatus.
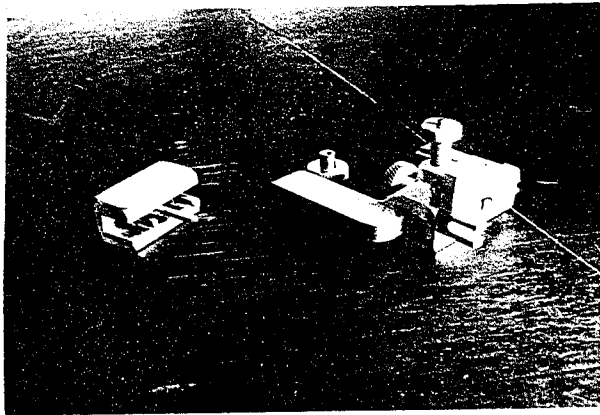
Fig. 8: Parts of the micrometer-
screw assembly.
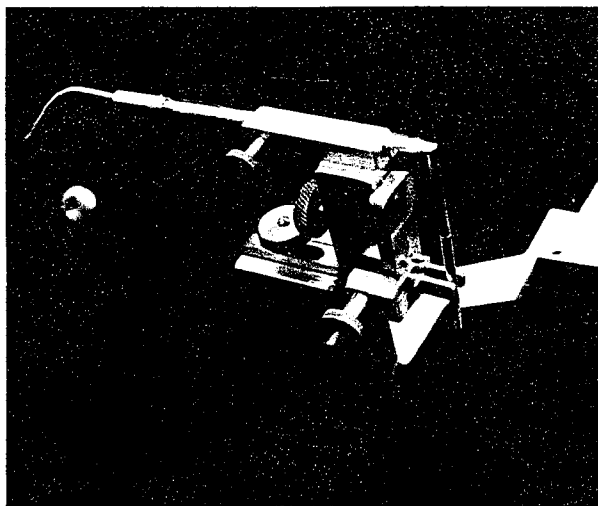
Fig. 9: The hot-wire probe
fixed in position.

Fig. 10: Bell-mouth entrance
to the supply tube.
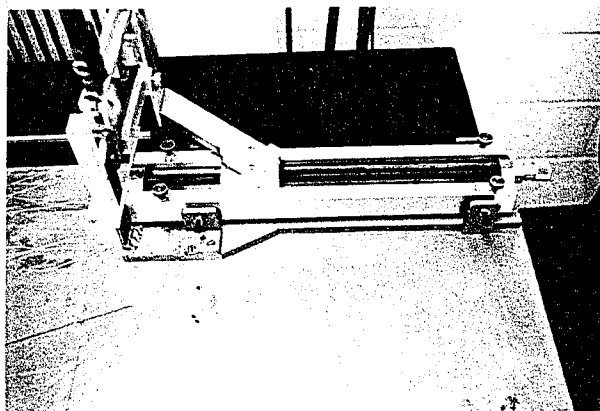
Fig. 11: Horizontal traver-
sing mechanism, also
showing the levelling
screws.

Fig. 13: Traversing horizontally
across the large jet.

Fig. 12: Traversing vertically
across the large jet.
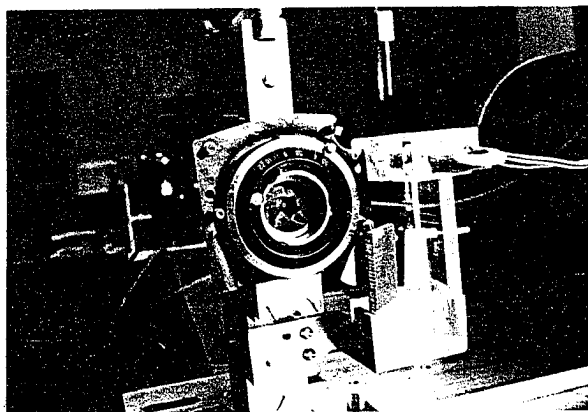
Fig. 14: Camera shutter mech-
anism used as valve
on control jet.
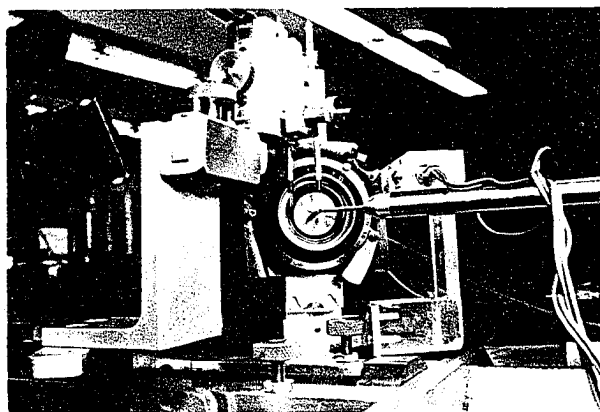
Fig. 15: The control jet
located at 30° to
the supply jet.
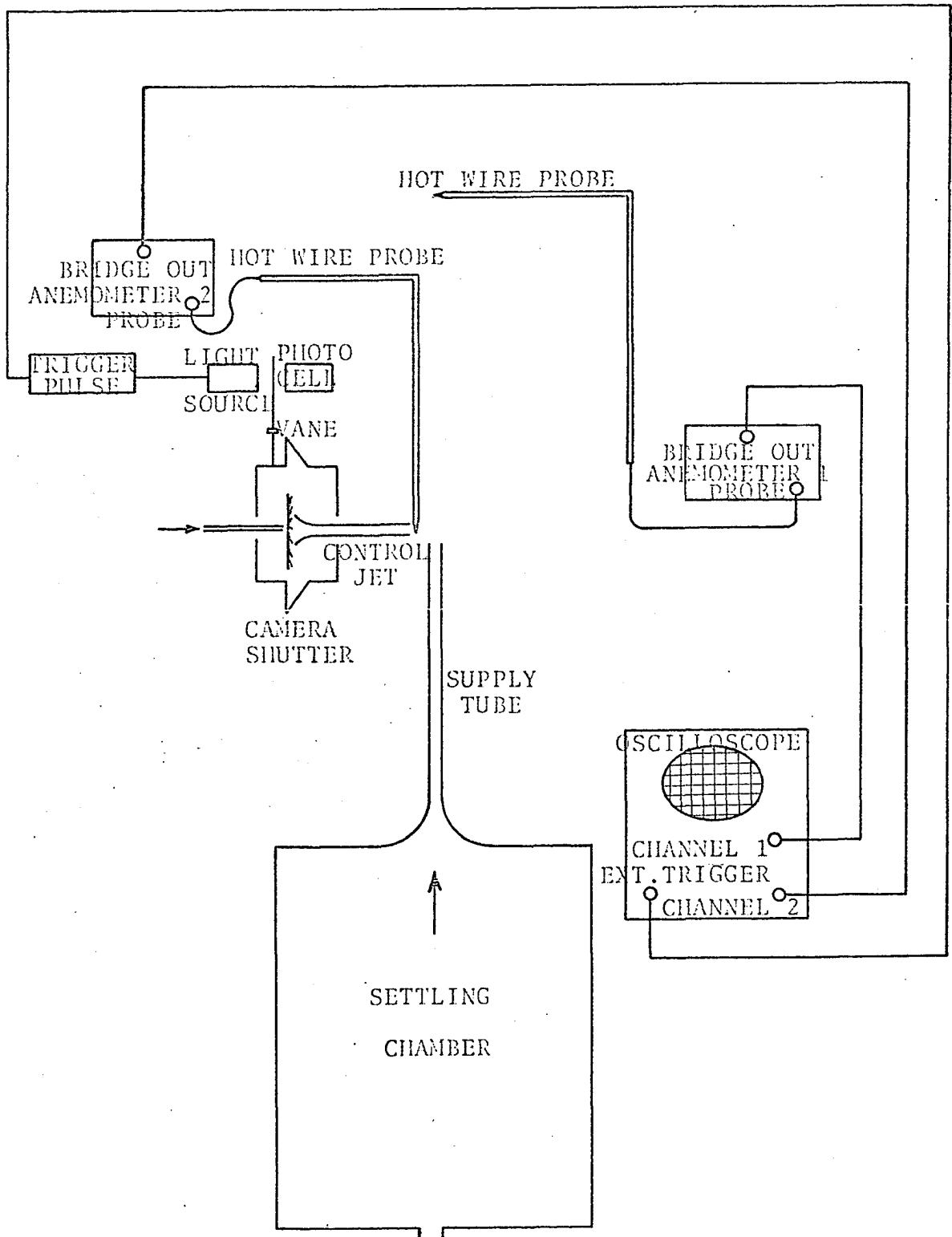
Fig. 16 : Details of the electrical connections

$$\text{Re}_s = 2000$$

$$d = 0.25"$$

○ Experimental points obtained

□ Points obtained using the equation of a parabola
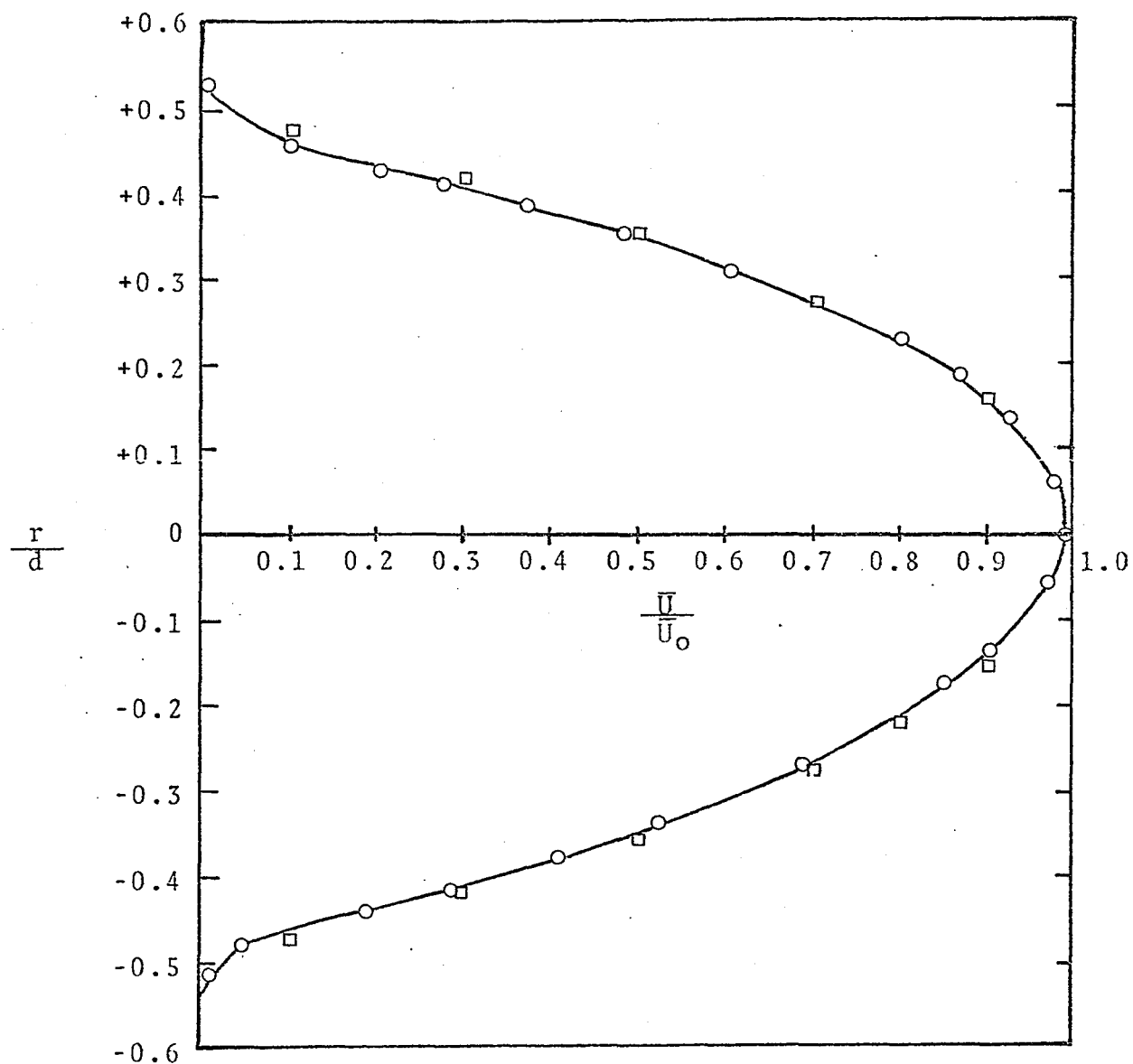
Fig. 17: Velocity distribution at exit of
tube   (x/d = 0.1)

△ d = 0.054"

○ d = 0.25"

$\dfrac{\overline{U}}{U_O} = 1$

$\mathrm{Re}_s = 2342$

$\dfrac{r}{d}$

+1.4
+1.2
+1.0
+0.8
+0.6
+0.4
+0.2
0
-0.2
-0.4
-0.6
-0.8
-1.0
-1.2
-1.4

x/d=4   x/d=8   x/d=12
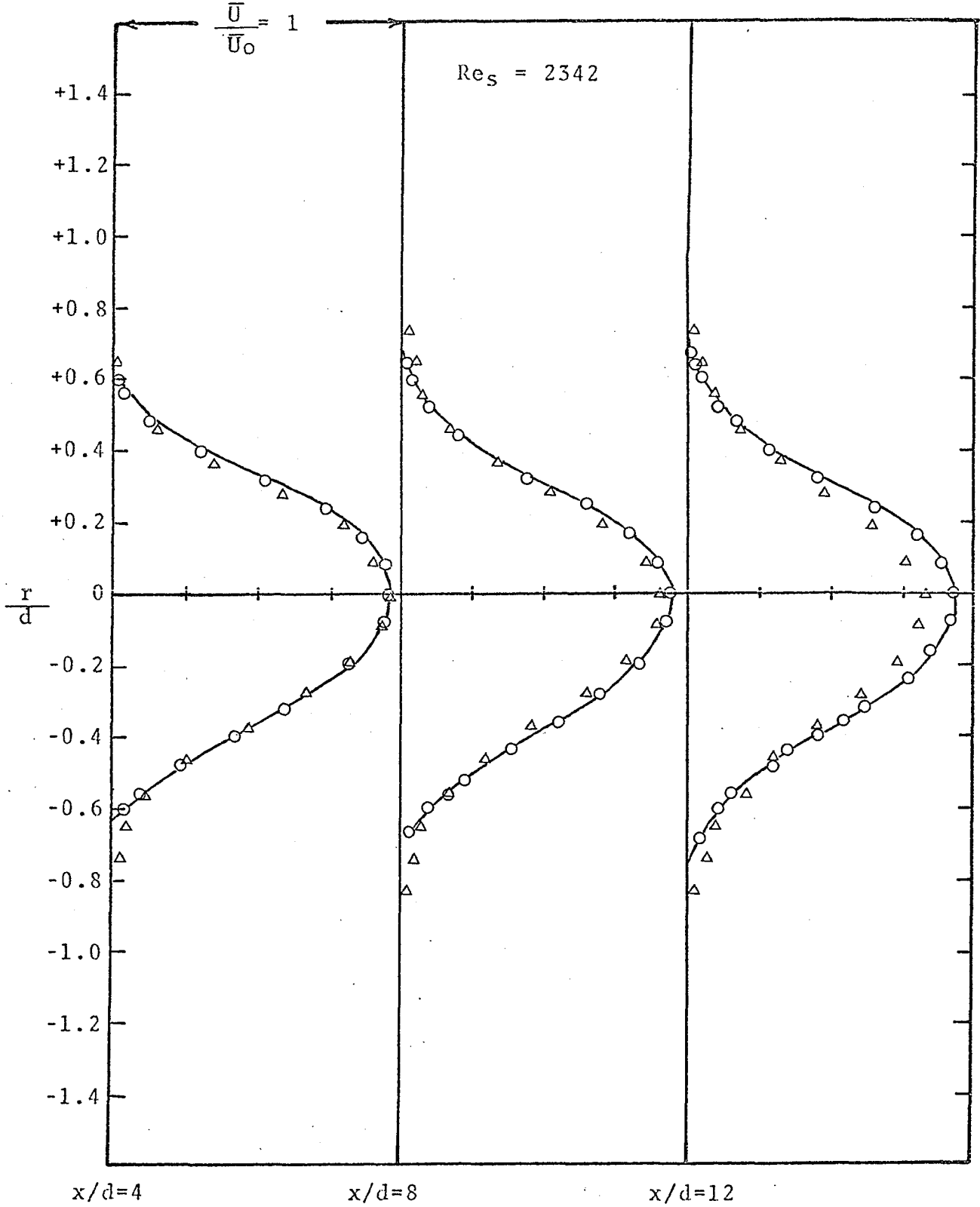
Fig. 18: Velocity distribution at different axial stations.

$\dfrac{r}{d}$

$Re_s = 2342$

x/d=16   x/d=20   x/d=24
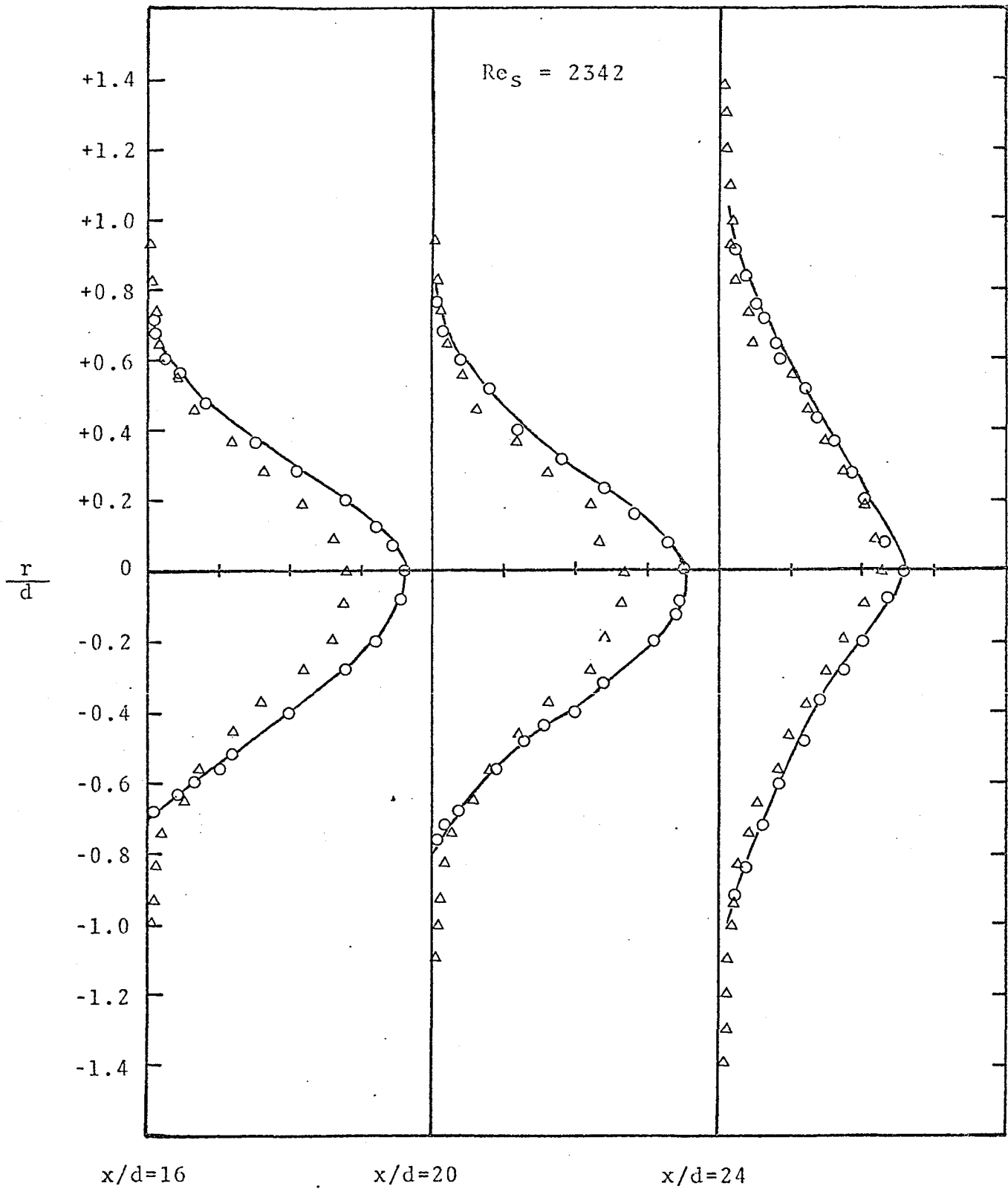
Fig. 19: Velocity distribution continued

Fig. 20: Velocity distribution at different axial stations.

Fig. 21: Velocity distribution continued

d = 0.25"
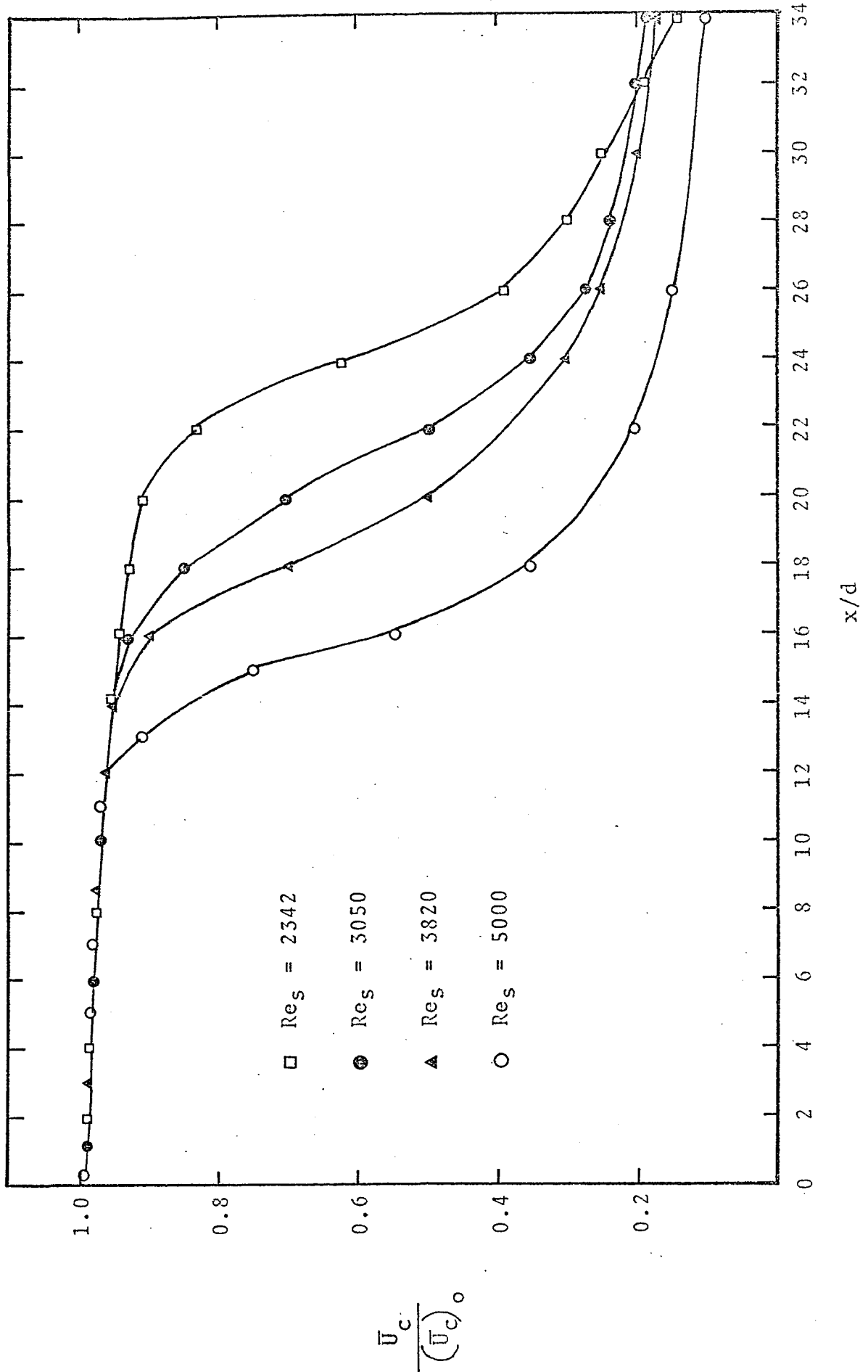
Fig. 22: Center-line mean-velocity distribution.

$\dfrac{\bar{U}_c}{(\bar{U}_c)_o}$

x/d

□ Re$_s$ = 2342

⬤ Re$_s$ = 3050

▲ Re$_s$ = 3820

◯ Re$_s$ = 5000
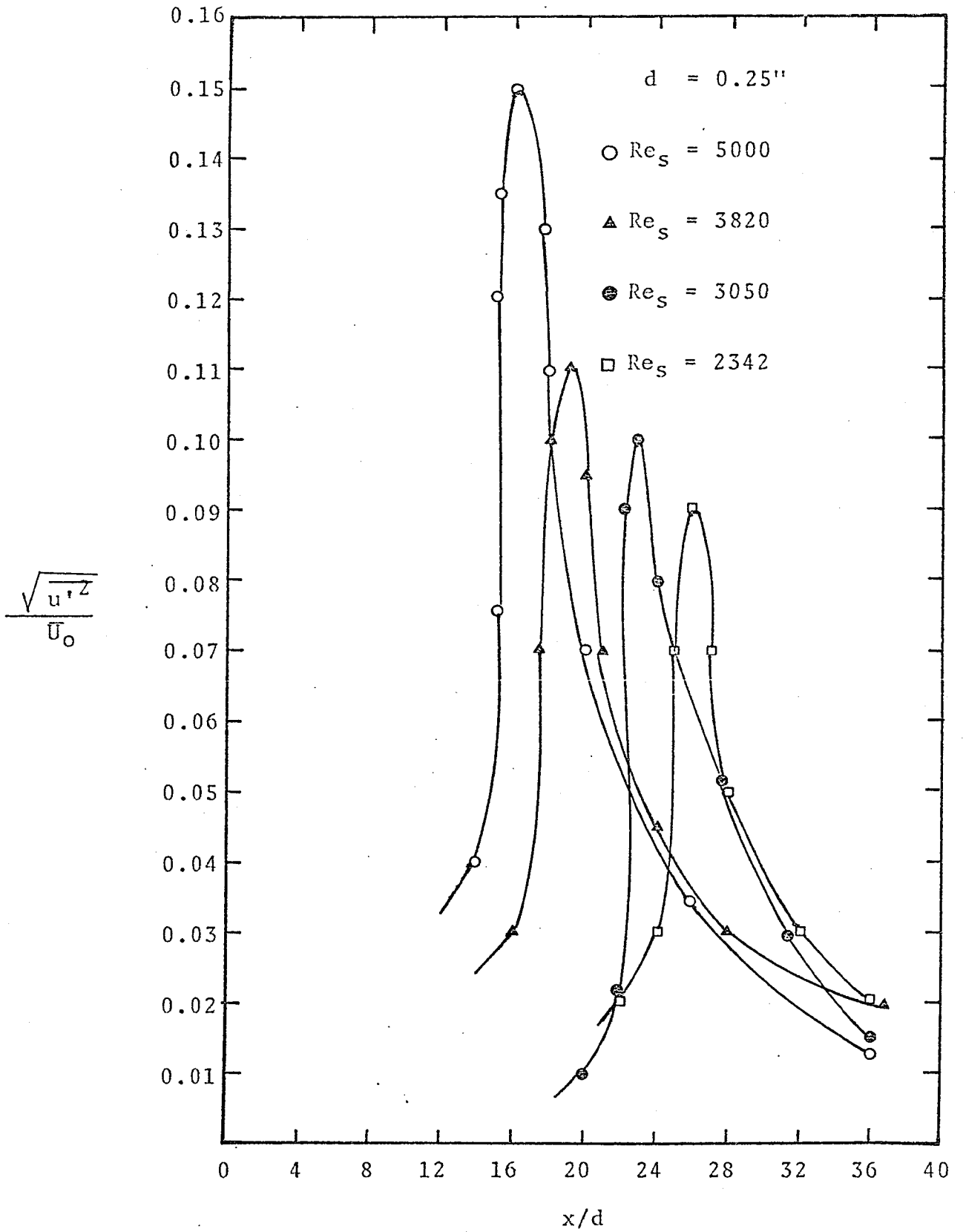
Fig. 23: Intensity of turbulence along the jet center-line.

d = 0.25"

Re_s = 3050

⊗ x/d = 0.1
□ x/d = 8
○ x/d = 12
△ x/d = 16
⬤ x/d = 18
▽ x/d = 22
▲ x/d = 24
⊙ x/d = 26
▼ x/d = 28

$\frac{r}{d}$

$\frac{\sqrt{\overline{u'^2}}}{\overline{U}_o}$
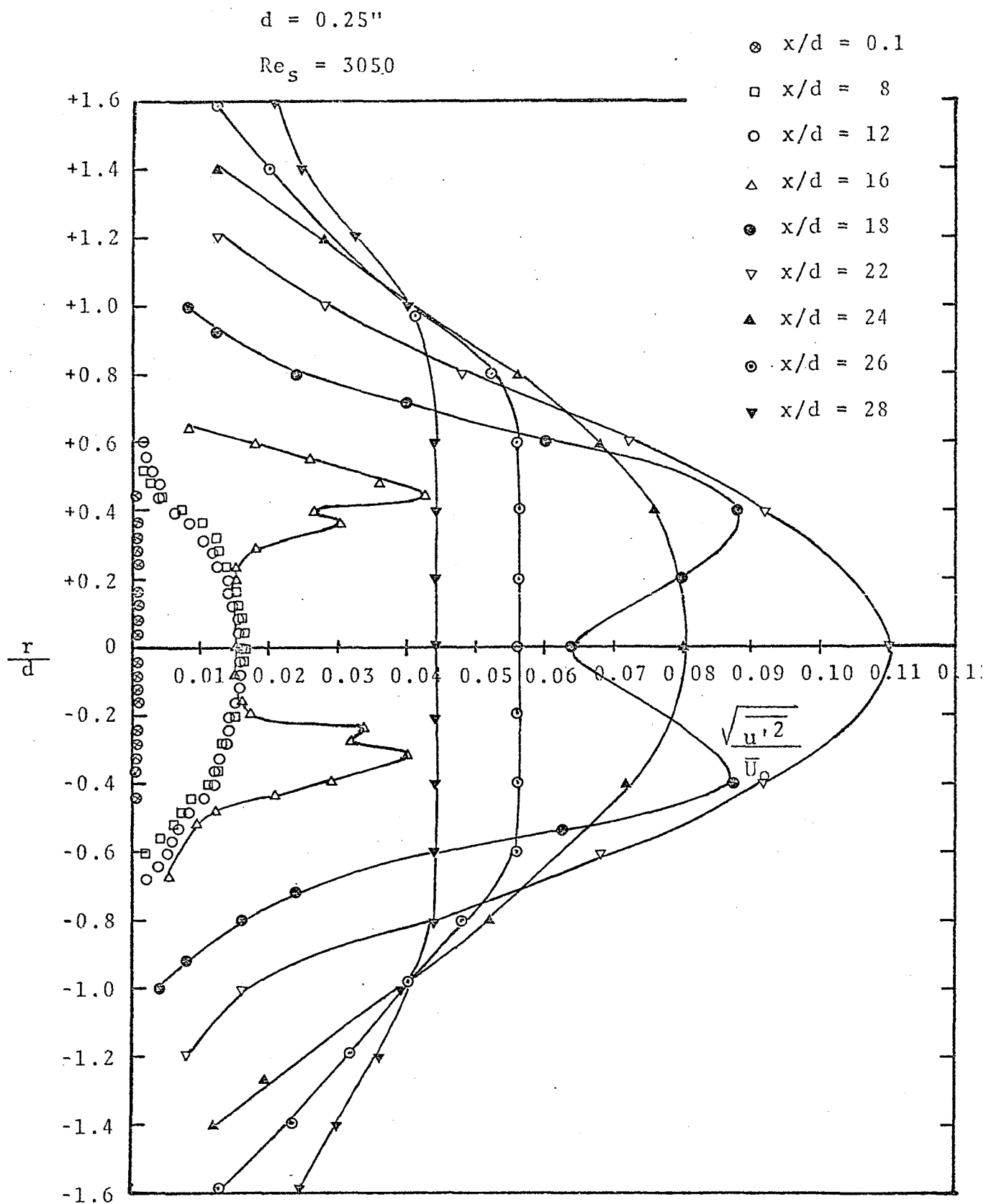
Fig. 24 : Turbulence intensity profiles

$$\frac{L}{d} = -0.00185Re + 22.33$$

d = 0.25"
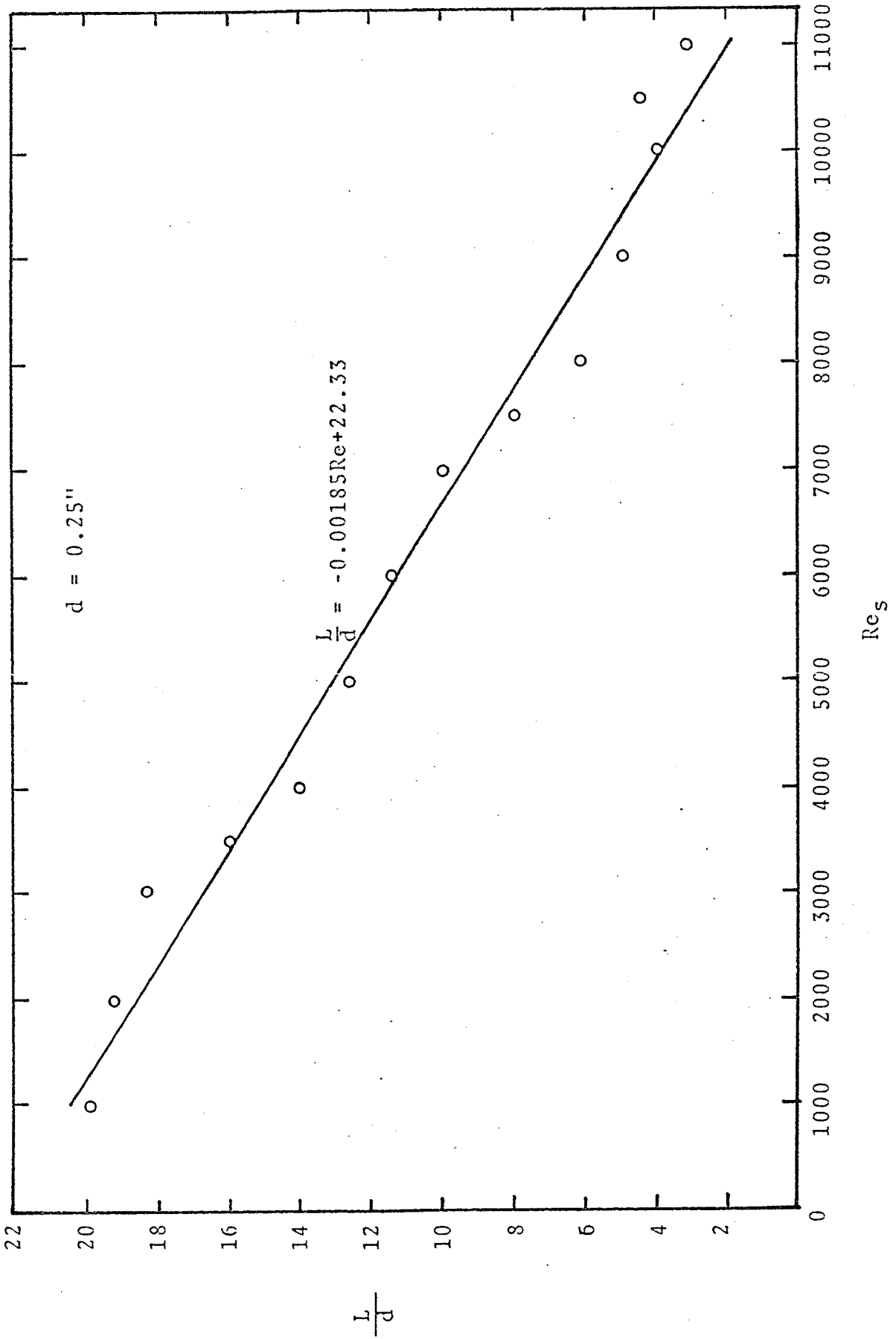
Fig. 25: Downstream distance of the transition point over a wide range of Reynolds numbers.
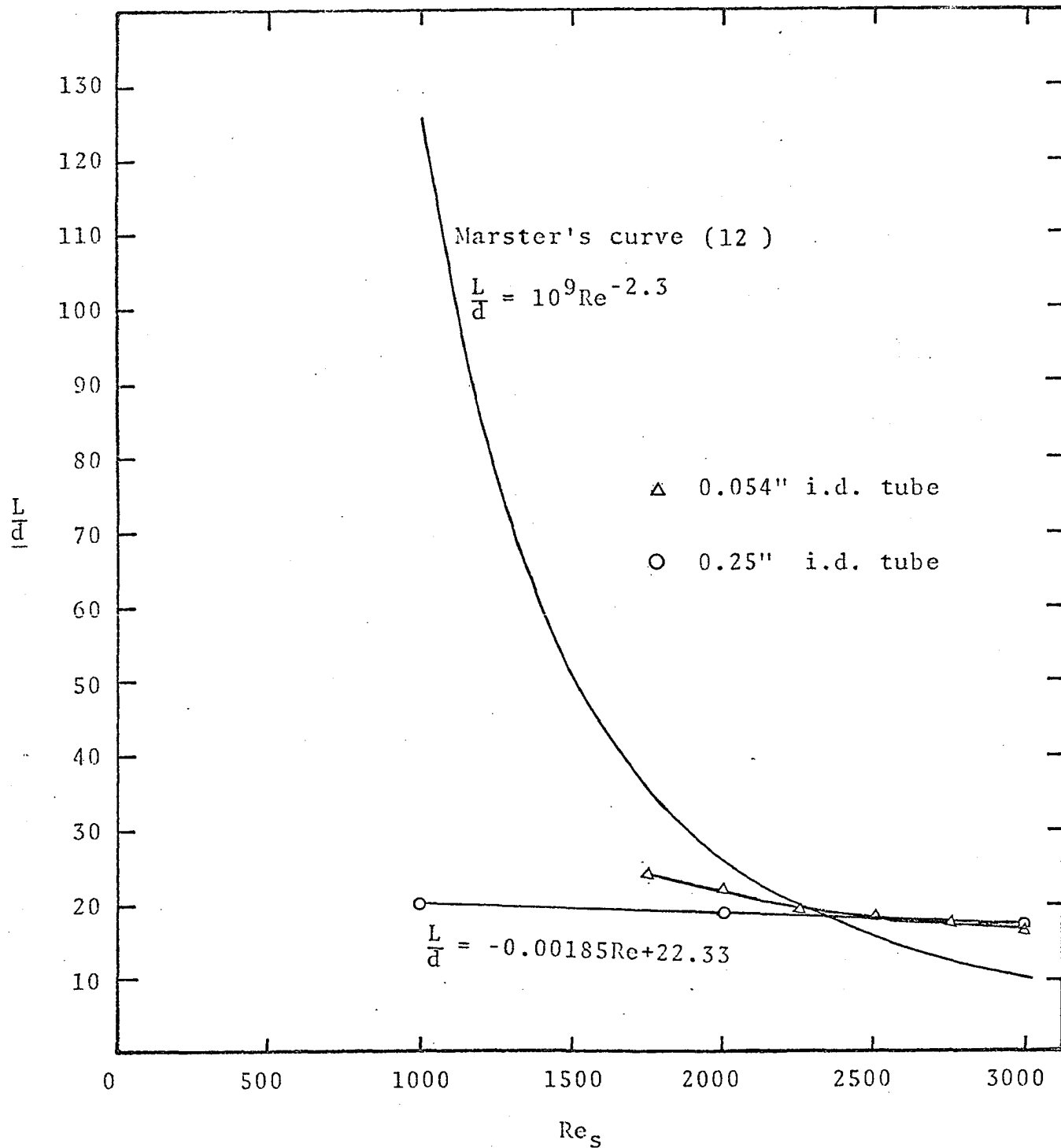
Fig. 26: Comparison of the laminar length of the jet.
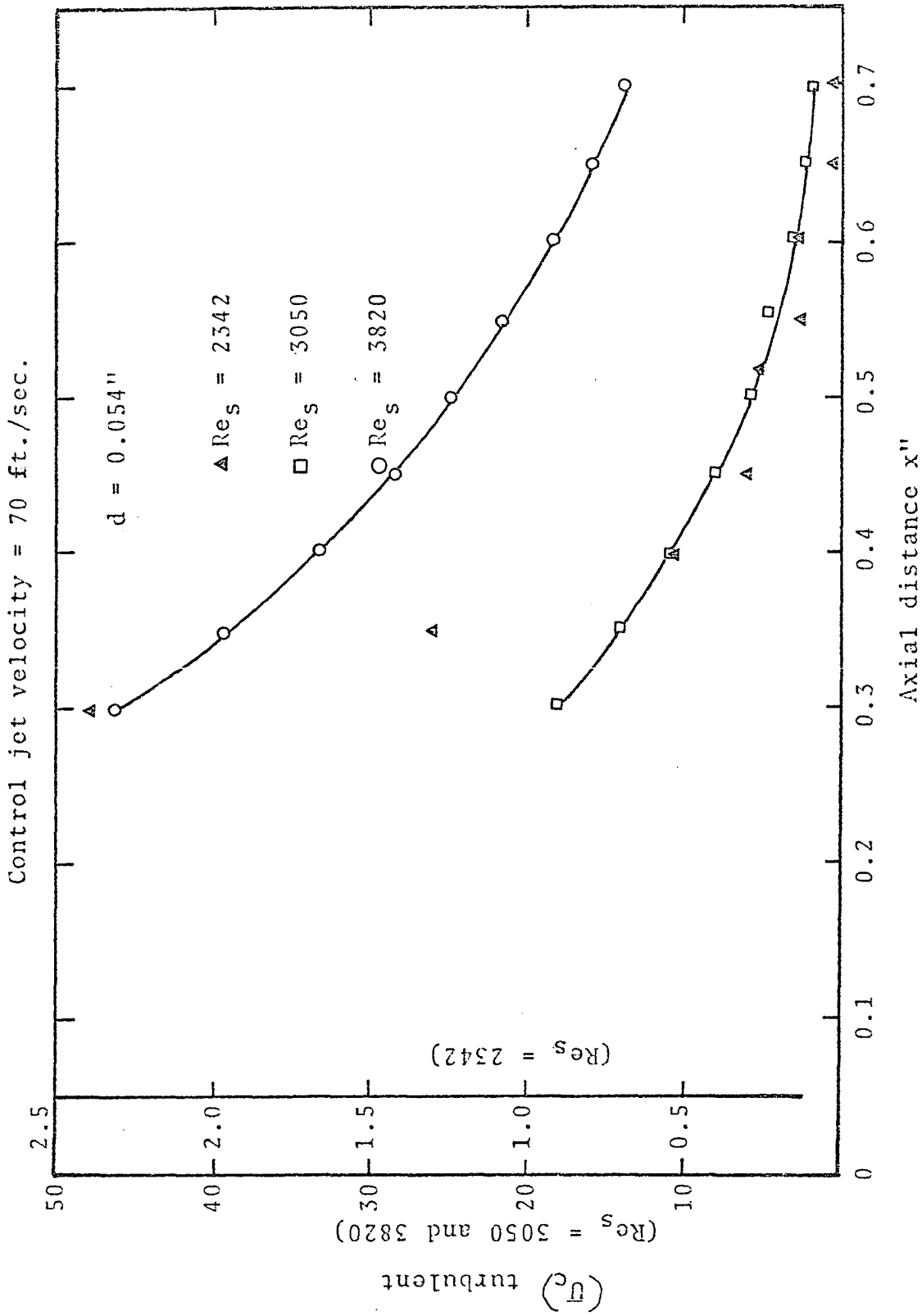
Fig. 27: Decrease in center-line velocity with control jet on.
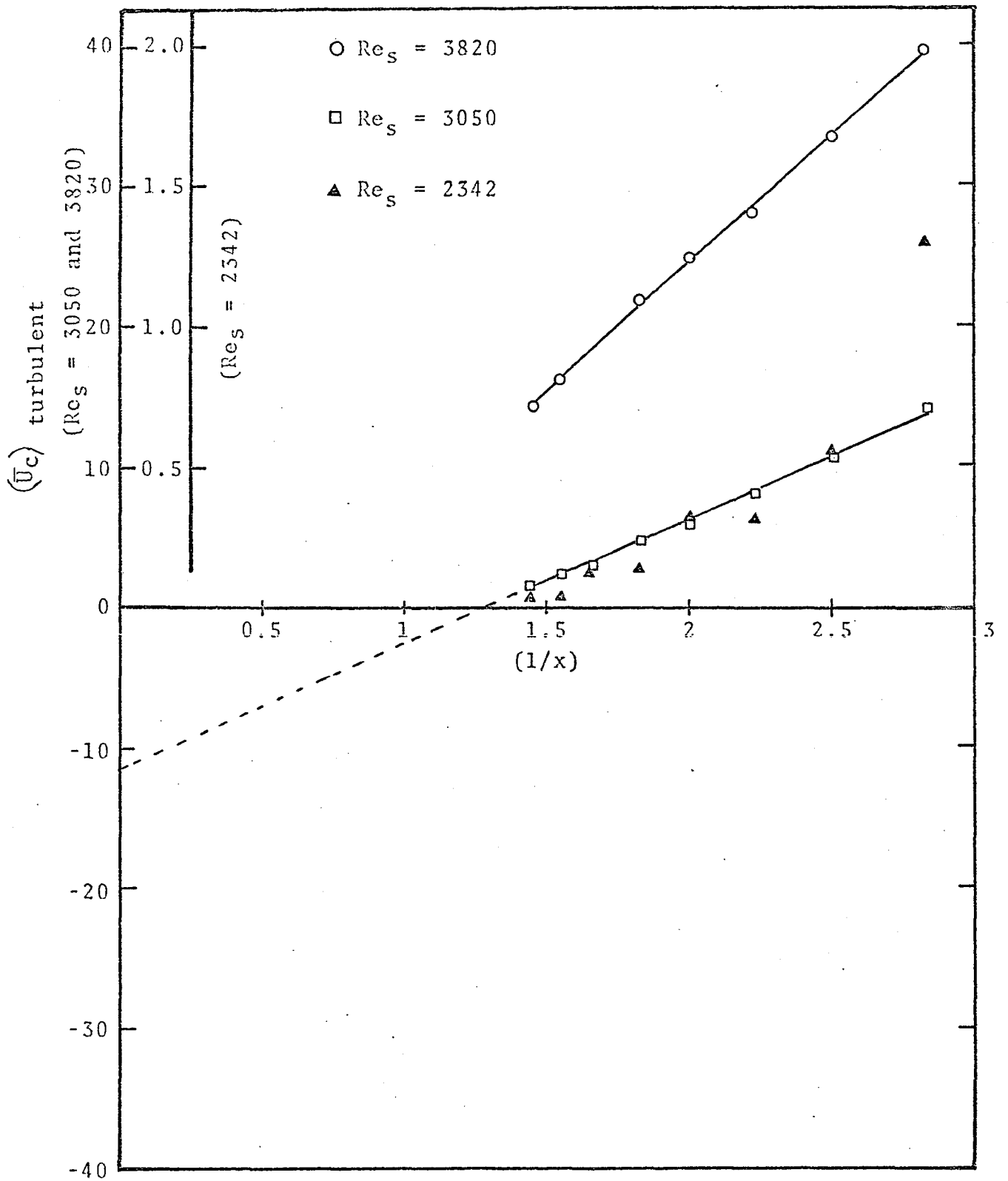
Fig. 28: Turbulent center-line velocity
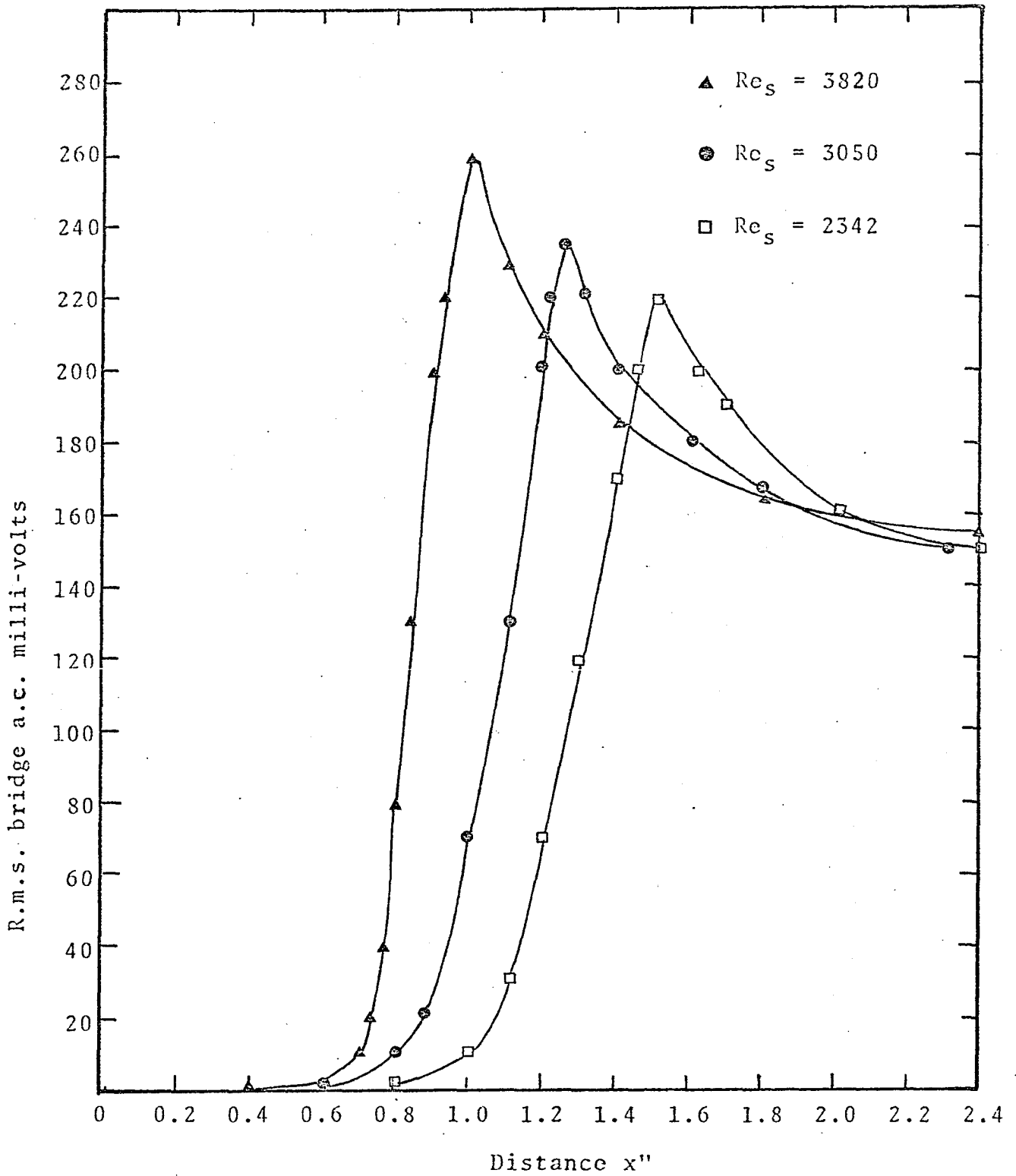
Fig. 29: R.m.s. milli-volt turbulence readings
versus axial distance.
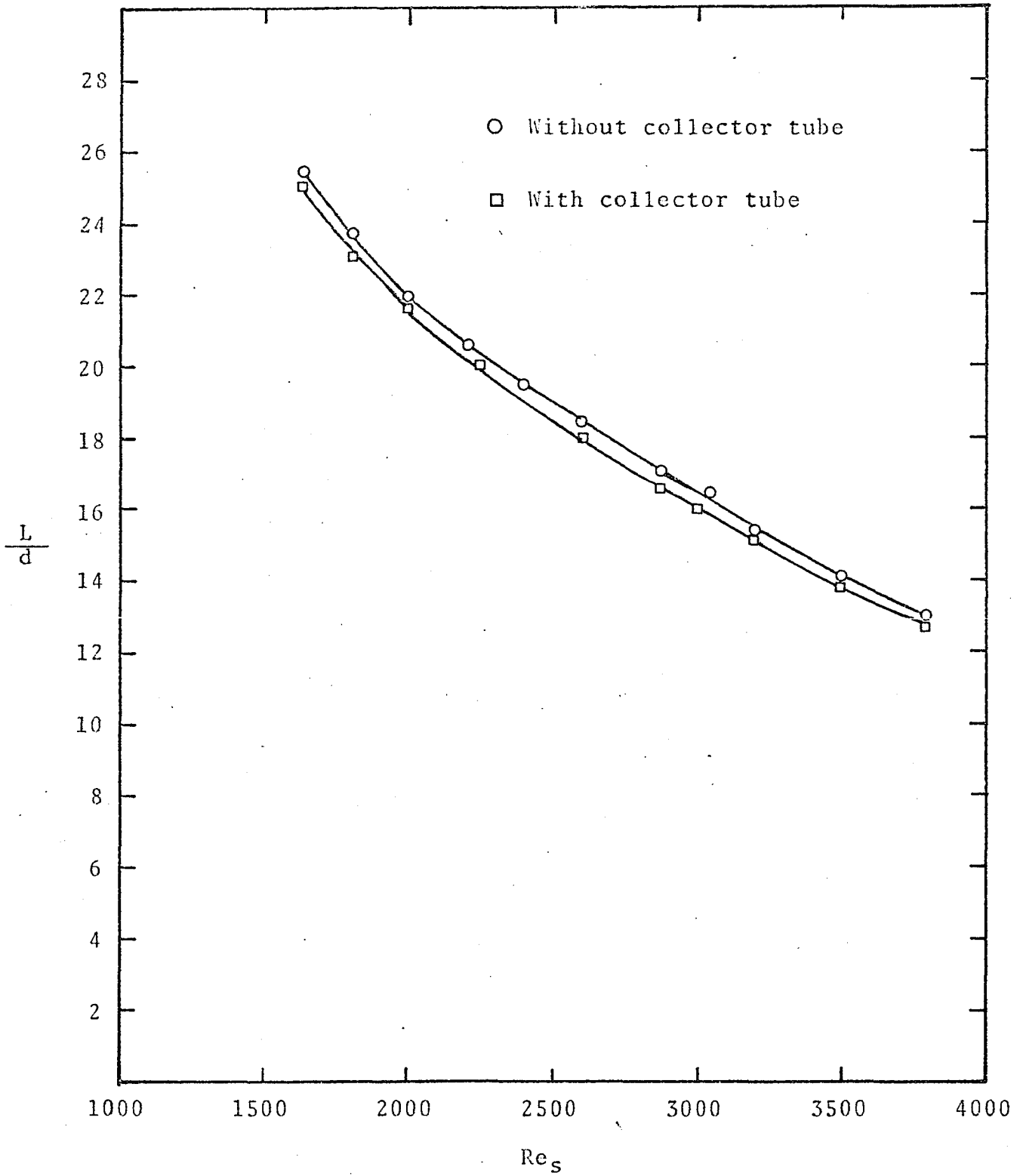
Fig. 30: The collectors influence on the transition point.
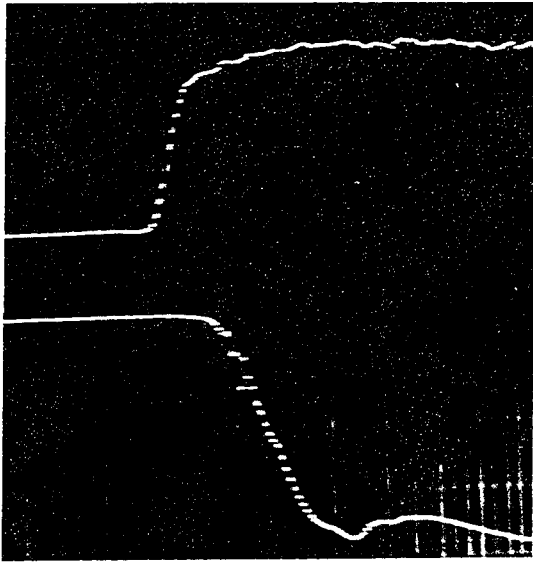
(a) $Re_S = 2342$

$x = 0.3"$

$V_c = 70$ ft./sec.
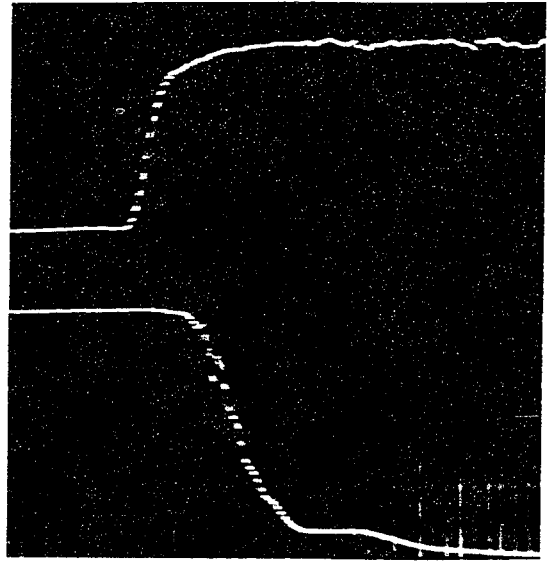
(b) $Re_S = 2342$

$x = 0.3"$

$V_c = 83$ ft./sec.
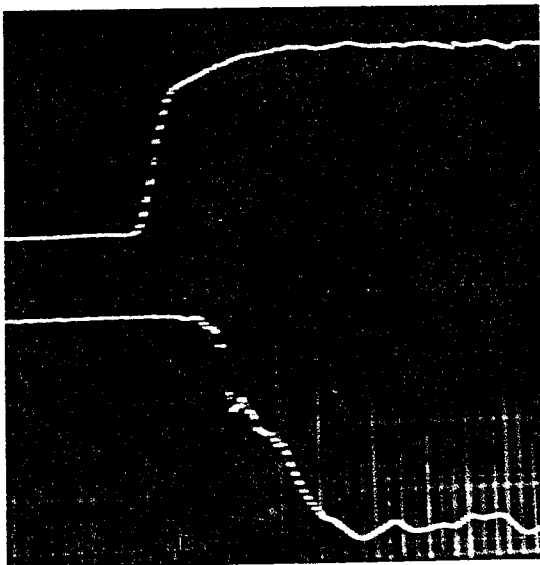
(c) $Re_S = 2780$

$x = 0.4"$

$V_c = 70$ ft./sec.
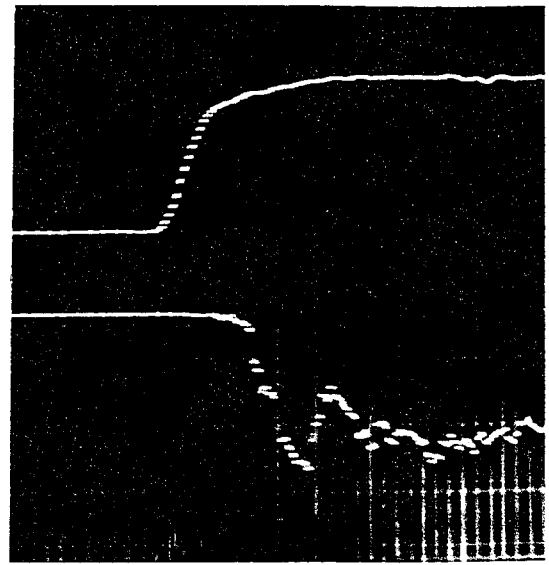
(d) $Re_S = 3050$

$x = 0.4"$

$V_c = 56.75$ ft/sec.

Fig. 31: Typical oscillograms for the ON-OFF transition of the turbulence amplifier.

Control jet velocity = 56.75 ft./sec.

$\blacksquare$ Re$_S$ = 2342 $\ominus$ Re$_S$ = 3050

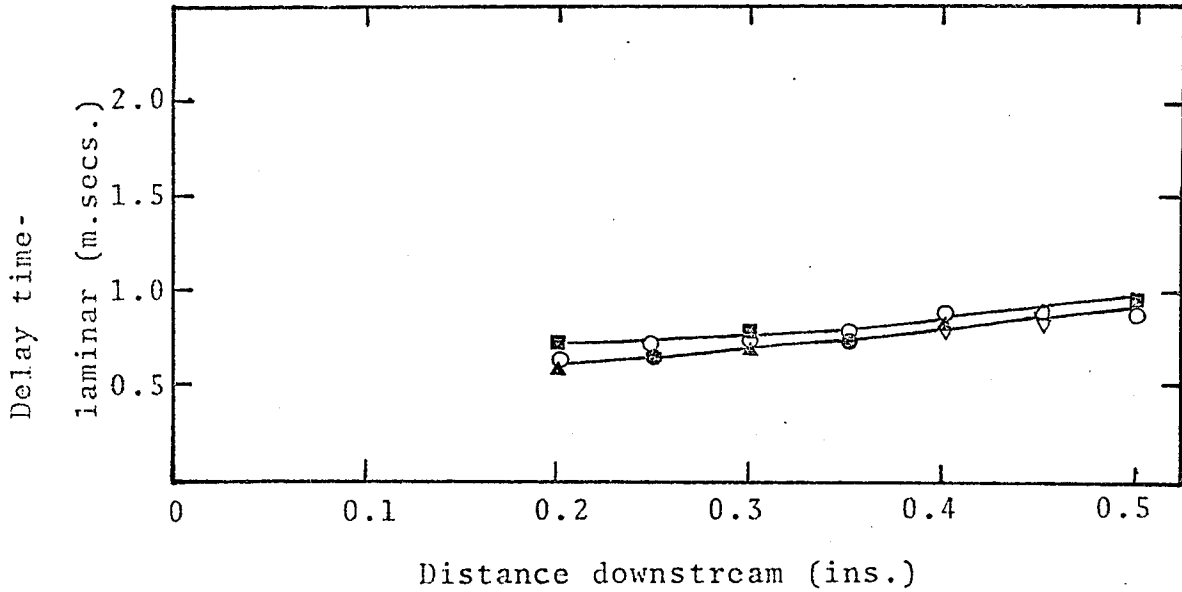$\blacktriangle$ Re$_S$ = 2780 ∇ Re$_S$ = 3540 $\circ$ Re$_S$ = 3820

Fig. 32: Delay time-laminar, control
jet velocity 56.75 ft./sec.
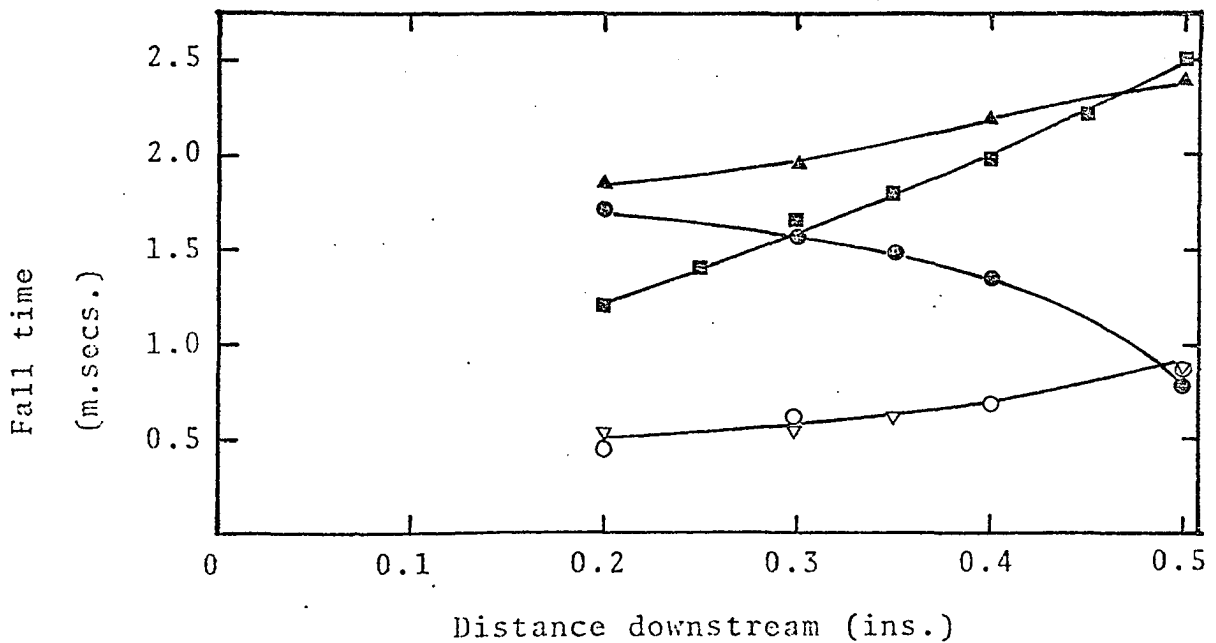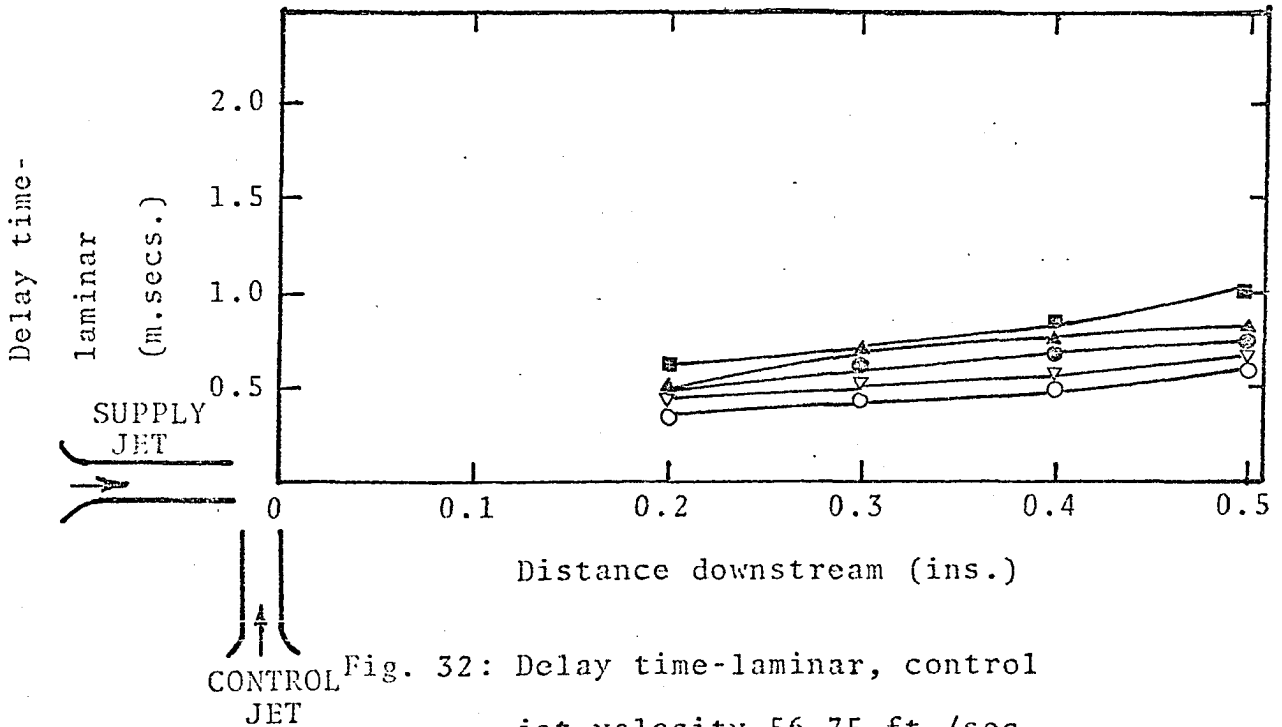
Fig. 33: Fall time, control jet
velocity 56.75 ft./sec.

Control jet velocity = 70 ft./sec.

  ▣ Re$_S$ = 2342   ⊕ Re$_S$ = 3050

                                            O Re$_S$ = 3820
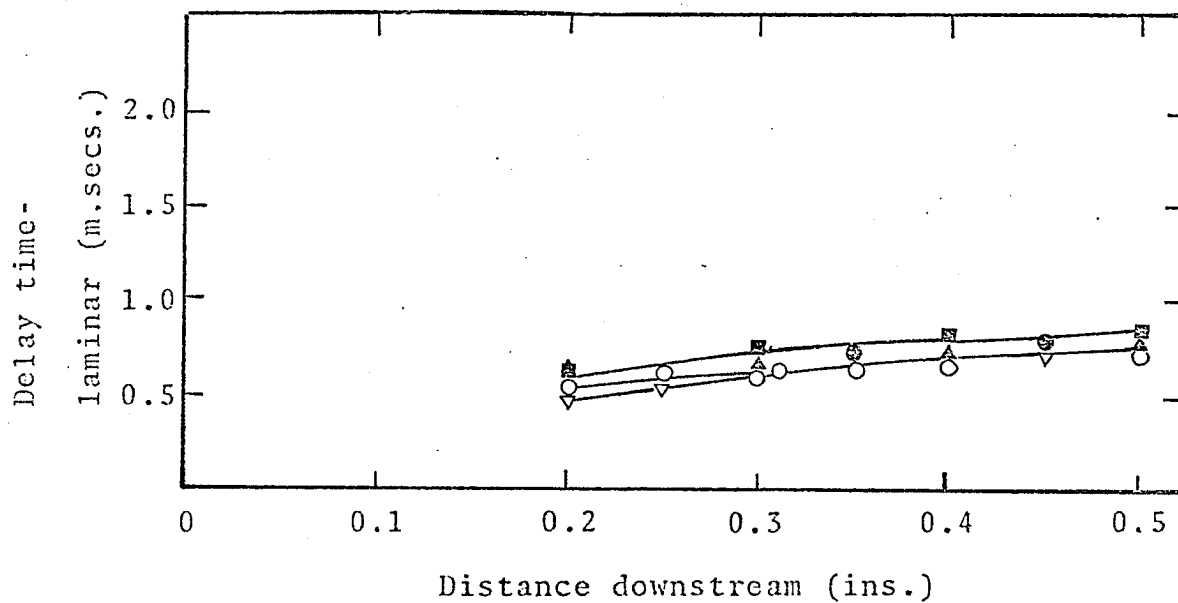
  ▲ Re$_S$ = 2780   ▽ Re$_S$ = 3540

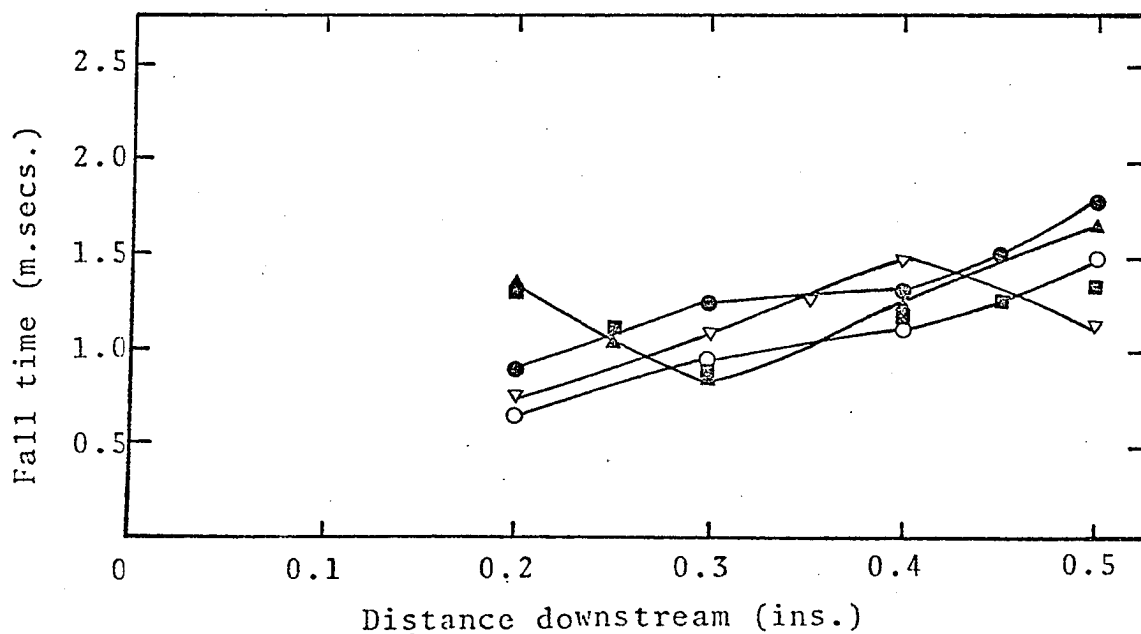Fig. 34: Delay time-laminar, control jet
velocity 70 ft./sec.
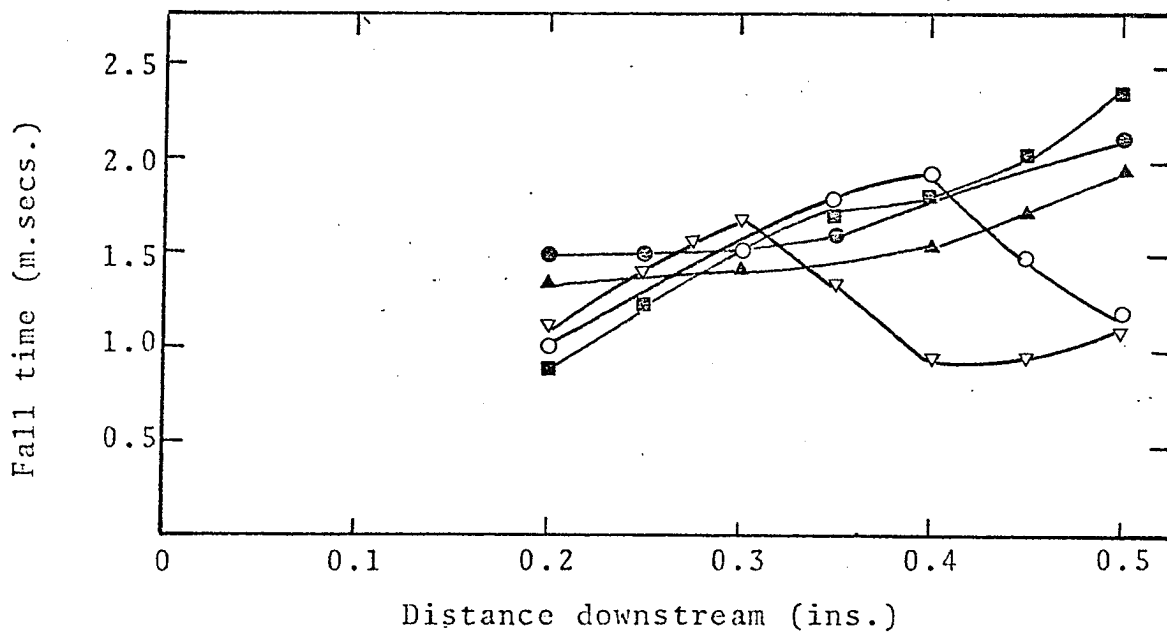
Fig. 35: Fall time, control jet velocity
70 ft./sec.

Control jet velocity = 83 ft./sec.

■ Re$_s$ = 2342   ◉ Re$_s$ = 3050   ○ Re$_s$ = 3820
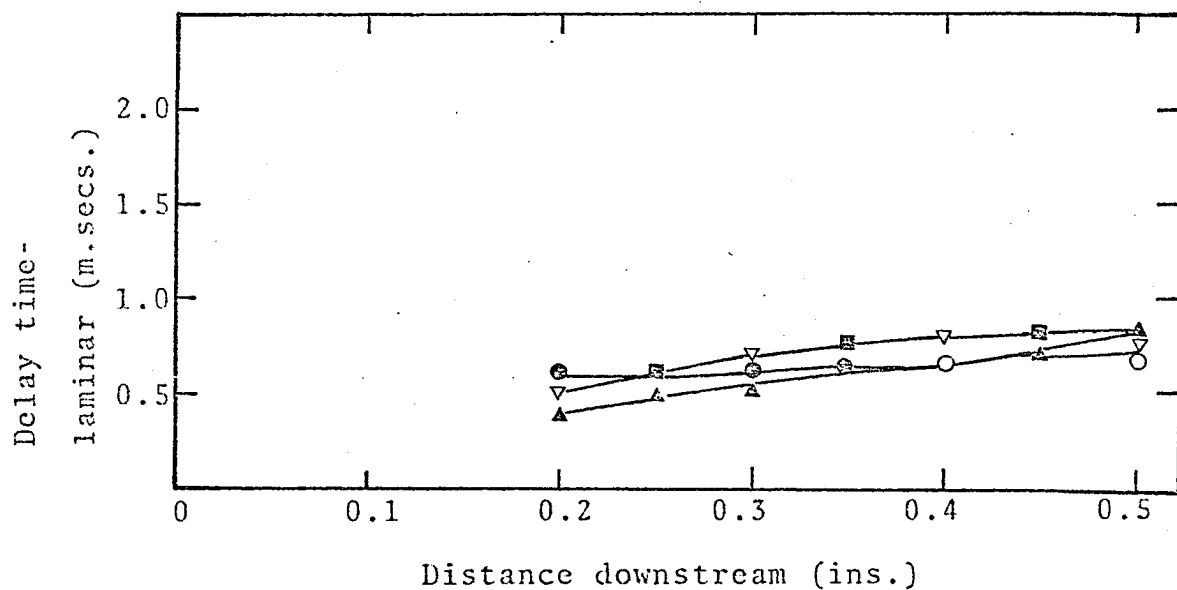
▲ Re$_s$ = 2780   ▽ Re$_s$ = 3540

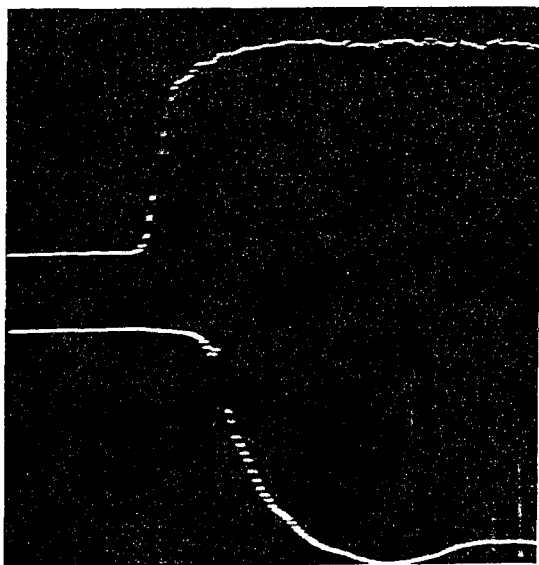Fig. 36: Delay time-laminar, control

jet velocity 83 ft./sec.
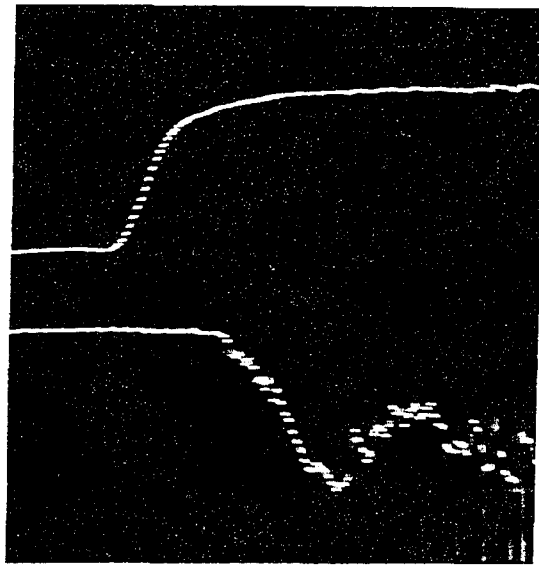

Fig. 37: Fall time, control jet velocity

83 ft./sec.

Fig. 38: Delay time-turbulent and Rise time, control jet velocity 56.75 ft./sec.
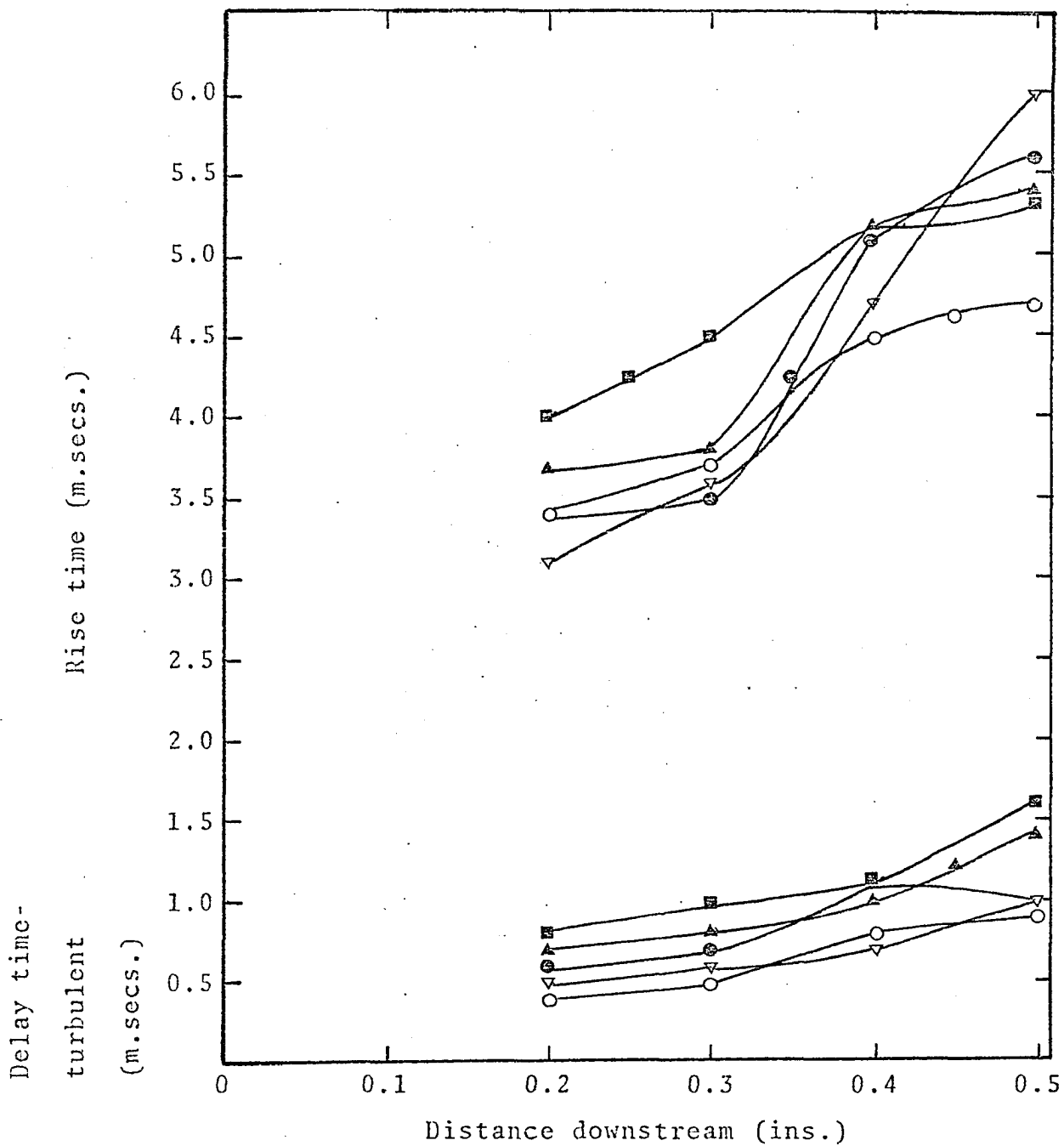
Fig. 39: Delay time-turbulent and Rise time, control jet velocity 70 ft./sec.

Control jet velocity = 83 ft./sec.

▣ Re_s = 2342   ⊕ Re_s = 3050   ○ Re_s = 3820

▲ Re_s = 2780   ▽ Re_s = 3540
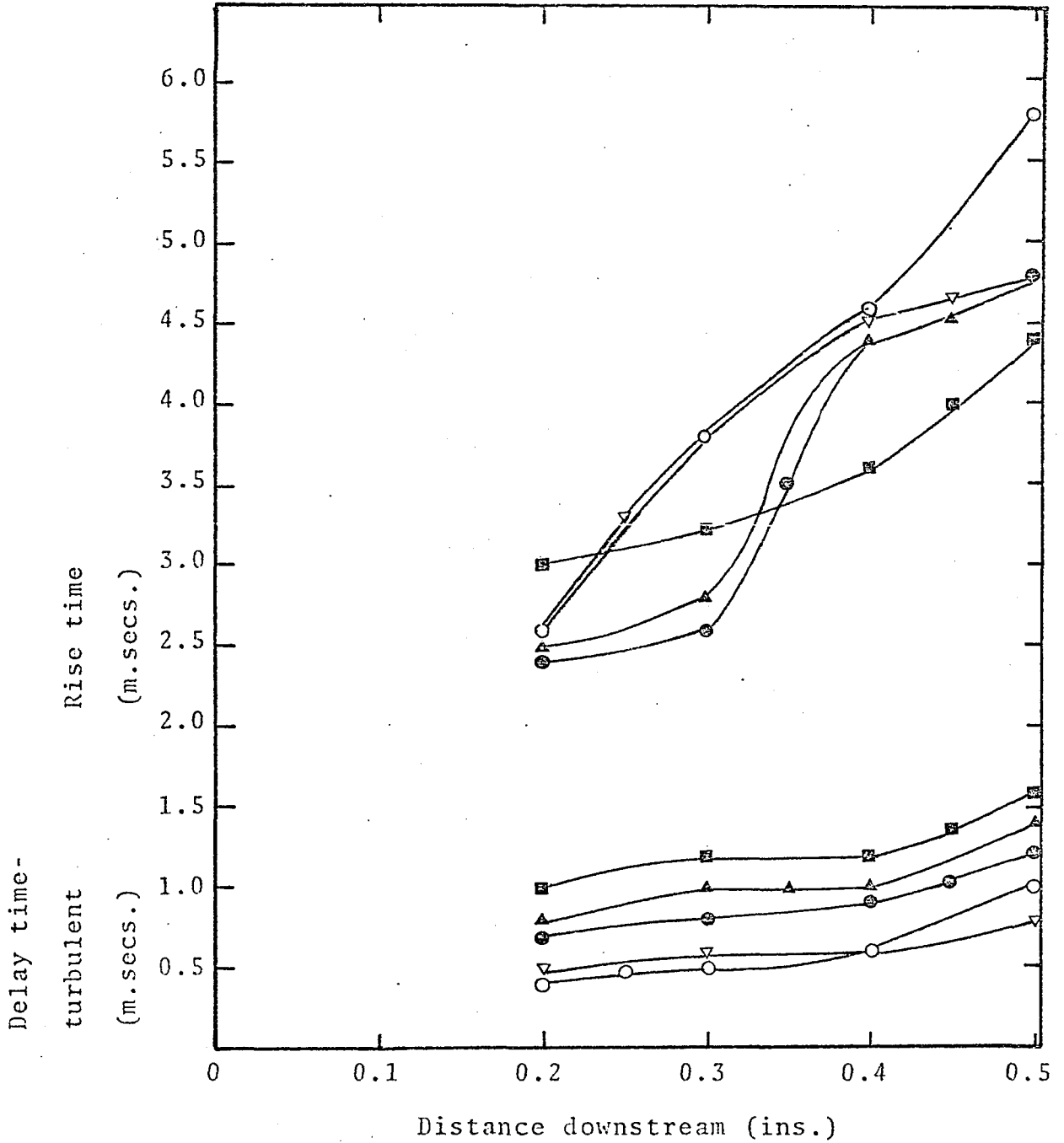
Fig. 40: Delay time-turbulent and Rise time, control jet velocity 83 ft./sec.
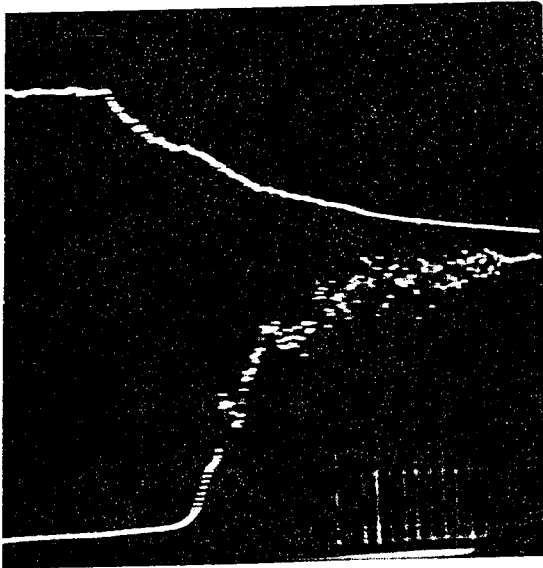
(a) Re_S = 2342

x = 0.5"

V_c = 70 ft./sec.
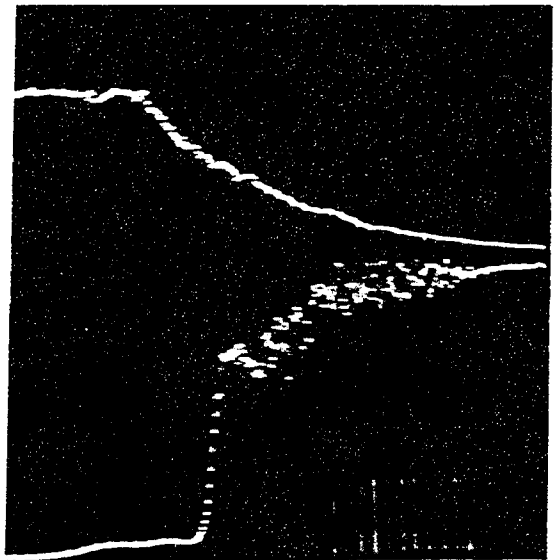
(b) Re_S = 2780

x = 0.4"

V_c = 83 ft./sec.
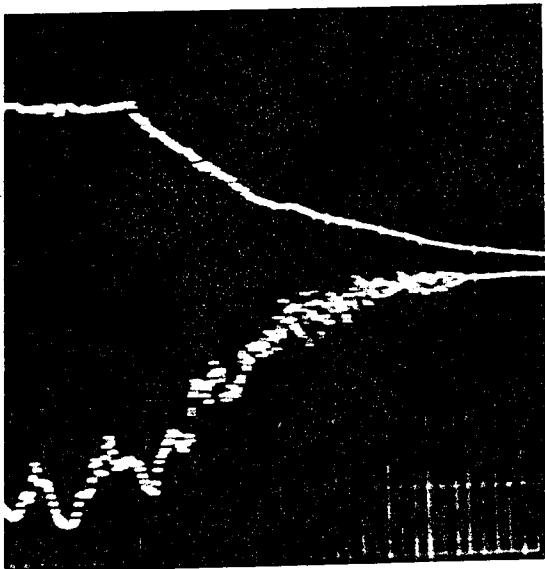
(c) Re_S = 3050

x = 0.4"

V_c = 70 ft./sec.
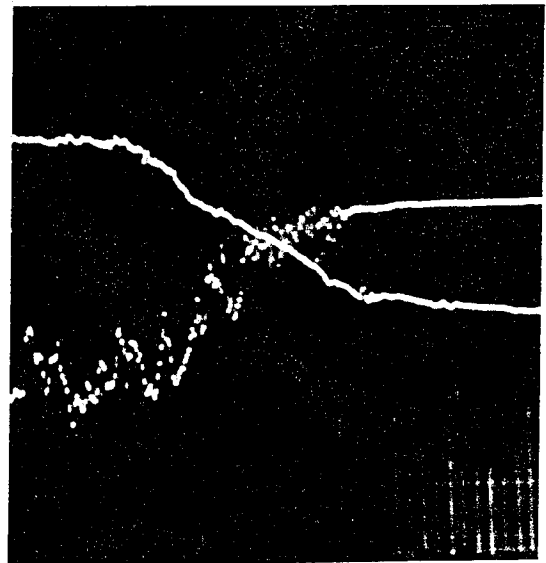
(d) Re_S = 3820

x = 0.4"

V_c = 56.75 ft./sec.

Fig. 41: Typical oscillograms for the OFF-ON transition of the turbulence amplifier.

Control jet velocity = 56.75 ft./sec.

Control jet turned through 30°

■ Re_s = 2342   ◉ Re_s = 3050   O Re_s = 3820
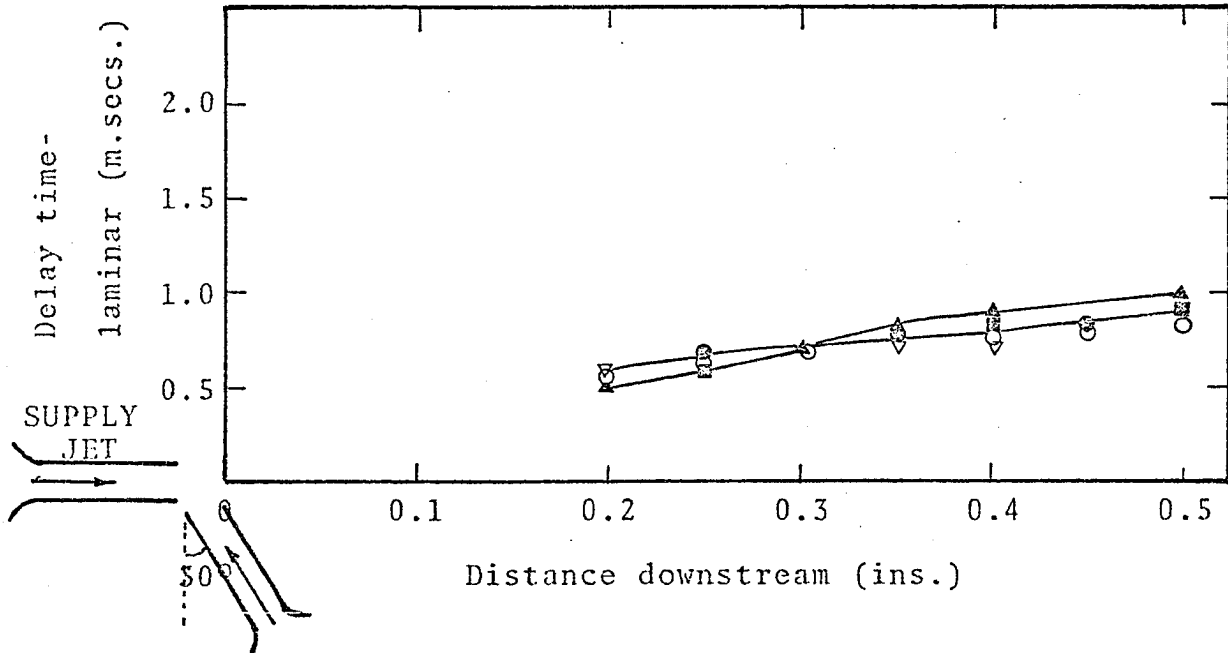
▲ Re_s = 2780   ▽ Re_s = 3540

Fig. 42: Delay time-laminar, control
jet velocity 56.75 ft./sec.
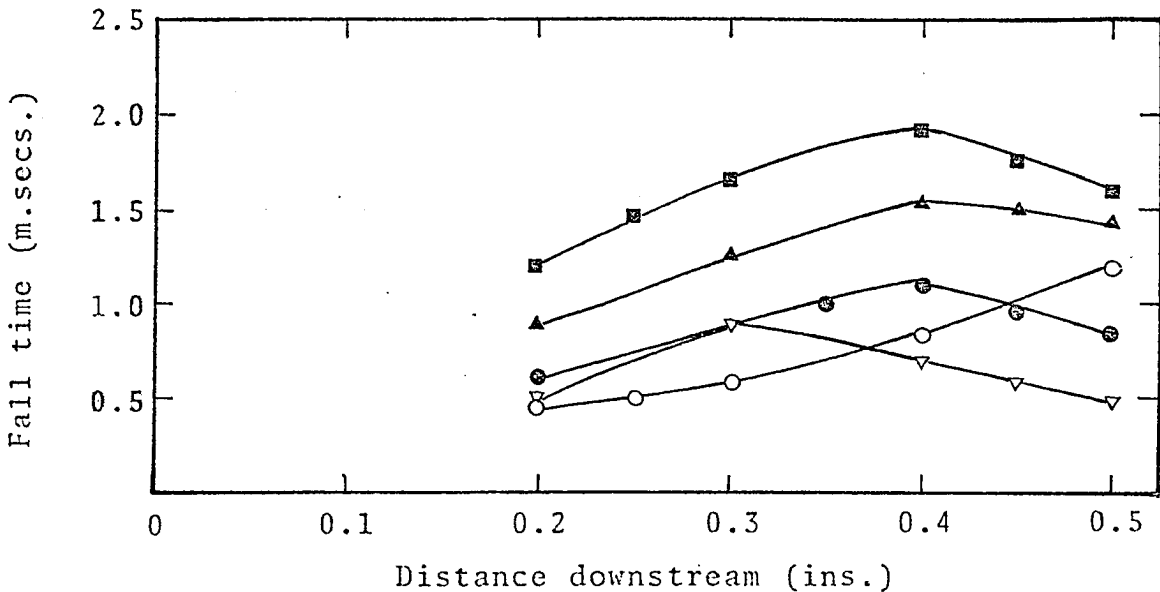
Fig. 43: Fall time, control jet velocity 56.75 ft./sec.

Control jet velocity = 70 ft./sec.

Control jet turned through 30°

☒ Re_S = 2342   ⊛ Re_S = 3050

▲ Re_S = 2780   ▽ Re_S = 3540

O Re_S = 3820
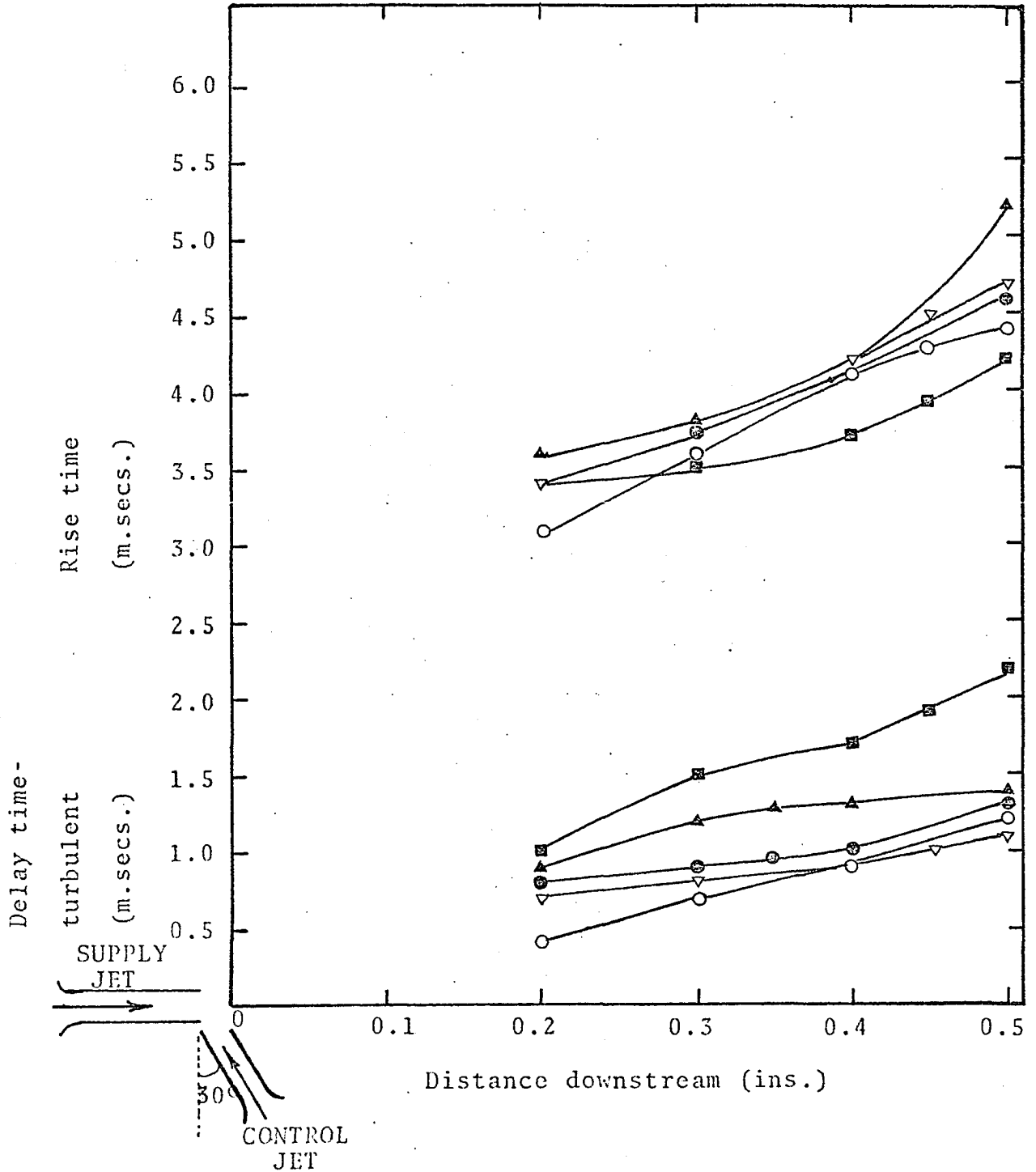

Fig. 44: Delay time-laminar, control jet
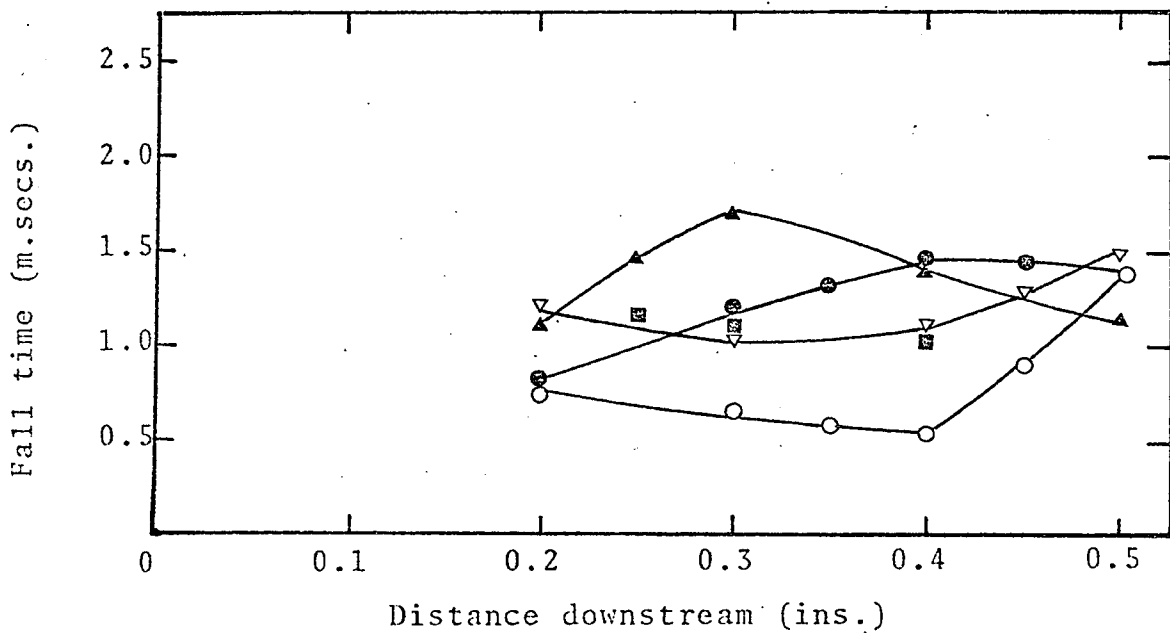
velocity 70 ft./sec.

Fig. 45: Fall time, control jet velocity

. 70 ft./sec.

Control jet velocity = 83 ft./sec.

Control jet turned through 30°

■ Re$_S$ = 2342   ● Re$_S$ = 3050   O Re$_S$ = 3820

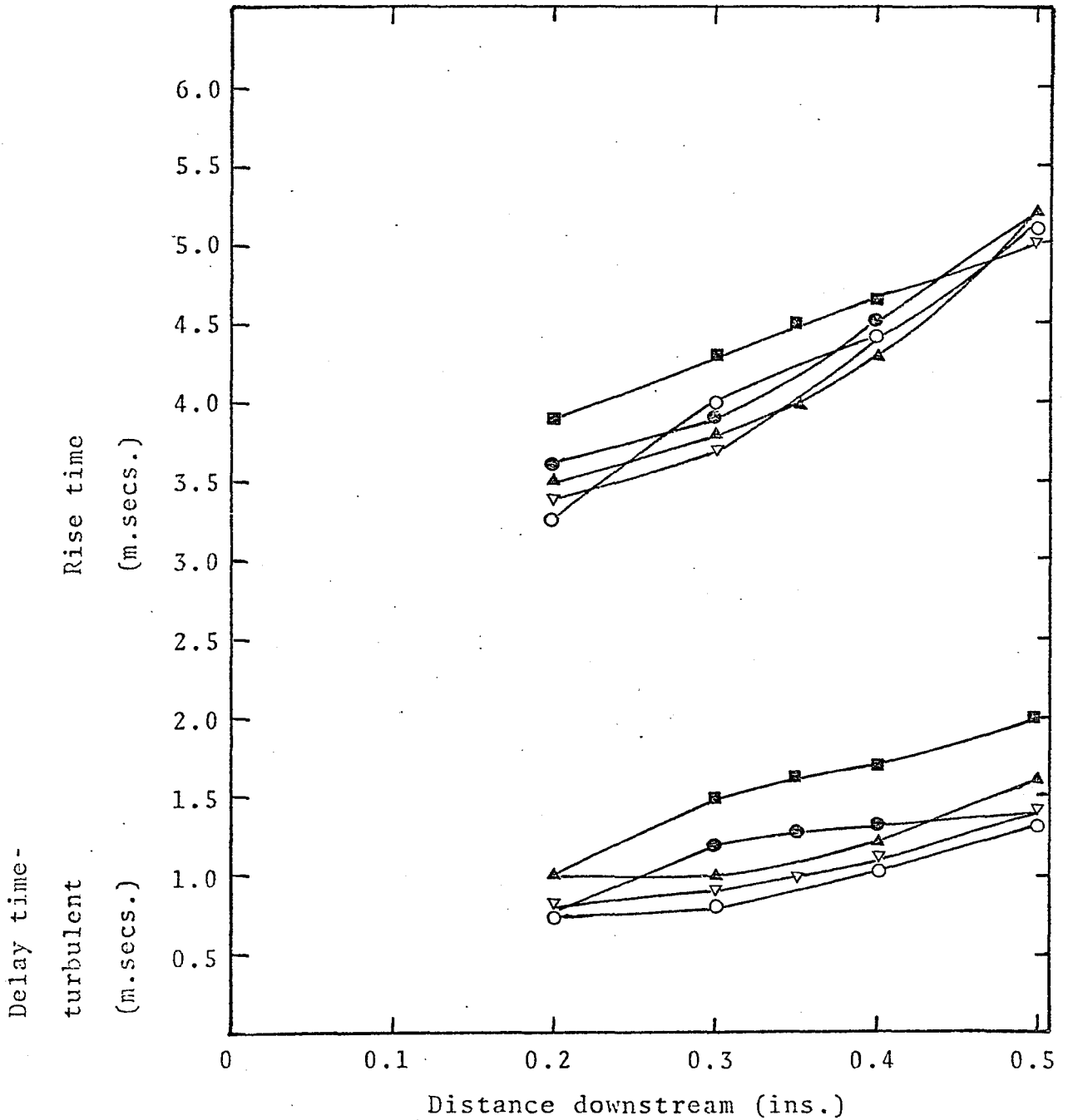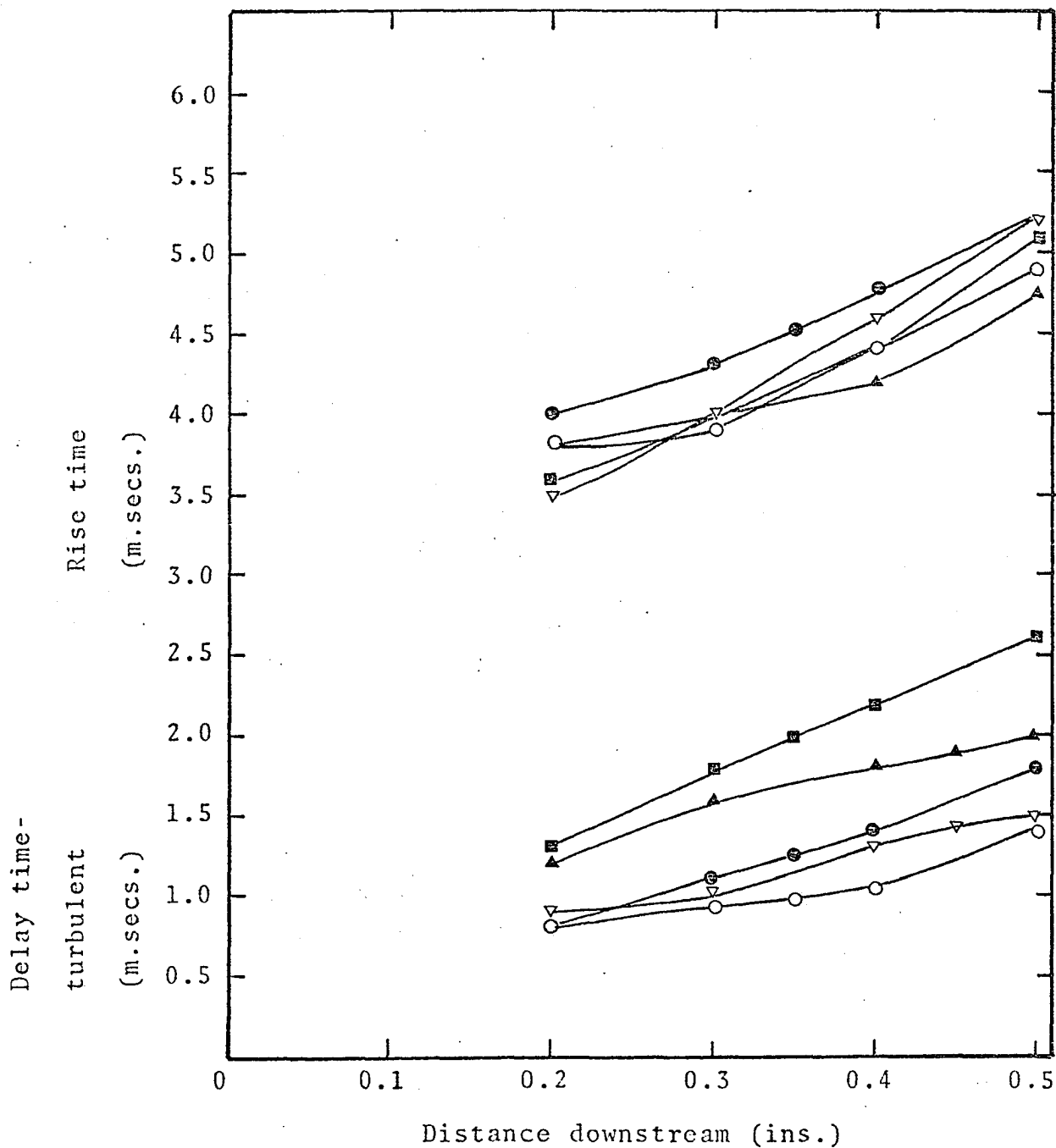▲ Re$_S$ = 2780   ▽ Re$_S$ = 3540
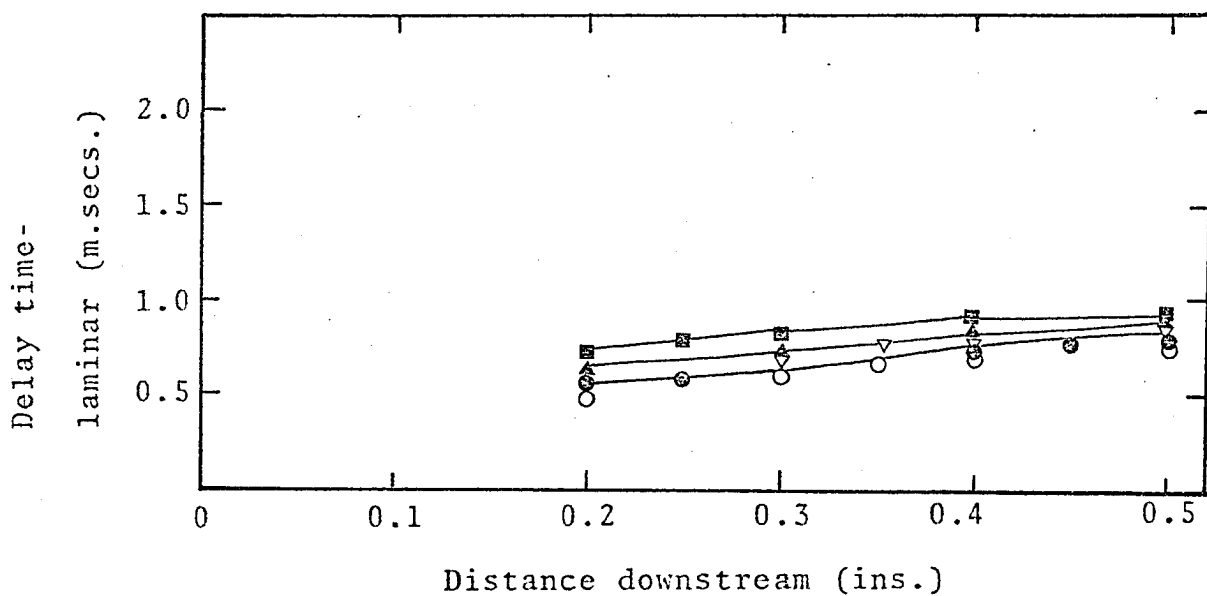
Fig. 46: Delay time-laminar, control jet

velocity 83 ft./sec.

Fig. 47: Fall time, control jet velocity

83 ft./sec.

(a) Re_s = 2342   CONTROL JET   (b) Re_s = 3050

    x = 0.3"   TURNED   x = 0.5"

    V_c = 83 ft./sec.   THROUGH 30° V_c = 56.75 ft./sec.

(c) Re_s = 3540   (d) Re_s = 3540

    x = 0.4"   x = 0.4"
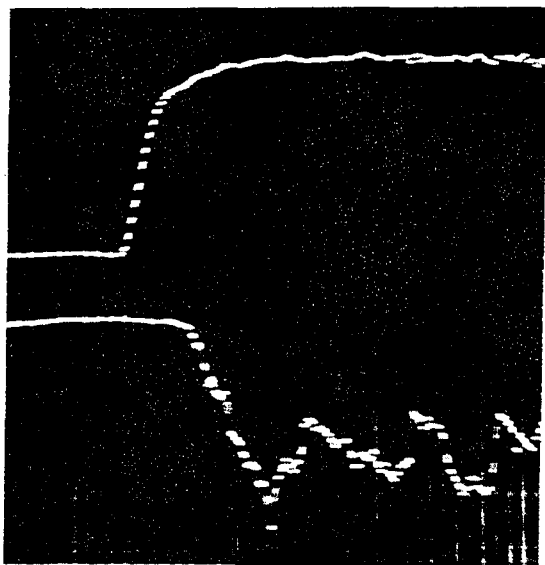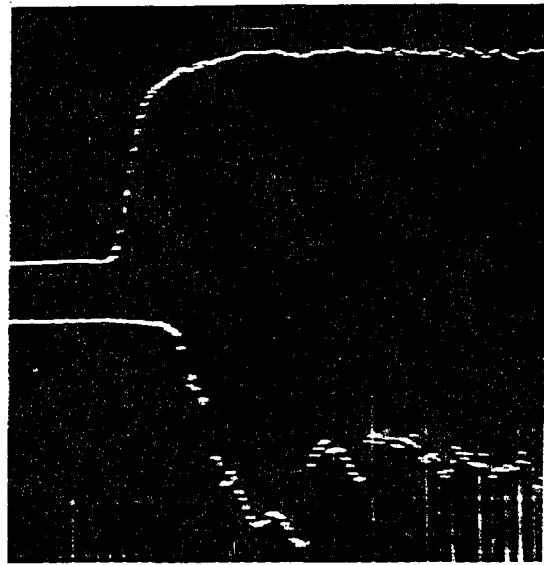
    V_c = 70 ft./sec. V_c = 83 ft./sec.

Fig. 48: Typical oscillogram for the ON-OFF transition of
the turbulence amplifier.

Control jet velocity = 56.75 ft./sec.

Control jet turned through 30°

◨ Re_s = 2342　　● Re_s = 3050

▲ Re_s = 2780　　▽ Re_s = 3540　　○ Re_s = 3820

Fig. 49: Delay time-turbulent and Rise time,
control jet velocity 56.75 ft./sec.

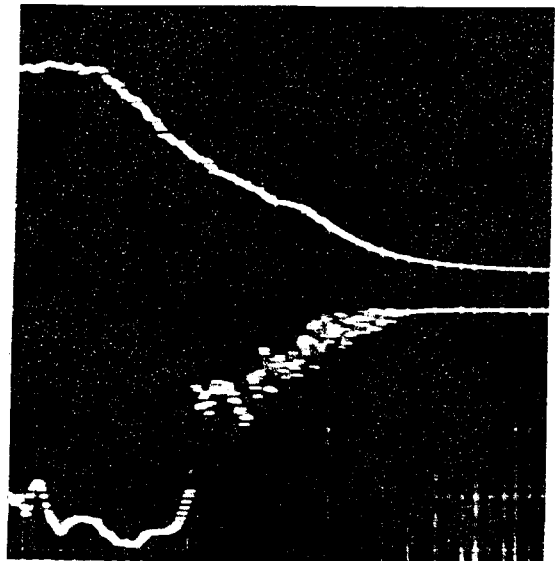Fig. 50: Delay time-turbulent and Rise time,
control jet velocity 70 ft./sec.

Control jet velocity = 83 ft./sec.

Control jet turned through 30°

   ■ Re_s = 2342   ⊖ Re_s = 3050

   ▲ Re_s = 2780   ▽ Re_s = 3540   O Re_s = 3820

Fig. 51: Delay time-turbulent and Rise time,

control jet velocity 83 ft./sec.

(a) Re_s = 2342   CONTROL JET   (b) Re_s = 2780

     x = 0.3"   TURNED   x = 0.4"
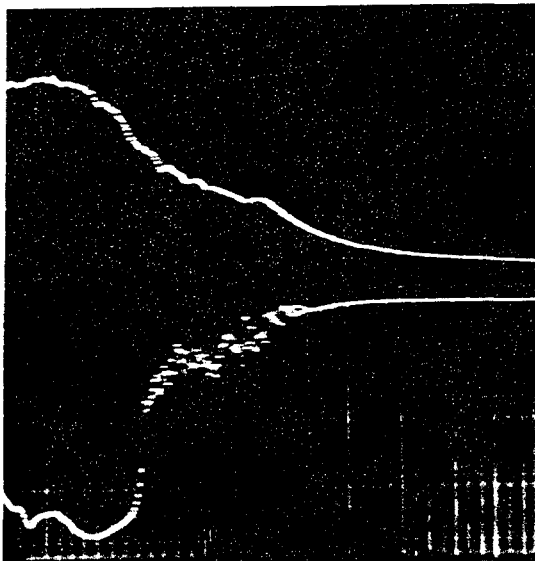
     V_c = 70 ft./sec.   THROUGH 30° V_c = 56.75 ft./sec.

(c) Re_s = 3050   (d) Re_s = 3540

     x = 0.5"   x = 0.4"
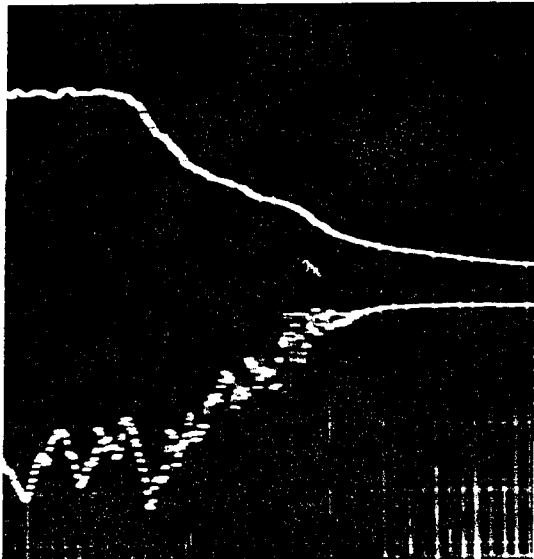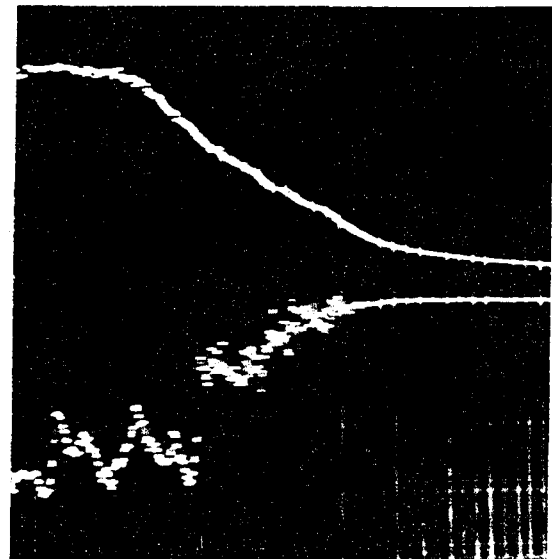
     V_c = 83 ft./sec V_c = 83 ft./sec.

Fig. 52: Typical oscillograms for the OFF-ON transition
of the turbulence amplifier.
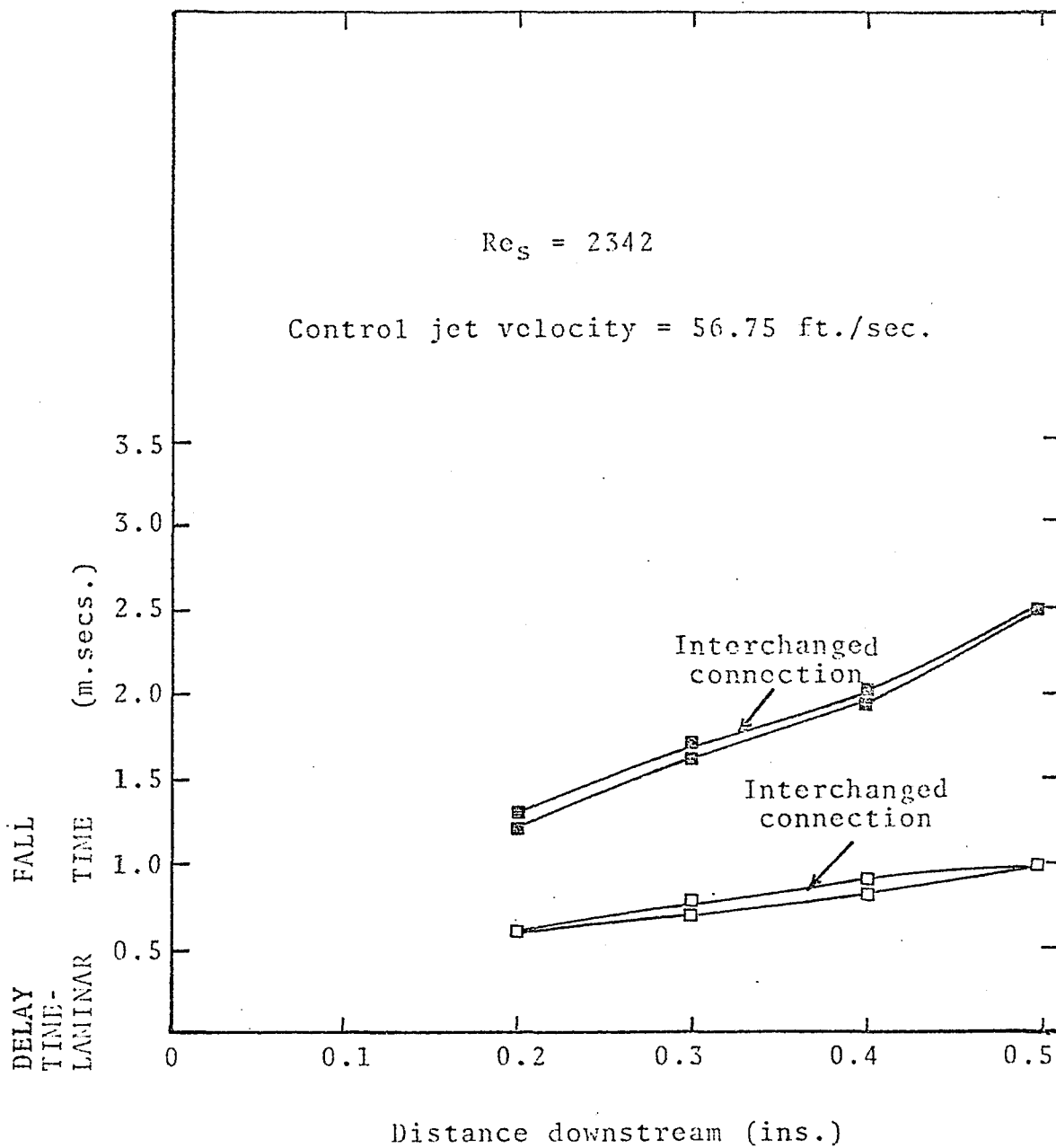
Fig. 53: Check on the response time of the
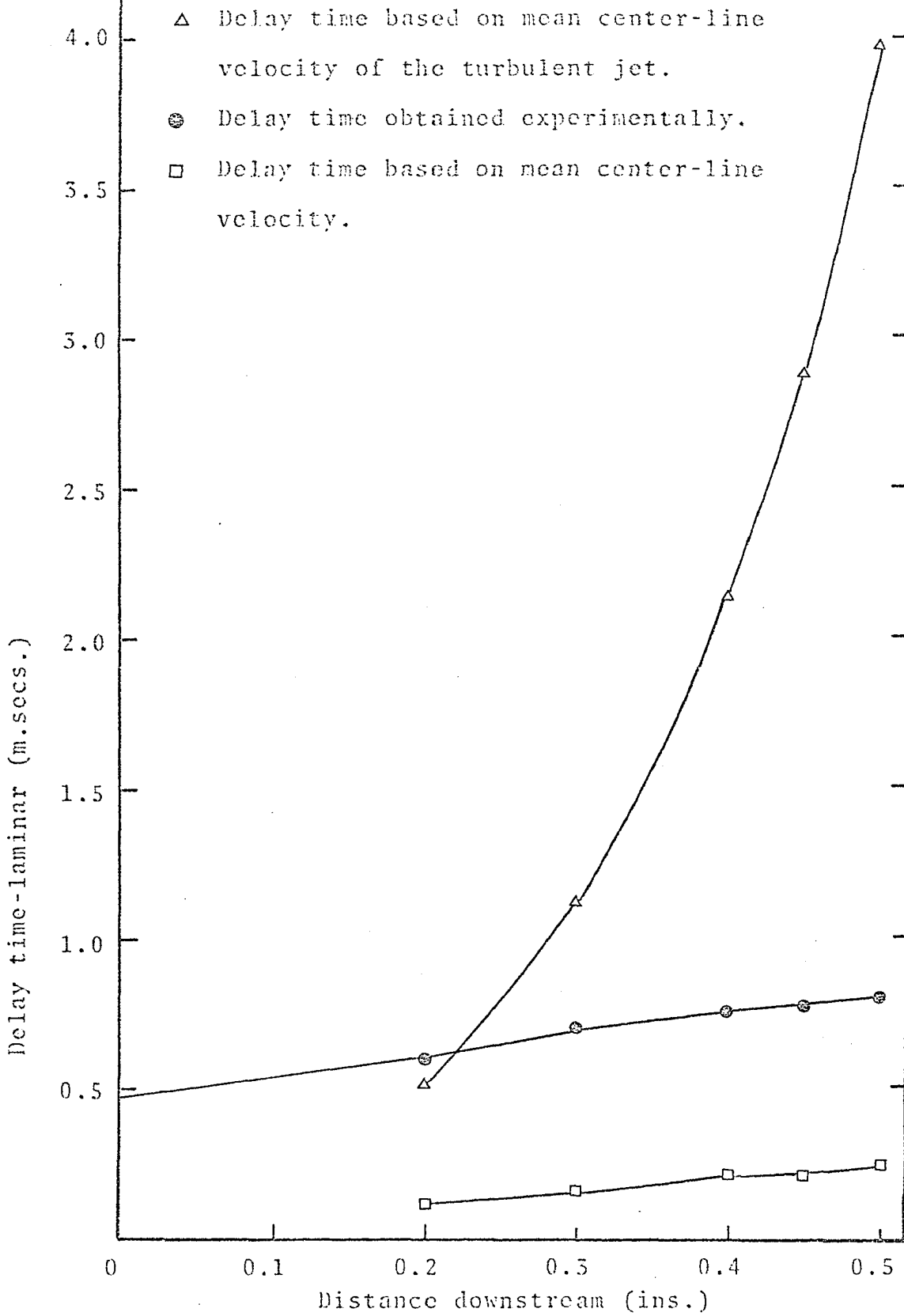hot-wire anemometers.

Fig. 54: Comparison of the experimental curve of the delay time-laminar with delay times based on mean center-line velocities.

Legend (on chart):
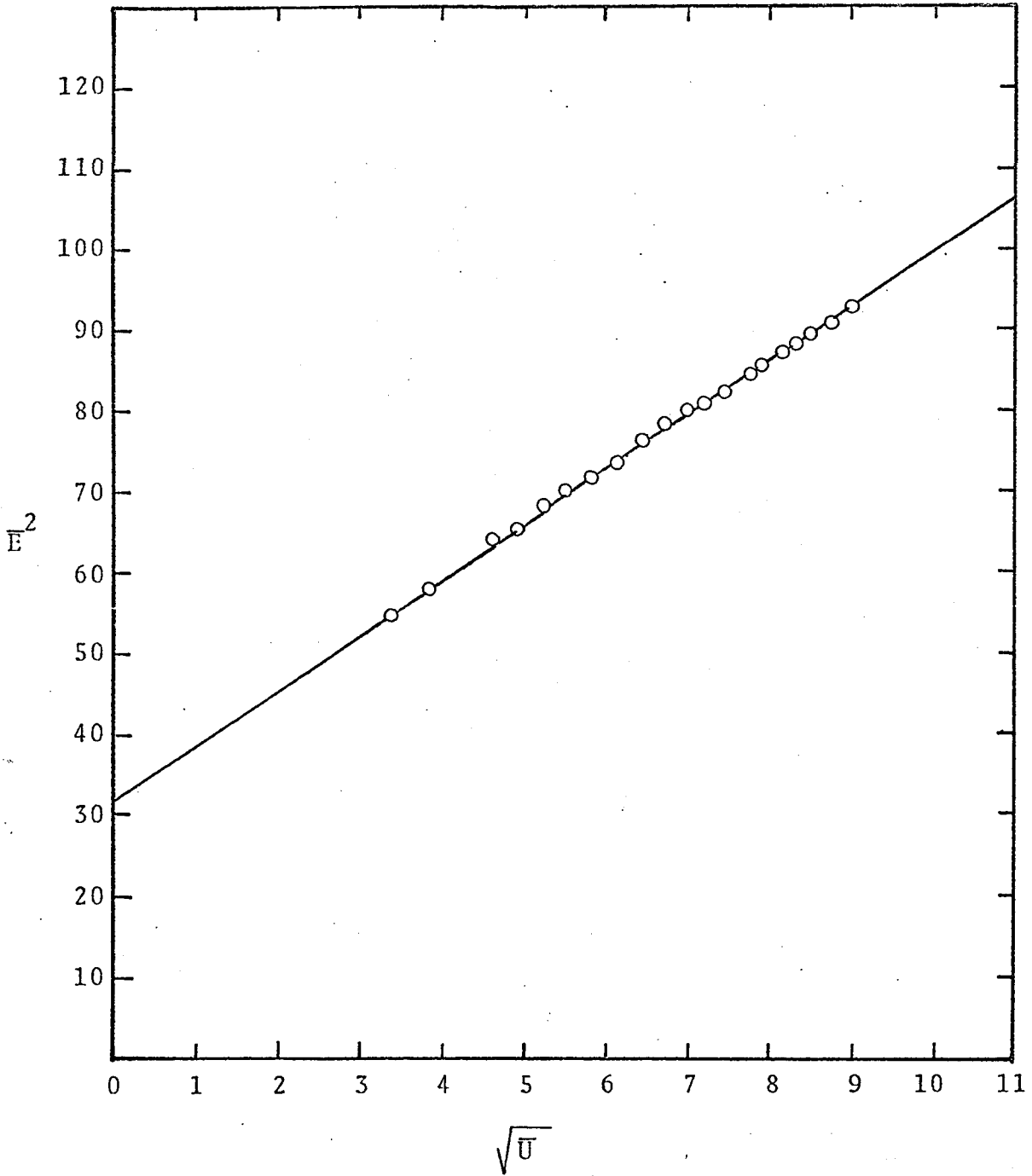△ Delay time based on mean center-line velocity of the turbulent jet.
⊛ Delay time obtained experimentally.
□ Delay time based on mean center-line velocity.

$Re_S = 3050$

Y-axis: Delay time-laminar (m.secs.)
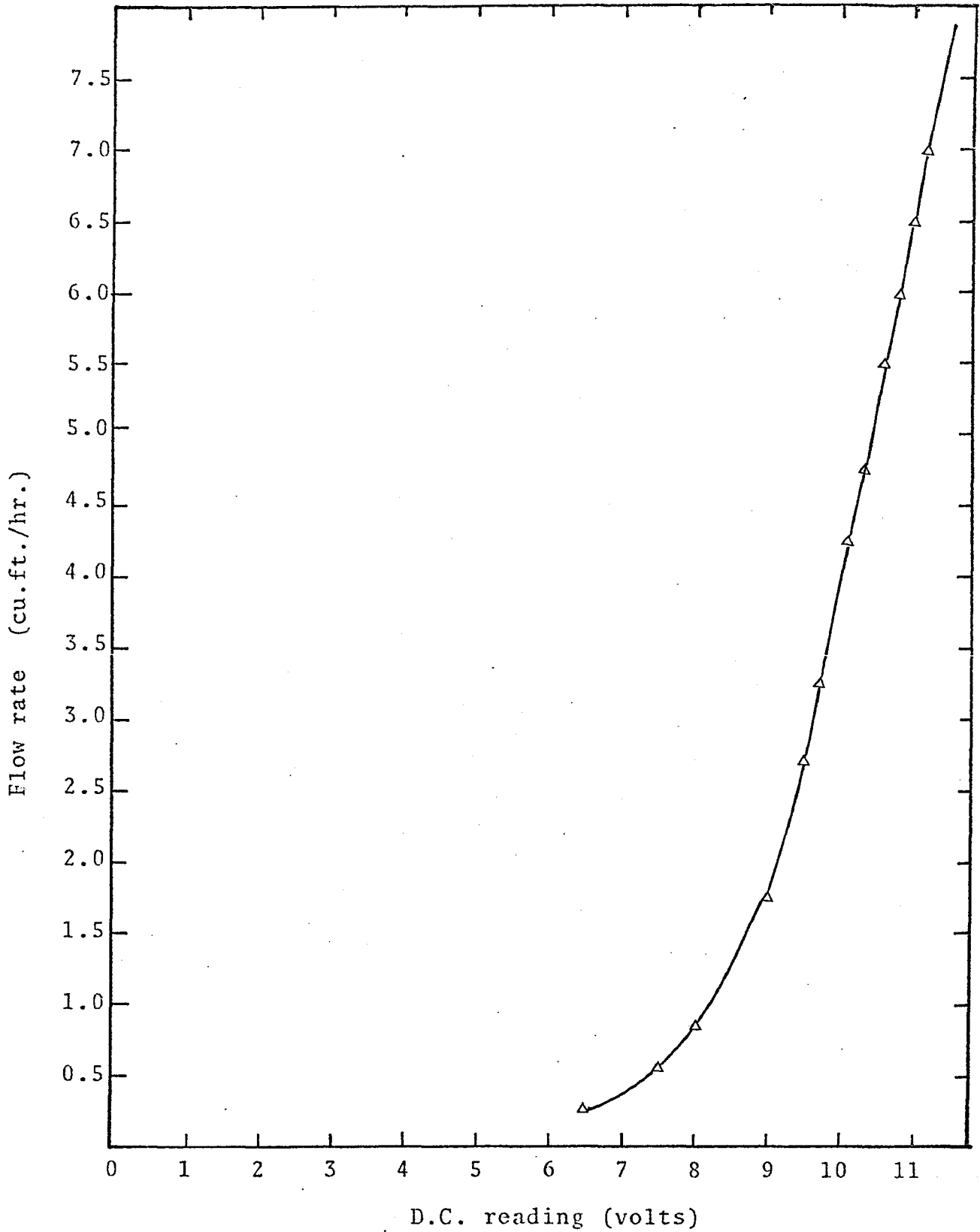X-axis: Distance downstream (ins.)

Fig. 55: Calibration curve for Type 55A25
hot-wire probe.

Fig. 56: Calibration curve for control jet.
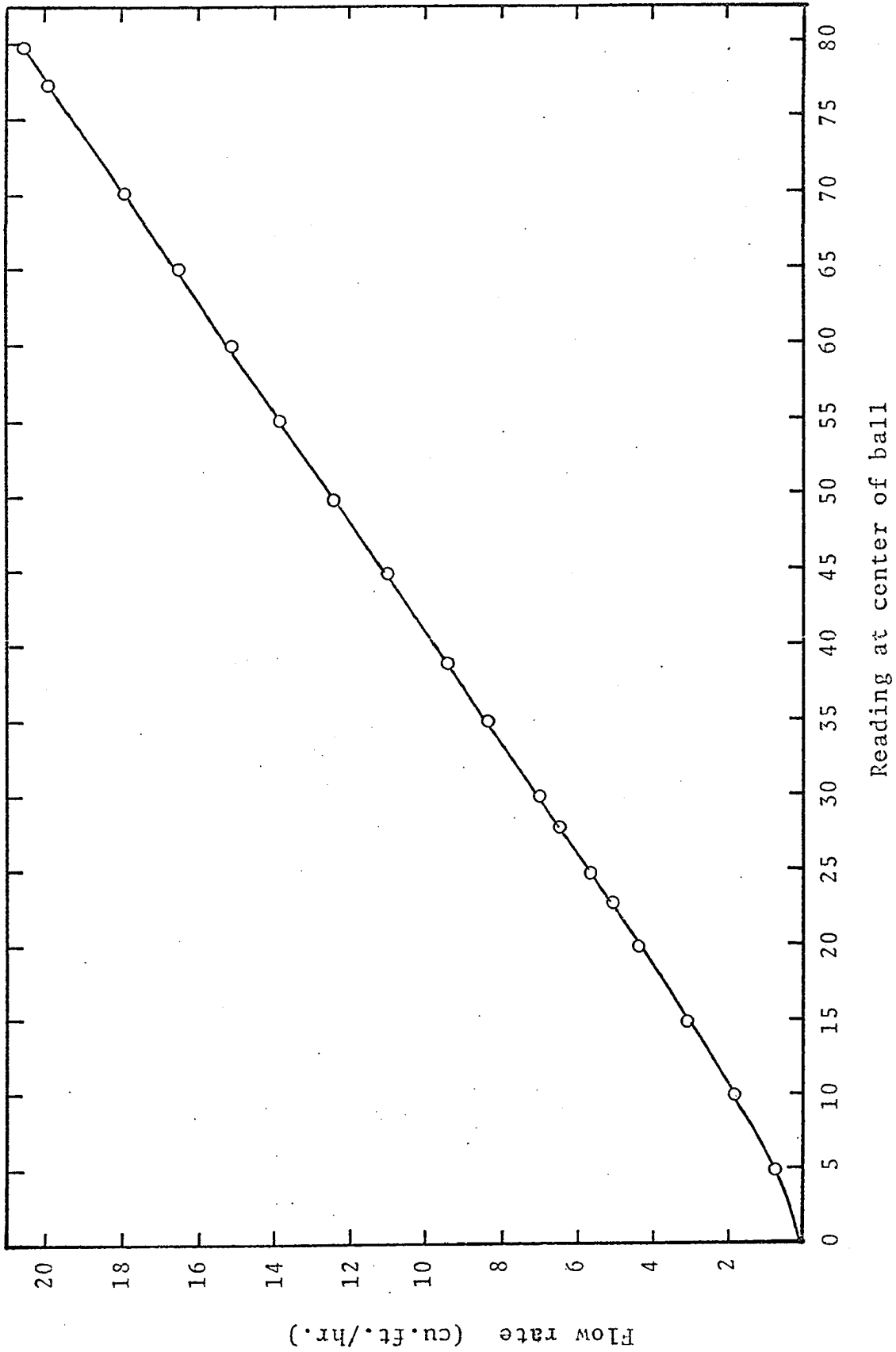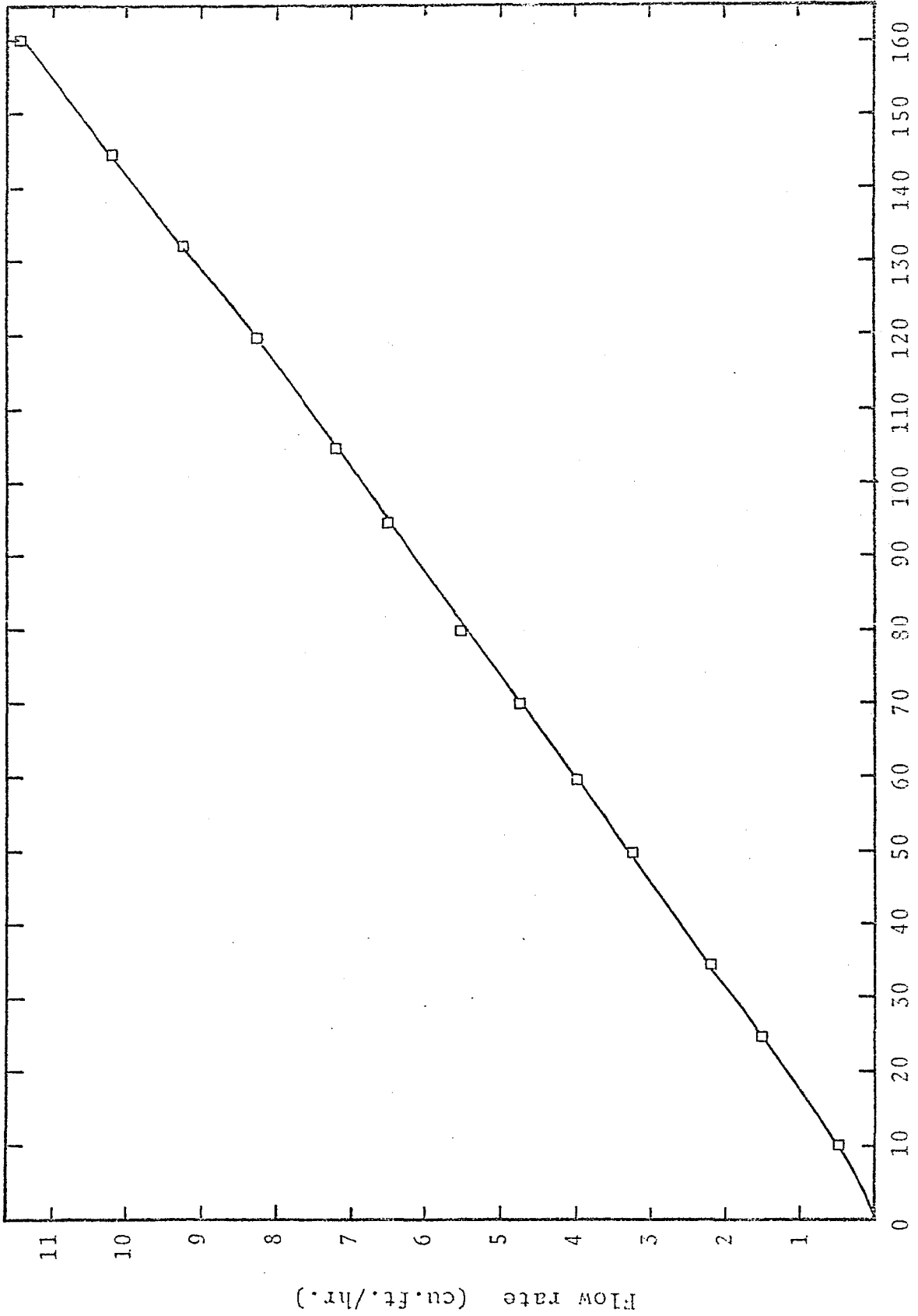
Fig. 57: Calibration curve for Roger Gilmont F1300 spherical float flowmeter.

Fig. 58: Calibration curve for Rotameter ROTA L 10 400-6185

VITA AUCTORIS

1944   Born in Mangalore, India on December 9th.

1960   Completed High School from St. Bede's High
        School, Madras, India.

1962   Passed the Pre-University Examination from
        Loyola College, Madras, India.

1968   Received Bachelor of Engineering (Mechanical)
        degree from College of Engineering, Guindy,
        Madras, India.

1970   Candidate for the degree of Master of Applied
        Science in Mechanical Engineering at the
        University of Windsor, Windsor, Ontario,
        Canada.